University of Cape Town

A Population Dynamics Model for Analysing the Effect of Rainfall Seasonality on Vegetation in the Karoo

Author:
Serayen Govender
GVNSER004

Supervisor:
Prof. Res Altwegg

M.Sc. AdvancedAnalytics

Abstract

The flora of the Cape Floristic Region is amongst the most diverse and unique on the planet, due mainly to the unique climate of this region. The effects of climate change are threatening many sensitive ecosystems around the world and so it is important to understand how factors of climate change may affect the Cape Floristic Region. This paper investigates the effect of changing rainfall seasonality on certain important species of plants in the Cape Floristic Region. The species are selected from different biomes and I focus on two growth forms, namely reseeder and resprouter. Data from an experiment conducted between two biomes in the Cape Floristic Region is used to model the growth of the two growth forms post-fire. Rainfall in this experiment is artificially manipulated on replicated plots at the two experiment sites. The population growth is modeled using state-space models, incorporating both an ecological process model and an observation model. This allows us to account for errors both in the observation of the data as well as in the natural variability in the biological state process that generated the data in order to account for both measurement and process error. My results suggest that increased summer rainfall in the Cape Floristic Region has a positive effect on the populations of reseeder species in both biomes and has little effect on the populations of resprouter species. A multivariate state-space model is also proposed to investigate the effects of interactions of species growth, within the replicated plots.

Acknowledgements

A large amount of gratitude is due to Prof. Res Altwegg for his continuous support and patience. His careful and insightful guidance has been of great support throughout this research.

This research would not have been possible without the efforts of Dr. Justin van Blerk and Prof. Adam West who have graciously provided the data of their experiment and provided careful explanations and assistance whenever required.

Contents

1 Introduction

The Cape Floristic Region is a vast natural region of South Africa. It has many complex ecological and geographical features that make it unique, such as it's Mediterranean climate in southern Africa and varieties of rare succulent flora. However, as with many natural regions around the world, the biomes of the Karoo may be vulnerable to threat of climate change.

The Succulent Karoo is located in the westerly portion of the region (covering part of the Western Cape and reaching as far as the southern portion of Namibia), whereas the Cape Floristic Region spans to the east and dominates a large portion of South Africa. Each biome has its own unique range of flora. The prevalence of these flora in each region is believed to be due to the differing climate and resource availability between the two biomes. The Fynbos and Renosterveld are biomes within the Cape Floristic Region and usually experiences its rainy season in winter where it receives 65% of its annual rainfall (Dean and Milton, 1999).

This research investigates the impact of changing rainfall patterns on the population sizes of various species of perennial woody shrub species found in different biomes of the Karoo, post-fire. Perennial woody shrubs make use of two post-fire growth strategies, reseeding or resprouting. Reseeders emerge from seeds post-fire, whereas, resprouters grow from root systems that survive post fire (Van Blerk, 2021). The growth of eight species of perennial woody shrub are investigated, from both the Renosterveld and Fynbos utilizing either of the post-fire growth strategies.

Fire in the Fynbos and Renosterveld is a crucial trigger that resets the 'succesional-clock' of the biomes. The growth of species of perennial woody shrubs in these areas is studied post-fire. It is then possible to investigate the sensitivity of the recovery of this vegetation to changing rainfall patterns during early post-fire years (van Blerk, West, Altwegg, and Hoffman, 2021).

The growth patterns of other plants in the ecosystem may also have an effect on the growth of perennial woody shrub species. This research will focus on one univariate interaction, the parasitic species, *Thesium strictum*, on certain species of perennial woody shrubs. In a multivariate setting the interaction of woody shrub species on other woody shrub will be analysed.

The population dynamics for the growth of these species, post-fire, are modeled using a state-space modeling approach. Such an approach allows for the incorporation of both an ecological process model and an observation model, it is therefore possible to account for errors during measurement (observations) and the process variation of the model (Auger-Méthé, Newman, Cole, Empacher, Gryba, King, Leos-Barajas, Flemming, Nielsen, Petris, and Thomas, 2020).

2 Literature Review

2.1 The Cape Floristic Region

The Cape Floristic Region (CFR) is a large floristic region in south western Africa, comprising several important biomes. It is a biodiversity hotspot of global significance and is considered the smallest of the six Floral Kingdoms of the world (Dupont et al., 2022).

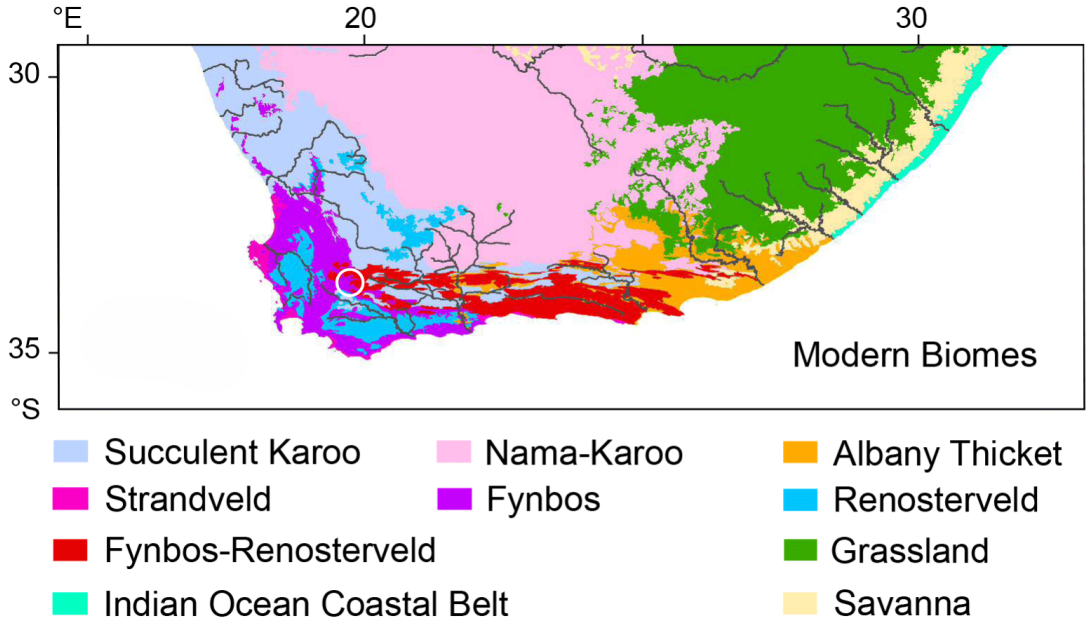

Figure 1: A Diagram showing the geographical layout of important biomes in South Africa. The central and western portions show the many biomes that comprise the CFR. The site of the experiment that this analysis was based on, was located in both the Fynbos and Renosterveld biome. The white circle indicates the approximate location of the Drie Kuilen Nature Reserve, where the experiment was conducted. The Fynbos-Renosterveld biome indicates a region that shares aspects of both the Fynbos and Renosterveld biomes. The biomes where the experiments are conducted are only between the Fynbos and Renosterveld and does not include the Fynbos-Renosterveld. Adapted from Dupont et al. (2022).

2.1.1 Rainfall

The distribution of mean rainfall in the Karoo shows that precipitation decreases uniformly westwards from the eastern escarpment across the plateau except for the

extreme south due to topographical irregularities in the Cape Fold Belt (van Blerk et al., 2021).

Over most of the eastern parts of the country, summer rainfall is prevalent. Over the western interior, to the east escarpment and north of the Cape Fold belt a winter-rainfall regime (Mediterranean Climate) dominates. Considered more meaningful in terms of distribution and characteristics of plant cover than general distribution patterns of rainfall are the duration, time of occurrence and degree of intensity of the rainy season (Dean and Milton, 1999).

Areas that experience winter-rainfall are floristically distinct from the rest of southern Africa (Born et al., 2006). The Fynbos and Renosterveld, within the Cape Floristic Region, experience winter-rainfall. The Cape Floristic Region has the highest endism and richness in relation to surrounding regions (Born et al., 2006). The Fynbos usually has more coarse and sandy soil derived from sandstone whereas the Renosterveld usually has more fine-particle loam soils derived from shale (van Blerk et al., 2021).

2.1.2 Flora of the Cape Floristic Region

Availability of water is generally considered the greatest limitation of plant growth and distribution (Dean and Milton, 1999). Several bio-geographic climate classifications of southern Africa have been conducted and in all cases, rainfall emerges as the primary driving variable (van Blerk et al., 2021). More importantly, the distinction between summer and winter rainfall maxima has emerged as the primary driving variable (van Blerk et al., 2021).

Flora of the CFR contains a variety of growth forms, with a range of size, shape and degree of succulence. In speciose vegetation, growth form classification is extremely useful in characterizing vegetation at a coarser level than taxonomic (Dean and Milton, 1999).

This research focuses on perennial woody shrubs having two main (post-fire) growth forms sprouters and seeders. Perennial woody shrub species regenerate post-fire either through reseeding or resprouting. Reseeding is a growth strategy whereby a plant regenerates through a seed whereas resprouting is a growth strategy whereby plants survive fire and resprout from surviving strucutres in the post-fire environment, they do not produce seedlings after fire. Reseeders and resprouters often present with different physiological and morphological characteristics, which may lead to a difference in sensitivity to rainfall patterns, particularly in a post-fire growth phase (van Blerk et al., 2021).

Thesium strictum is a flowering plant in the family Santalaceae that is prevalent

in the Cape Floristic Region. It has a parasitic relationship with the plants that it grows near, especially woody shrubs (van Blerk et al., 2021).

2.2 State-Space Modeling

State-space Models (SSMs) are hierarchical models, commonly used in ecology to analyze ecological time series, often to model population dynamics. State-space models present a flexible class of models that allow for the modeling of the natural variation in ecological processes separately from observation error. This allows for the separation of the two stochastic sources in the model and therefore the separation of biological stochasticity and imprecision in sampling methodology (Auger-Méthé et al., 2020).

The hierarchical structure of an SSM allows the modeling of two time series, a state (process) time series that attempts to reflect the true, hidden, state of the population and an observation process that are observations or measurements of the true, hidden state. The two stochastic components act at different levels of the model hierarchy and an SSM allows them to be modeled seperately. The SSM allows the seperation of these two stochastic processes with the assumptions that:

1. The process (hidden) states are auto-correlated. The value of the hidden state at time (t + 1) depends on its value at time t.
2. Observations are independent of each other and depend only on their true, hidden state.

Fitting an SSM to a time series requires the estimation of the parameters of the process and observation models as well as the hidden state. The estimates generally reflect the true state of nature better than the observation (Auger-Méthé et al., 2020).

A Normal Dynamic Linear Model (NDLM) is a linear time series model with an SSM where the process variance and observation error are modeled with a Gaussian distribution (Auger-Méthé et al., 2020).

This research has modeled SSMs in a Bayesian framework, using a Gibbs sampler. A Bayesian approach provides a means to fit increasingly complex SSMs with multiple hierarchical levels (Auger-Méthé, Newman, Cole, Empacher, Gryba, King, Leos-Barajas, Flemming, Nielsen, Petris, and Thomas).

Priors for the distributions of parameters of the state variation and observation errors must be selected. Uniform prior distributions may be favoured over gamma priors as they are less informative (Lopes, McCulloch, and Tsay, 2021).

Parameters of the Bayesian model can be estimated using Monte Carlo Markov Chain (MCMC) algorithms. These algorithms yields samples of arbitrary size of auto-correlated draws from a distribution and can be constructed so that this distribution approximates the desired posterior distribution (Kery and Schaub, 2011).

A Gibbs Sampler is a MCMC algorithm that takes a set of random initial parameters and through repeated sampling creates a Markov chain that has a stationary distribution which approximates the required posterior distribution (Gelfand, 2000).

2.3 Multivariate State-Space Models

Populations are structured by various methods such as spacial subdivision. Spread out across multiple sites populations covary to a restricted degree (Hinrichsen and Holmes, 2009).

Ecological time series analyses often have three main purposes, to approximate general patterns of measured variables over time, check for interactions between measured variables and to analyse the relationships between measured and explanatory variables (Zuur, Fryer, Jolliffe, Dekker, and Beukema, 2003a). State-space models can be extended into the multivariate space so as to address these questions. The multivariate model used in this paper is known as the multivariate auto-regressive state space model or dynamic factor analysis. With advances in computing, more computationally intensive time series techniques can now be applied to short non-stationary multiple time series (Zuur, Fryer, Jolliffe, Dekker, and Beukema, 2003a).

The objectives of this model is to estimate stochastic growth rates and variances that drive the dynamics of the population across the sites and to infer the correlation across sites (Hinrichsen and Holmes, 2009). This multivariate time-series analysis technique is used to estimate common patterns in a set of time series. These patterns can be common trends, common seasonal effects or common cycles (Zuur, Tuck, and Bailey, 2003b). The time-series are modelled in terms of, a linear combination of trends, explanatory variables, a level parameter and a noise component (Zuur et al. 2003b; Riga and Knape 2022).

Dynamic Factor Analysis can also be used for dimension reduction technique to model N observed time series in terms of M common trends (Zuur et al., 2003b). In this paper, in a multivariate context, N common trends are modeled by N time series, thus dimension reduction, while possible, is unnecessary. These models are important not only in an ecological context but are also used in the fields of economics, engineering and physics (Holmes, Ward, and Wills, 2012).

Most literature regarding multivariate state-space modeling relies on a frequentist approach for parameter estimation using maximum likelihood techniques (Hinrichsen

and Holmes 2009; Holmes et al. 2012), such as the Expectation-Maximisation (EM) algorithm (Zuur et al., 2003a). In this paper parameters for the multivariate state-space models are estimated within a Bayesian framework, using a hierarchical model and a Gibbs sampler.

3 Methods

3.1 Experimental Design

The data used in the present project was provided by an experiment set up by Dr. Justin Van Blerk and Prof. Adam West in the Drie Kuilen Nature Reserve, a semi-arid area with a Mediterranean type climate.

The experiment was set up in two biomes, Fynbos and Renosterveld. The experimental sites were approximately 2.4 kilometers apart and there was approximately 200m of altitude between them. These sites usually experience winter rainfall with 65% of mean annual rainfall experienced during winter months (van Blerk et al., 2021).

At each site, land was divided into twelve plots, each, four meters by four meters. This allowed for the observation of sixteen square meters of vegetation in each plot. Twenty-four plots were set up in total, twelve at each Biome. Of the twelve plots at each biome, six were designated as treatment plots and six as controls. Plots were arranged in blocks using a randomised complete block design across the landscape (van Blerk et al., 2021).

The plots that were designated as control plots were allowed to experience rainfall patterns as they usually would. For the six that were designated as treatment plots, their rainfall pattern was shifted, i.e., treatment plots that usually experienced winter rainfall seasonality were induced into now experiencing summer rainfall seasonality.

To achieve this, shelters were built over the treatment plots that allow the vegetation to experience half of the rainfall that occurs during the appropriate rainy season. The other half of the water was reserved and given to the plants in the treatment plot in the season opposite to the natural rainy season of the biome.

At the beginning of the experiment in May of 2016, all plots within the sites were subjected to a controlled burn where all above ground biomass was lost. The sites were allowed to repopulate until November of 2016 when the first survey -the baseline survey- was done. After this, surveys were conducted roughly every six months on the plots until May of 2019. Figure 2 shows the timeline of surveys from the initial burn to the final winter survey in May 2019.

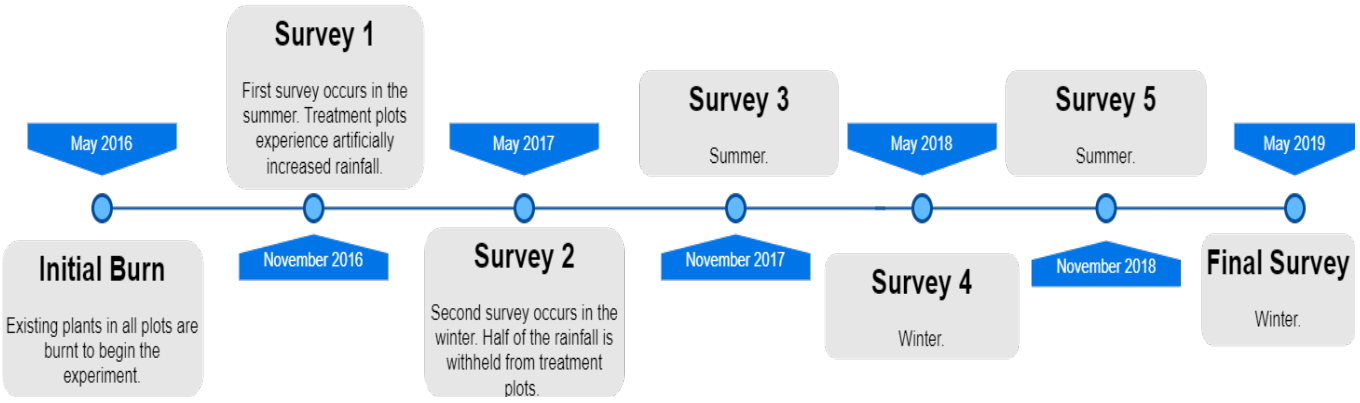

Figure 2: A Diagram showing the timeline of the recording of data from the experiment.

3.2 State-Space Models

The population growth of plant species in each plot was modeled so that the effect of the engineered shift of rainfall patterns could be analysed. With such an experiment, surveys can be a difficult task and often population counts are observed imperfectly (Bolker, 2007).

As with most population dynamics models the change in population size was assumed to be a Markovian process. State-space models were chosen to model population sizes as they are useful to describe Markov processes that are "hidden" because they are imperfectly observed thus, providing allowance to deal with observation errors in the analysis of population dynamics (Auger-Méthé et al., 2020).

State-space models are a set of hierarchical models that decompose an observed time series of counts into a process variation and observation error component (Kery and Schaub, 2011). Process variation represents the stochastic process that changes the population size through time. While observation error reflects the differences between the hidden state and the observed data.

A state-space model consists of two sets of equations (Auger-Méthé et al., 2020):

1. The process equations that describe the true but unknown development of the state
2. The observation equations that maps the true state of the process based on the observed data

A simple example of a state-space model is:
Process equation:

$$z_t = \beta z_{t-1} + \epsilon_t. \tag{1}$$

Where:

1. z_t represents the true, hidden state of the population size at time t.
2. β captures the autocorrelation between states.
3. $\epsilon_t \sim N\left(0, \sigma_p^2\right)$.

Observation equation:

$$y_t = \alpha z_t + \eta_t. \tag{2}$$

Where:

1. y_t represents the observed population at time t.
2. α allows the observation at time t to be a biased estimate of the state at time t.
3. $\eta_t \sim N\left(0, \sigma_o^2\right)$.

Equations 1 and 2 show an example of a general SSM that may not only be used for ecological purposes but also, for example, in the fields of economics or physics (Auger-Méthé et al., 2020).

Figure 3:A is a representation of the dependence relationship between states. It shows a dataset that is modeled with a state-space model as described above. The values of the observations, y_t, are autocorrelated only because the true state, z_t, is autocorrelated through time. The discrepancy between the true population size and the observation is not correlated through time. Once the dependence of the observations, y_t, on the states, z_t, are accounted for, the observations are assumed independent (Auger-Méthé et al., 2020).

These models can be treated as hierarchical Bayesian models and their parameters were estimated in a Bayesian framework using a Gibbs Sampler. The parameters of these models have been estimated in R using the JAGS(Just Another Gibbs Sampler) package (Plummer (2023), see also; R Core Team (2021)).

3.3 State-Space Model for a single species

The first set of state-space models that were run use a basic population dynamics format and Gaussian prior distributions and are therefore classified as normal dy-

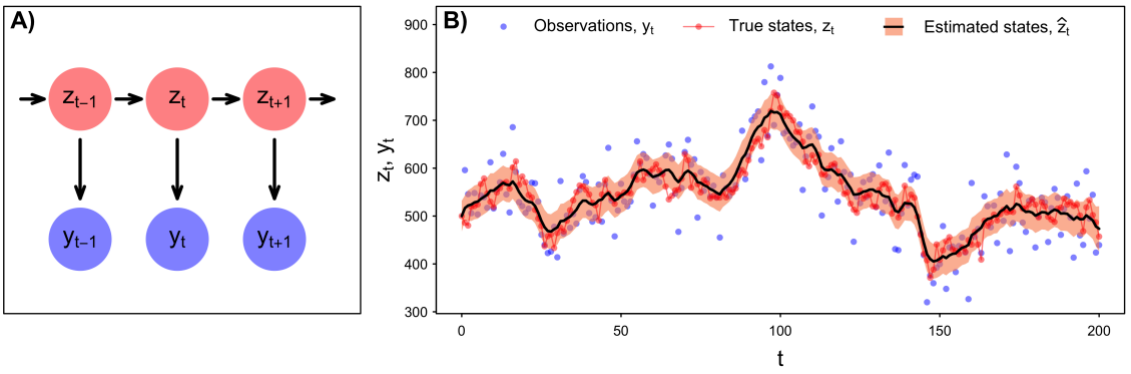

Figure 3: A visualization of state-space modeling adapted from Auger-Méthé et al. (2020).
A: A diagram showing the dependence relationship between states in a state space model, where, the observed value y is dependent only on the true state z at time t.
B: An example of a state space model with observed, estimated and true states represented. This example shows how the estimation of true states may differ from observations and are a closer approximation of the true state.

namic linear models. The type of population dynamics model was changed to an exponential growth model.

The equations for an example of the model is:

Process equation:

$$N_{i,t+1} = N_{i,t} \times e^{\lambda_{i,t}} \quad \text{where} \quad \lambda_{i,t} \sim N\left(\mu_{\lambda_{i,t}}, \sigma^2_{\text{process}}\right), \tag{3}$$

where:

1. $N_{i,t}$ is the estimated population size at time step t and at plot i.
2. $\lambda_{i,t}$ is the intrinsic growth rate at time step t and at plot i.
3. $\mu_{\lambda_{i,t}}$ is the mean of the intrinsic growth rate.

$\mu_{\lambda_{i,t}}$ was modeled as:

$$\mu_{\lambda_{i,t}} = \beta_0 + \beta_1 X_{\text{treatment }_i} + \epsilon_{\text{plot}}, \tag{4}$$

where, $X_{\text{treatment}}$ is a binary variable indicating whether or not the current experimental plot is a treatment or control plot, i.e. takes a value of 1 for a treatment plot and 0 for a control plot and $\epsilon_{\text{plot}} \sim N\left(0, \sigma^2_{\text{plot}}\right)$ is the random effect of the plot, which encompasses the variability of plant growth geographically. The β coefficients determine the relationship between the mean intrinsic growth rate and the effect of treatment.

Observation equation:

$$Y_{i,t} = N_{i,t} + \epsilon_{\text{observation}} \,. \tag{5}$$

Where, $\epsilon_{\text{observation}} \sim N\left(0, \sigma^2_{\text{observation}}\right)$. The assumption of a Gaussian prior allows the error to be negative so as to account for the possibility of under-counting.

The model parameters were estimated in a Bayesian framework using a Gibbs Sampler so the hyperparameters, $\sigma^2_{\text{process}}$, σ^2_{plot} and $\sigma^2_{\text{observation}}$ were assumed to have distribution. In this model they were assumed to have a uniform distribution, the parameters of which will vary for each model depending on the data from observations.

Each species was modeled at one experimental site over every plot that it is present at, at that site (usually 12 plots, half of which are treatment plots). By analysing the difference in growth rates between treatment and control plots some insight was gained as to the effect of a changing rainfall on a certain species. The β_1 variable, the coefficient of the treatment variable, in determining the mean of the intrinsic growth rate $\mu_{\lambda_{i,t}}$ at plot i, can give us some insight into the response of the growth rate of a species to the experimental treatment as opposed to at a control plot.

The state-space models (hierarchical Bayesian models) were modeled using a Gibbs sampler in R, using the rjags and R2jags packages (Plummer (2023); see also Su and Yajima (2021)). The Gibbs sampler was set to use 5 chains and 10000 iterations, with a burn in of 5000 iterations and a thinning rate of 3. The initial values for the Gibbs sampler were set to be random numbers; between 0 and 5 for variance parameters, 0 and 1 for β parameters and between 0 and 50 000 for population (N) parameters. These settings were chosen after several variations were tested and the best settings for fit and convergence were found. These settings were sufficient to achieve convergence in most parameters of the models. For those where it was not, the autojags function, from the R2jags package, was used to update the model until convergence.

3.4 Univariate Interaction Models

Another model that can potentially give insight into the growth rate of a population of a species within a plot is one that accounts for the interaction of the abundance of certain species of plants on other species. In particular this research focuses on the effect of the abundance of *Thesium strictum*, a root parasite on the growth rate of shrubs within the same plot (van Blerk et al., 2021). These models gave insight into how different growth forms of shrubs react to the presence of parasitic plants and what effect this has on the sensitivity to a change in rainfall pattern. *Thesium strictum* is found almost entirely within the Renosterveld so models with interactions have only been attempted with species that were found mainly in the Renosterveld.

An example of such a model would be:

Process equation:

$$N_{i,t+1} = N_{i,t} \times e^{\lambda_{i,t}} \quad \text{Where} \quad \lambda_{i,t} \sim N\left(\mu_{\lambda_{i,t}}, \sigma^2_{\text{process}}\right), \tag{6}$$

where:

1. $N_{i,t}$ the estimated population size at time step t and at plot i.
2. $\lambda_{i,t}$ the intrinsic growth rate at time step t and at plot i.

It is assumed that the intrinsic growth rate has a Gaussian prior with mean:

$$\mu_{\lambda_{i,t}} = \beta_0 + \beta_1 X_{\text{treatment }_i} + \beta_2 N_{\text{Thesium}(i,t)} + \beta_3 N_{\text{Thesium}(i,t)} X_{\text{treatment }_i} + \epsilon_{\text{plot}}\ , \tag{7}$$

where, $\epsilon_{\text{plot}} \sim N\left(0, \sigma^2_{\text{plot}}\right)$, and $N_{\text{Thesium}(i,t)}$ is the population size of *Thesium strictum* in plot i at time step t. This allows for the analysis of the effect of the interaction of *Thesium strictum* on the population in both treatment and control plots.

The observation model remains the same as it is assumed that the observations are dependent on the process variation only.
Observation equation:

$$Y_{i,t} = N_{i,t} + \epsilon_{\text{observation}}\ , \tag{8}$$

where, $\epsilon_{\text{observation}} \sim N\left(0, \sigma^2_{\text{observation}}\right)$. As with the previous model the variance hyperparameters of the model are assumed to be uniformly distributed.

In this model it was assumed that the abundance of *Thesium strictum* plants had an effect on the intrinsic growth rate of plants of a particular species, within a given plot.

Therefore this model incorporated the effect of the abundance of *Thesium strictum* in the calculation of the mean of the intrinsic population growth rate.

3.5 Forecasting

Using the models described in Section 3.3, a forecast of population growth rates both under control and experimental conditions has been attempted. The reliability of predictions may be called into question due to the short period of observation of the experiment.

In order to forecast the population growth rates in the time series data, the parameters for the relevant state-space models were estimated in a Bayesian framework (using a Gibbs sampler). The process equation of the state-space model was then estimated into further time periods, not yet observed. The model no longer estimates a value of the population size using the observation as an unbiased estimator, as there is no observation to estimate from (Kery and Schaub, 2011).

Estimations of population size after the initial time-series were a result of a stochastic model of population growth. The parameters of the model for these estimates were informed by the state-space model that relied on observations to estimate the true state. Therefore the process equations for the state-space models may be used to predict population growth as a regular time-series population dynamics model with parameters informed by a state-space model.

Forecasting was only conducted on one model in this analysis to demonstrate its effectiveness. It was demonstrated that forecasting for this model is not reliable due to the short length of the time series analysis. It, however, remains a useful tool that may be adapted to future analysis.

3.6 Multivariate State-Space Model

A more popular approach to account for interactions between species (as well as interactions with other potential covariates) within a site is a multivariate state-space model (Hinrichsen and Holmes, 2009).

In this paper a linear multivariate autoregressive state-space (MARSS) model is proposed to model the growth of selected species within a given site.

Like other SSMs the MARSS model includes a process and observation model. Gaussian errors are assumed to time series data (Zuur et al., 2003b). In the MARSS model the process model is a multivariate first-order autoregressive model (Holmes et al., 2012) taking the form:

$$\mathbf{N}_t = \mathbf{B}\mathbf{N}_{t-1} + \mathbf{u} + \mathbf{w}_t; \quad \mathbf{w}_t \sim \text{MVN}(0, \mathbf{Q}), \tag{9}$$

where:

1. $\mathbf{N}_t$ is an $m \times 1$ vector of state values, in this paper the sizes of populations of species, equally spaced through time. Where m represents the number of latent trends considered.
2. $\mathbf{B}$, $\mathbf{u}$ and $\mathbf{Q}$ are state parameters.
3. The $\mathbf{B}$ matrix is an $m \times m$ matrix that allows for interaction between state processes.
4. The diagonal elements of $\mathbf{B}$ can be interpreted as coefficients of auto-regression in state vectors (Holmes et al., 2012).
5. The $m \times 1$ vector $\mathbf{u}$ describes the mean trend.
6. The $m \times m$ matrix $\mathbf{Q}$ defines the correlation of the process deviation.

The MARSS process model for two state processes can be written out as:

$$\begin{gathered}\begin{bmatrix} N_1 \\ N_2 \end{bmatrix}_t = \begin{bmatrix} b_{11} & b_{12} \\ b_{21} & b_{22} \end{bmatrix} \begin{bmatrix} N_1 \\ N_2 \end{bmatrix}_{t-1} + \begin{bmatrix} u_1 \\ u_2 \end{bmatrix} + \begin{bmatrix} w_1 \\ w_2 \end{bmatrix}_t', \\ Where: \begin{bmatrix} w_1 \\ w_2 \end{bmatrix}_t \sim \text{MVN}\left(0, \begin{bmatrix} q_{11} & q_{12} \\ q_{21} & q_{22} \end{bmatrix}\right).\end{gathered} \tag{10}$$

The multivariate observation component can be expressed as:

$$\mathbf{y}_t = \mathbf{Z}\mathbf{N}_t + \mathbf{a} + \mathbf{v}_t; \quad \mathbf{v}_t \sim \text{MVN}(0, \mathbf{R}), \tag{11}$$

where:

1. $\mathbf{y}_t$ is an $n \times 1$ vector of observation values equally spaced through time. Where n is the number of species.
2. The $\mathbf{Z}$ matrix is an $n \times m$ matrix that contains the factor loadings of the state estimate on the observation and determines the exact form of the linear combinations of the common trends (Zuur et al., 2003b).
3. The $n \times 1$ vector $\mathbf{a}$ describes the mean trend.
4. The $n \times n$ matrix $\mathbf{R}$ defines the correlation structure of observation errors.

It is not always required to include the $\mathbf{Z}$ and $\mathbf{a}$ variables, but they are used when state processes are observed multiple times and when observations are linear combinations of the state process (Holmes et al., 2012). They were not used for this analysis.

Written for three observation processes and two state processes, the observation model would be:

$$\begin{gathered}\begin{bmatrix} y_1 \\ y_2 \\ y_3 \end{bmatrix}_t = \begin{bmatrix} z_{11} & z_{12} \\ z_{21} & z_{22} \\ z_{31} & z_{32} \end{bmatrix} \begin{bmatrix} N_1 \\ N_2 \end{bmatrix}_t + \begin{bmatrix} a_1 \\ a_2 \\ a_3 \end{bmatrix} + \begin{bmatrix} v_1 \\ v_2 \\ v_3 \end{bmatrix}_t, \\ Where: \begin{bmatrix} v_1 \\ v_2 \\ v_3 \end{bmatrix}_t \sim \text{MVN}\left(0, \begin{bmatrix} r_{11} & r_{12} & r_{13} \\ r_{21} & r_{22} & r_{23} \\ r_{31} & r_{32} & r_{33} \end{bmatrix}\right)\end{gathered} \tag{12}$$

MARSS process and observation models are flexible and many multivariate time-series models can be written in MARSS form (Holmes et al., 2012).

The main purpose in fitting a multivariate model to this ecological data is to investigate the interactions between species in a given plot (Zuur et al., 2003b). The $\mathbf{B}$ matrix in the state process is the interaction matrix that gives inference on the effect of state variables on other state variables. The diagonal elements of $\mathbf{B}$ indicate the strength of density dependence, values near 1 indicate no density dependence and those near 0 indicate strong density dependence. The off diagonal elements represent the effect of one species on the per-capita growth rate of another (Ives, Dennis, Cottingham, and Carpenter, 2003).

4 Species To Be Modeled

The data from the experiment described in Section 3.1 was surveyed on a six month basis. Six surveys occured between November 2016 and May 2019.

The data recorded the working name, species, genus, family, functional group, area, height, width and volume of plants found within each specific plot at every time period, as well as the growth form of the plant i.e. a plant can be classified as either a reseeding or resprouting plant after the burn.

In the experimental plots over the six time intervals 37 unique species of plants from five functional groups were recorded. These species included 28 species of herbaceous shrubs, three species of tall shrubs, two species of graminoids, three species of geophyte bulbs and one species of a root parasite.

Perennial woody shrubs (which includes herbaceous shrubs and tall shrubs) were chosen to be modeled as they not only encompass some of the most important and unique plant life in the Cape Floristic Region but also may show the greatest sensitivity to a changing rainfall pattern (van Blerk et al., 2021). It was also possible to compare the population growth between different growth forms of these plants under changing rainfall conditions. The population of eight of the most commonly observed species of perennial woody shrubs were modeled across the six intervals of the survey.

Of the eight species of perennial woody shrubs that were selected, two resprouters and two reseeders that were more present in the Renosterveld and two resprouters and two reseeders that were more present in the Fynbos were selected. Species population growth under changing rainfall patterns were modeled only in the biome in which they were more if not only present. The species modeled are listed in Table 1

Thesium strictum is a parasitic species of plant that is known to grow on shrubs in the Karoo. A model was created to attempt to study the effect of the presence of this species on the growth of certain species of shrubs in an experimental plot.

	Species	Biome	Growth Form	Count
1	*Agathosma capensis*	Fynbos	Resprouter	600
2	*Agathosma capensis*	Renosterveld	Resprouter	0
3	*Aspalathus shawii*	Fynbos	Reseeder	278
4	*Aspalathus shawii*	Renosterveld	Reseeder	1
5	*Elytropappus rhinocerotis*	Renosterveld	Resprouter	353
6	*Elytropappus rhinocerotis*	Fynbos	Resprouter	36
7	*Microdon polygaloides*	Renosterveld	Reseeder	2697
8	*Microdon polygaloides*	Fynbos	Reseeder	0
9	*Othonna parviflora*	Renosterveld	Reseeder	50
10	*Othonna parviflora*	Fynbos	Reseeder	13
11	*Passerina obtusifolia*	Renosterveld	Resprouter	531
12	*Passerina obtusifolia*	Fynbos	Resprouter	1
13	*Selago glabrata*	Fynbos	Reseeder	254
14	*Selago glabrata*	Renosterveld	Reseeder	0
15	*Thesium strictum*	Renosterveld	Root Parasite	201
16	*Thesium strictum*	Fynbos	Root Parasite	6
17	*Wahlenbergia nodosa*	Fynbos	Resprouter	1351
18	*Wahlenbergia nodosa*	Renosterveld	Resprouter	1

Table 1: Species of Perennial woody shrubs modeled and studied. The total counts of species of interest recorded at each site at the last survey period is represented in the count column.

Table 1 shows the sum of the observations of the species modeled at each experimental site at the final survey. This gives an idea of which site each species was more prevalent and where a state-space model may be more useful. From Table 1 it is clear that *Thesium strictum* was present mainly at the Renosterveld site, therefore models accounting for interactions of populations with this species was only attempted for species that were more prevalent in that site.

Counts of the population data was deemed to be the most reliable method of modeling population data due to the nature of other metrics recorded. Volumes of plant density or area covered that were captured were unreliable due to how they were recorded and the shape of the plants being inconsistent.

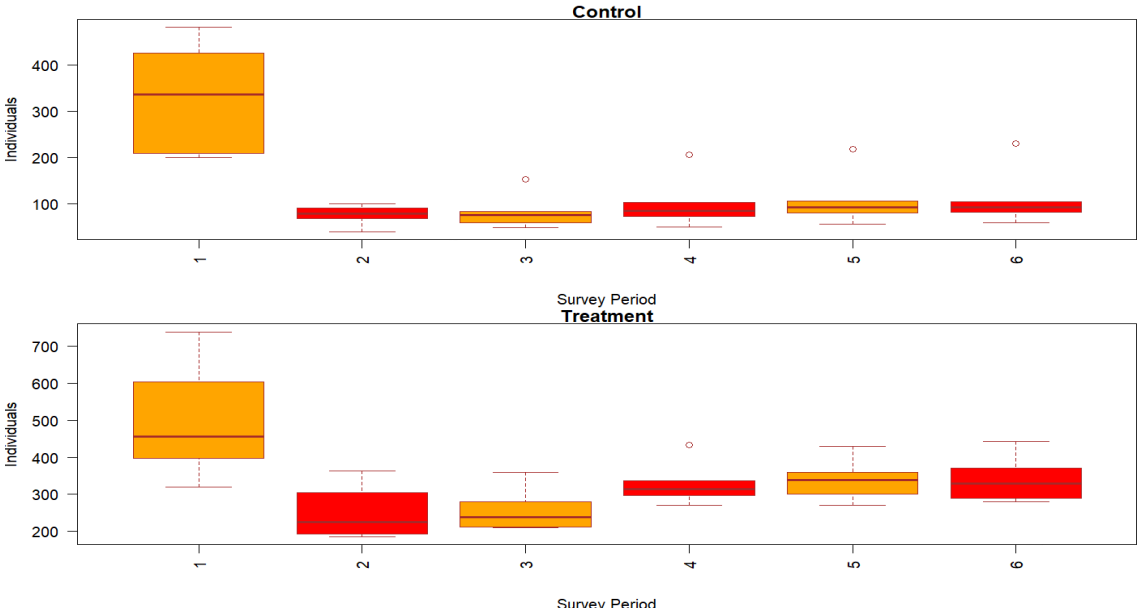

Figure 4: Two box plots showing the dispersion of *Microdon polygaloides* plants in both treatment and control plots in the Renosterveld. The y-axis represents the abundance of the population in the biome and the x-axis represents the time period.

Figure 4 shows a pair of box plots for the population of *Microdon polygaloides* in the Renosterveld. Figures 54 - 60 in Appendix 7.4 show similar box plots for the other species modeled (as highlighted in Table 1). The box plots show that for all species there were different levels of dispersion at different time periods. Due to this inconsistency and the relatively even spread of data of many species at many time periods, Gaussian priors were selected for variance parameters in state-space models.

5 Results

The state-space models were modeled in a Bayesian framework using a Gibbs sampler to estimate for parameters as outlined in Section 3.2. Each Species was modeled separately over six periods in a specific biome (Fynbos or Renosterveld).

5.1 *Microdon polygaloides*

Microdon polygaloides is a species of perennial woody shrub that is classified as a reseeder as it grows from a seedling post-fire. In the survey data it was only recorded as growing in the Renosterveld.

5.1.1 Normal Dynamic Linear Model

A state-space model was used to model the population density of *Microdon polygaloides*. The model is a Normal Dynamic linear model described in Section 3.3.

The parameters and hyperparameters are given the following prior distriutions:

1. $N_{i,0} \sim U\,(0, 10000)$.
2. $\beta_0 \sim N\,(0, 1000)$.
3. $\beta_1 \sim N\,(0, 1000)$.
4. $\sigma_{\text{process}} \sim U\,(0, 500)$.
5. $\sigma_{\text{plot}} \sim U\,(0, 500)$.
6. $\sigma_{\text{observation}} \sim U\,(0, 500)$.

The initial value of the population was given a uniform distribution as it acts as a location parameter in the model. The lower bound was set to zero (as there can be no negative counts) and the upper bound was set to a value sufficiently higher than the maximum number of observations. The beta parameters were modeled using a non-informative Gaussian prior with mean 0 and variance 1000 to flatten this distribution and keep it non-informative. Uniform priors with a wide range were used for the variance statistics as they are popular for variance statistics in hierarchical models (Lopes et al., 2021). Other formulations of distributions and parameters were attempted and this formulation was the most acceptable. This was decided by the prediction accuracy, level of fit and MCMC convergence of the resulting models.

As described in Section 3.3, the parameters of the model were estimated using a Gibbs sampler. Convergence in parameters in the sampling process was ensured

using the autojags function, in the R2jags package (Su and Yajima, 2021). Each model estimates 198 parameters, so it was not feasible to show all trace plots. Examples of trace plots for the β parameters of this model are included in Appendix 7.2, these plots showed convergence after the burn-in period. The trace plots of other estimates show similar trends. The Gelman-Rubin statistic ($\hat{R}$), of all parameters were observed to be close to 1.00, and none were greater than 1.1, indicating convergence of MCMC chains. Effective sample sizes estimated from MCMC algorithms of all estimates is close to and mostly significantly greater than 100. This was also observed in all subsequent models. The observation standard deviation $\sigma_{\text{observation}}$, estimated by the model was 9.98, whereas the process standard deviation σ_{process}, was estimated to be 0.53.

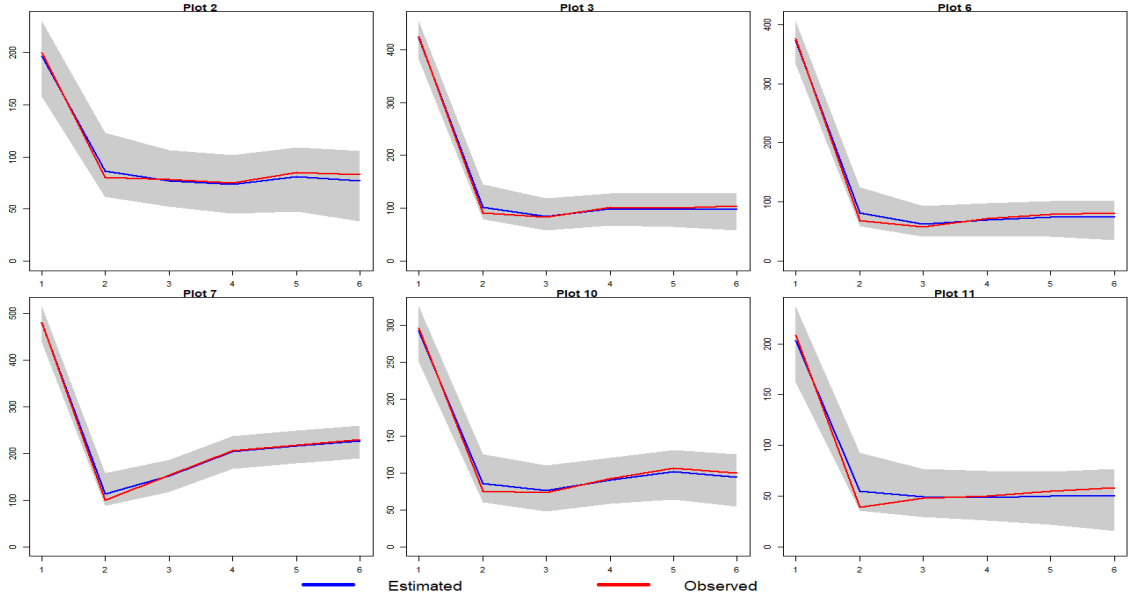

Figure 5: The population of *Microdon polygaloides* plants in six control plots in the Renosterveld. These plots experience winter rainfall patterns, which is not changed by the experiment. The y-axis represents abundance of the population and the x-axis represents the time period. The grey bands represent a 95% credibility interval for the estimations given by the state-space models.

The control plots represented are plot numbers: 2, 3, 6, 7, 10 and 11 from the Renosterveld experiment site.

The estimations of population size from the state space models seem to follow the same general trend as the observations but show slight variations due to observation errors according to the model. With more data points there may be more deviation from the true state of population density from the observed population growth due

to observation error as the model would have more parameters to estimate.

All models represented in Figure 5 contain the observed population growth within the 95% credibility interval of the true state estimated by the SSM. By visual inspection of the graphs it is apparent that most of these credibility intervals are relatively wide. It should be remembered that the model is fitted only over six intervals and with more recordings of data more precise credibility intervals may be expected.

	Plot	1	2	3	4	5
1	2	-0.84	-0.11	-0.05	0.09	-0.06
2	3	-1.43	-0.18	0.15	-0.01	-0.00
3	6	-1.54	-0.27	0.12	0.07	-0.02
4	7	-1.46	0.31	0.29	0.06	0.05
5	10	-1.25	-0.12	0.18	0.12	-0.08
6	11	-1.35	-0.08	-0.02	0.01	-0.03

Table 2: The estimates, from the SSM, of the growth rates, λ, of *Microdon polygaloides* in six control plots over six periods.

Table 2 shows the intrinsic growth rates, $\lambda_{i,t}$, (at plot i and time t) of the population of *Microdon polygaloides* in control plots over the six periods surveyed, estimated by the state-space model. Five growth rates are recorded between the six surveys.

From Figure 5 and Table 2 it is apparent that amongst all control plots there was a dramatic decrease in the population from the first to second time period. There was not much recovery from this decrease with the exception of plot seven. Other control plots experience a plateau in the abundance of *Microdon polygaloides* after this period. Only plot seven shows some recovery with a growth of 36.34% ($e^{0.31} - 1$) after the second survey 33.64% ($e^{0.29} - 1$) after the third survey. The credibility intervals for λ for this species and all others are included in Appendix 7.1. The credibility interval for the growth rate in plot 7 after the first period shows a lower bound (2.5%) of -0.14 (a decrease of 13%) and an upper bound (97.5%) of 0.58 (an growth of 78%). This is a relatively wide interval and shows that there is not much certainty about the estimate from the model. This may be due to the model being influenced by the trends of growth in other plots at this time period, as well as, the short duration of the experiment. In a longer time-series analysis smaller intervals may be expected.

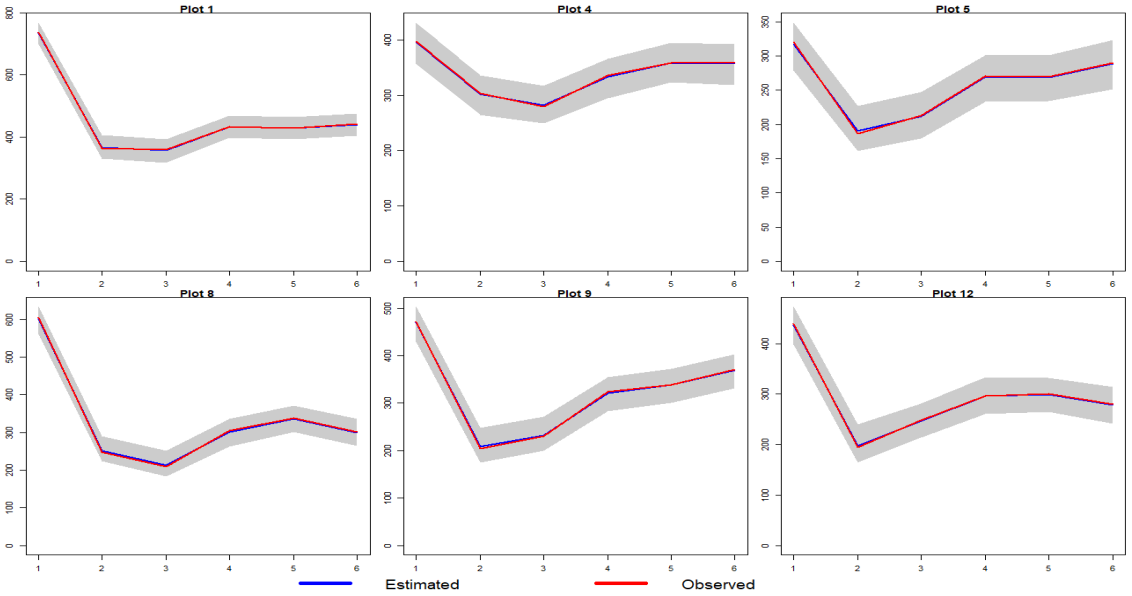

Figure 6: The population of *Microdon polygaloides* plants in six treatment plots, in the Renosterveld. These plots experience a changed rainfall pattern as described by the experimental design (Section 3.1). The y-axis represents abundance of the population and the x-axis represents the time period. The grey bands represent a 95% credibility interval for the estimations given by the state-space models.

The plots represented are plot numbers: 1, 4, 5, 8, 9 and 12 from the Renosterveld experiment site.

Table 3 shows the intrinsic growth rates, $\lambda_{i,t}$, of the population of *Microdon polygaloides* in treatment over the six periods surveyed, estimated by the state-space model.

From Figure 6 it is apparent that amongst treatment plots there was some consistent recovery in the abundance of the species after the initial drop on population as compared to control plots. It is apparent that this recovery mainly takes place in time period 3. This is supported by Table 3 as the third time period shows a positive λ parameter, for all plots, indicating growth of the population. The largest amount of growth after period 3 was recorded in plot 8 where the population was estimated to grow by $41.9\%(e^{0.35} - 1)$. The credibility intervals for λ for this species and all others are included in Appendix 7.1. It is apparent that these credibility intervals are also relatively wide. The credibility interval $(CI_{0.025}(\lambda), CI_{0.975}(\lambda))$ for plot 8 in period 3 was recorded as (0.13, 0.52). This shows that while growth was more certain, the rate of growth was more in line with growth in other plots at this period at the lower bound and much higher at the upper bound. It is again noted that a

	Plot	1	2	3	4	5
1	1	-0.70	-0.02	0.19	-0.01	0.03
2	4	-0.27	-0.07	0.17	0.07	-0.01
3	5	-0.51	0.11	0.24	-0.00	0.07
4	8	-0.87	-0.17	0.35	0.11	-0.12
5	9	-0.82	0.11	0.33	0.05	0.09
6	12	-0.79	0.22	0.18	0.01	-0.07

Table 3: The estimates, from the SSM, of growth rates, λ, of *Microdon polygaloides* in six treatment plots over six periods.

longer time series analysis may result in more precise intervals.

In Section 3.3 the mean of the intrinsic growth rate λ was assigned the Gaussian prior distribution, $\lambda_{i,t} \sim N\left(\mu_{\lambda_{i,t}}, \sigma^2_{\text{process}}\right)$.

The mean of that distribution is described in Equation 4 as:
$\mu_{\lambda_{i,t}} = \beta_0 + \beta_1 X_{\text{treatment }_i} + \epsilon_{\text{plot}}$.

The estimation of the parameter β_1 was analysed to give some insight into the effect of the plot being either a treatment or control plot on the mean of the intrinsic growth rate μ_λ.

	Coeffecient	sd	lower(2.5%)	upper(97.5%)
β_0	-0.25	0.10	-0.44	-0.05
β_1	0.18	0.14	-0.10	0.45

Table 4: Table of beta parameters estimated by the SSM as well as the standard deviation and 95"%" credibility intervals.

Table 4 shows that the state-space model estimates the β_1 parameter to be 0.18. $X_{\text{treatment}}$ is a binary variable that is set as 1 if the plot in the model is a treatment plot and 0 otherwise. Therefore there is an increase of 0.18 in the mean of the intrinsic growth rate μ_λ when the plot modeled is a treatment plot. From the credibilty intervals for β_1, it is apparent that the model does not predict this change with high accuracy. At the lower 2.5% level of credibility, the model estimates a value of -0.1, and at the upper 97.5%, a value of 0.45. It should be noted that, at the 5% level some variability is expected, but the high level of variance in this model (captured by the standard deviation of 0.14), may be explained by the short period of the time series analysis. This is apparent in the analysis of other species as well, and the analysis would benefit from a longer period of experimentation.

By using the coeffecients in the Equation 4, μ_λ can be calculated as: $\mu_\lambda = -0.25 +$

$0.18 = -0.07$ for treatment plots and $\mu_\lambda = -0.25 + 0 = -0.25$ for control plots. Thus it can be asserted that in control plots on average, every six months there was a decrease of the *Microdon polygaloides* population by 22.1% ($1 - e^{-0.25}$), whereas in treatment plots there was only a decrease of 6.67%.

From this it can be asserted that the population *Microdon polygaloides* benefits from the experimental treatment, of experiencing summer rainfall instead of winter rainfall.

5.1.2 Interaction with *Thesium strictum*

A state-space model as suggested in Section 3.4 was used to determine the effect of the presence of *Thesium strictum*, a parasite, on the growth of *Microdon polygaloides* within a plot.

The same prior distributions given in Section 5.1.1 are used in this model.

The prior distributions of the additional β parameters are:

1. $\beta_0 \sim N(0, 1)$
2. $\beta_1 \sim N(0, 1)$
3. $\beta_2 \sim N(0, 1)$
4. $\beta_3 \sim N(0, 1)$

In Section 3.4 the mean of the intrinsic growth rate λ is defined in Equation 7 as: $\mu_{\lambda_{i,t}} = \beta_0 + \beta_1 X_{\text{treatment }_i} + \beta_2 N_{\text{Thesium}(i,t)} + \beta_3 N_{\text{Thesium}(i,t)} X_{\text{treatment }_i} + \epsilon_{\text{plot}}$.

By comparison of Figures, 5 and 6 with Figures 7 and 8 it is apparent that adding complexity to the model has negatively effected the precision of the model. With more data points, the effect of this may be reduced (Warton, Blanchet, O'Hara, Ovaskainen, Taskinen, Walker, and Hui, 2015b). The observation standard deviation $\sigma_{observation}$, estimated by the model was 14.4, whereas the process standard deviation $\sigma_{process}$, was estimated to be 0.5. The increase in the observation error in the interaction model reflects the loss of accuracy in the more complex model.

Table 5 shows that the estimate for β_0 and β_1 are similar to that of the estimates for the model without interaction. The estimate of the β_2 parameter shows a strong negative effect of the abundance of *Thesium strictum* plants on the mean intrinsic growth rate of *Microdon polygaloides* in the control plots (when $X_{\text{treatment }_i}$ is 0). The estimate for β_3 shows a positive effect of the abundance of *Thesium strictum*

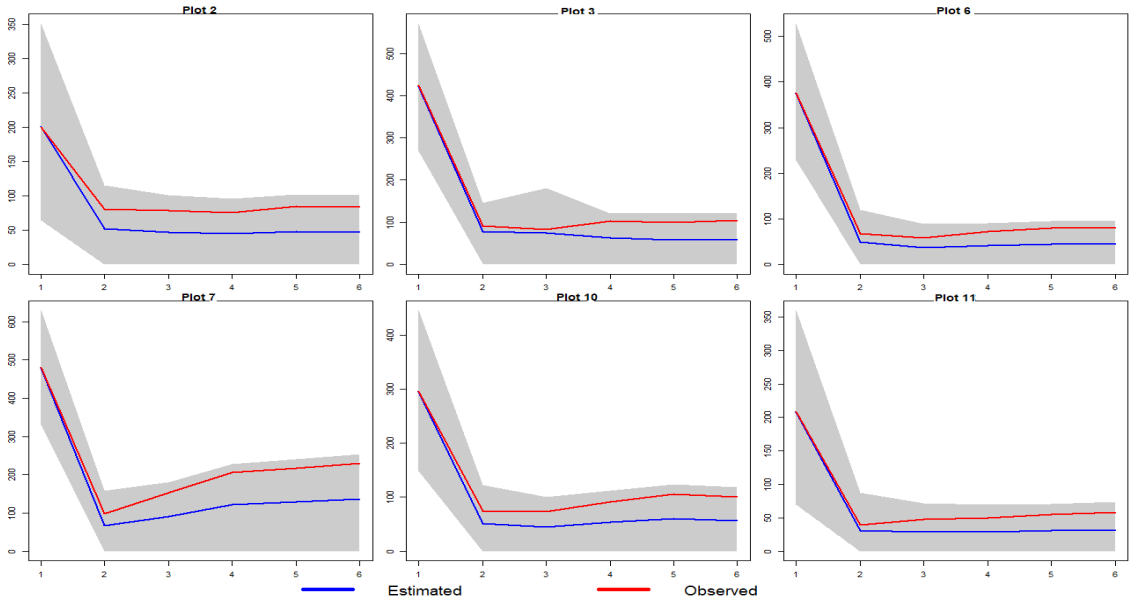

Figure 7: The population of *Microdon polygaloides* plants in six control plots, in the Renosterveld, modeled with the effect of the *Thesium strictum* population density. The y-axis represents abundance of the population and the x-axis represents the time period. The grey bands represent a 95% credibility interval for the estimations.

	mean	sd	lower(2.5%)	upper(97.5%)
β_0	-0.32	0.29	-0.98	0.24
β_1	0.19	0.32	-0.41	0.89
β_2	-0.29	0.57	-1.86	0.04
β_3	0.30	0.57	-0.04	1.86

Table 5: Table of beta parameters estimated by the interaction SSM.

plants on the mean intrinsic growth rate in the treatment plots. The net effect of the presence of *Thesium strictum* can be calculated as $\beta_2 + \beta_3$. From this it can be asserted that the effect of the parasitic plant on the population of *Microdon polygaloides* is reduced under experimental conditions, i.e. when the Renosterveld experiences mostly summer rainfall instead of winter rainfall.

Again, it is noted that the credibility intervals for estimated β parameters are relatively wide and that longer time series may result in more accurate estimates.

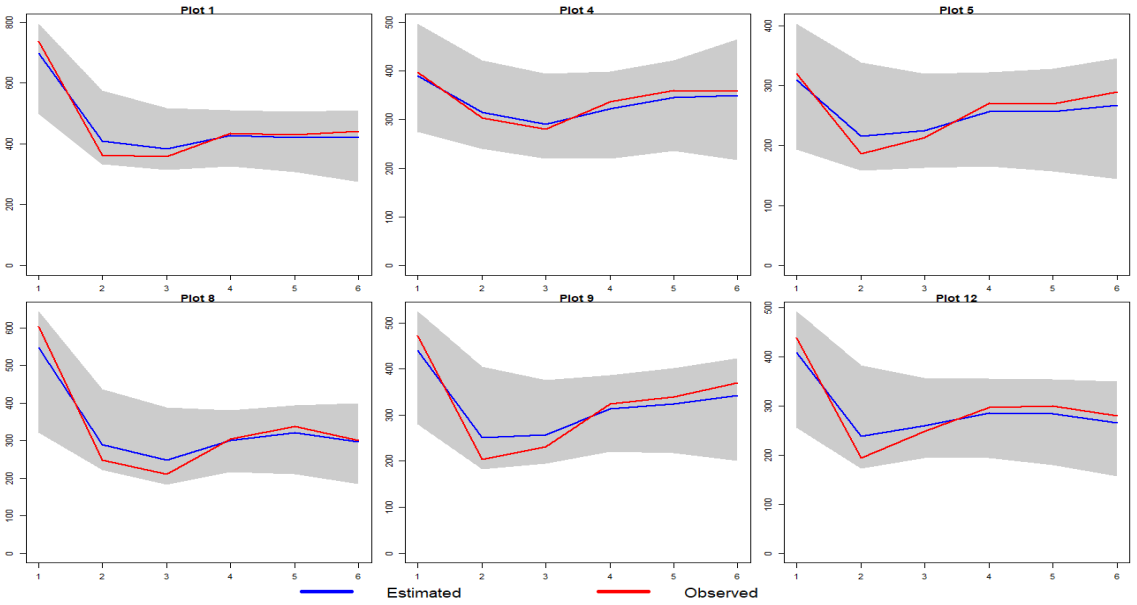

Figure 8: The population of *Microdon polygaloides* plants, in six treatment plots in the Renosterveld, modeled with the effect of the *Thesium strictum* population density. The y-axis represents abundance of the population and the x-axis represents the time period. The grey bands represent a 95% credibility interval for the estimations.

5.1.3 Forecasting

Figures 9 and 10 show an attempt at using the SSMs to forcast population sizes, as described in Section 3.5. Most plots show population density is predicted to follow the pattern of growth from the previous period. From these figures, it appears as though predictions, particularly those beyond one time period are very unreliable, this is highlighted by the greatly increased range of the 95% credibility intervals of the predictions. This may be due to the fact that there were very few observations for each model at the plot level, as only 6 time periods are recorded. Therefore it is not very beneficial to attempt to forecast at this point. However, with a data set where more surveys are recorded, forecasting may become a more useful tool.

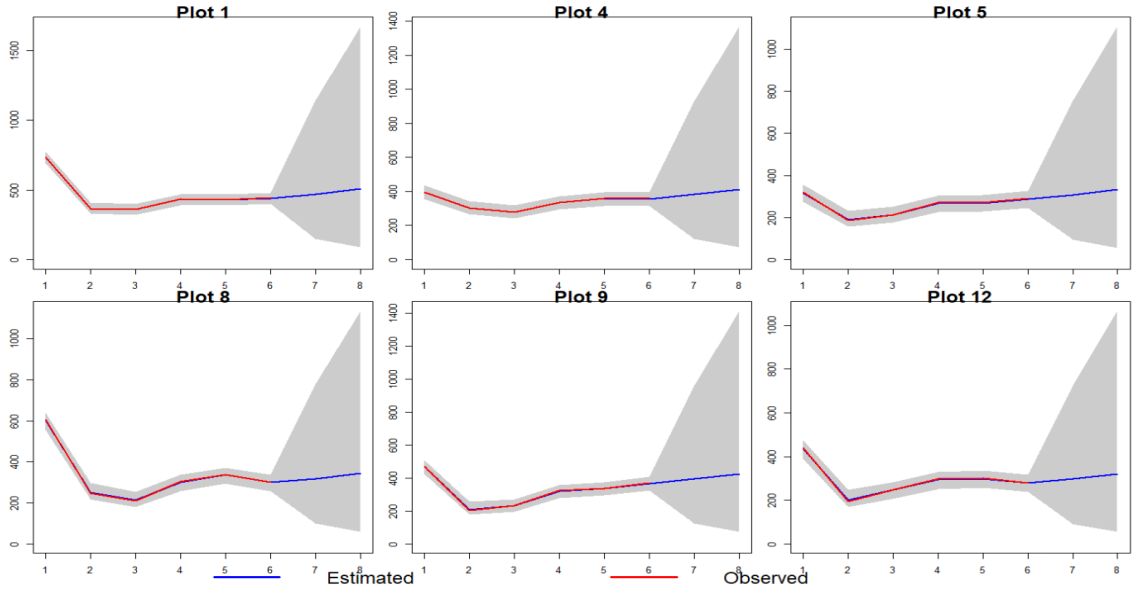

Figure 9: The population of *Microdon polygaloides* plants in six treatment plots in the Renosterveld, modeled with a forecast two time periods ahead. The y-axis represents abundance of the population and the x-axis represents the time period. The grey bands represent a 95% credibility interval for the estimations.

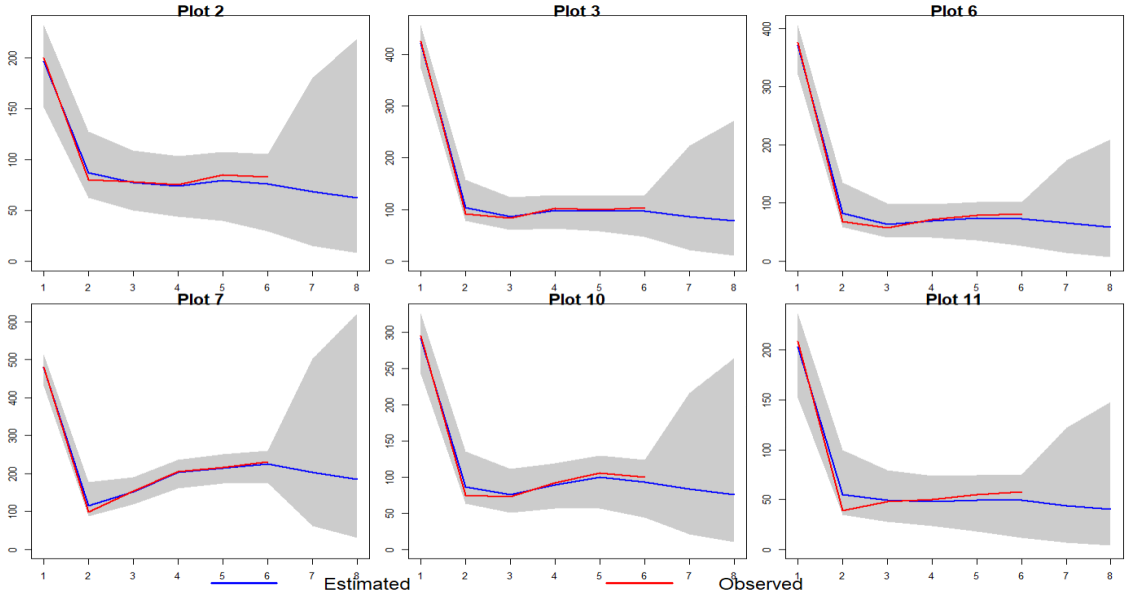

Figure 10: The population of *Microdon polygaloides* plants in six control plots in the Renosterveld, modeled with a forecast two time periods ahead. The y-axis represents abundance of the population and the x-axis represents the time period. The grey bands represent a 95% credibility interval for the estimations.

5.2 *Othonna parviflora*

Othonna parviflora is another species of perennial woody shrub, with a growth form classified as a reeseder. *Othonna parviflora* is present mainly in the Renosterveld site and the population will be modeled in this site only.

5.2.1 Normal Dynamic Linear Models

The population of *Othonna parviflora* in the experiment plots over the six time periods of recording are modeled using the normal dynamic linear models described in Section 3.3

The parameter and hyperparameters prior distributions, used in modeling this species, are the same as those given in Section 5.1.1.

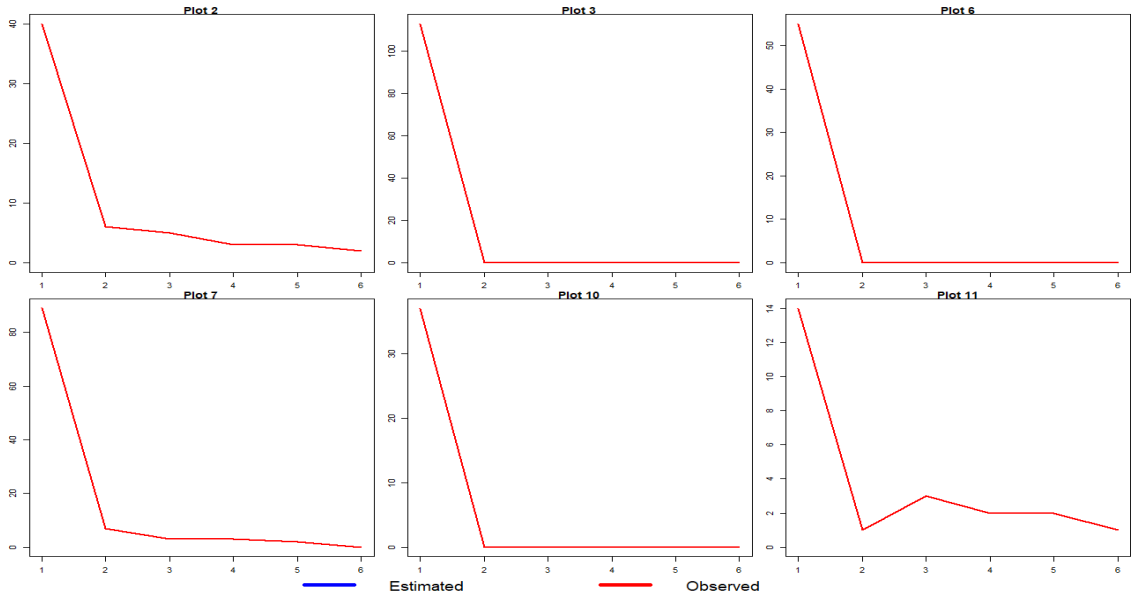

Figure 11: The population of *Othonna parviflora* plants in six control plots in the Renosterveld. The y-axis represents abundance of the population and the x-axis represents the time period.

Figure 11 shows the observed population of *Othonna parviflora* in the Renosterveld as well as the true states estimated by the SSM, in plots designated as control plots. For these plots the estimations of the true state of the population, from the SSMs are very close to the observed population of *Othonna parviflora*. In most plots the credibility intervals for the estimation of population size is very narrow. The observation standard deviation $\sigma_{observation}$, estimated by the model was 0.004,

whereas the process standard deviation $\sigma_{process}$, was estimated to be 2.23. The small observation error estimated explains the very narrow credibility intervals.

	Plot	1	2	3	4	5
1	2	-1.90	-0.18	-0.51	0.00	-0.41
2	3	-12.60	-10.10	-10.09	-10.08	-10.05
3	6	-11.92	-9.59	-9.56	-9.54	-9.55
4	7	-2.54	-0.85	0.00	-0.41	-7.02
5	10	-11.79	-9.62	-9.61	-9.57	-9.61
6	11	-2.64	1.10	-0.41	0.00	-0.69

Table 6: The estimation of growth rates, λ, of $Othonna\,parviflora$ in six control plots, over six periods.

Table 6 shows the intrinsic growth rates, $\lambda_{i,t}$, (at plot i and time t) of the population of *Othonna parviflora* in control plots over the six periods surveyed, estimated by the state-space model.

Referring to Figure 11 and Table 6 it is apparent that like *Microdon polygaloides* species the population of *Othonna parviflora* experiences a massive decrease in population at the first interval. In plots 3, 6 and 10 the population did not survive the initial decrease, post-fire, and are not found in these plots after the initial survey. Plot 11 experiences a brief growth period between the second and third surveys experiencing a growth rate 200%, a winter period where control plots experience a rainy season. However in this plot there is a relatively small population (at most 14) so this may not represent the population trend very well. The credibility intervals, (Appendix 7.1), for the estimates of the growth rate (λ) in this model are generally much narrower than those in the model for *Microdon polygaloides* (Section 5.1.1). The credibility interval for the growth at plot 11 at period 2 $(CI_{0.025}(e^{\lambda}-1), CI_{0.975}(e^{\lambda}-1))$, is (197%, 203%). This may be due to the growth trends of *Othonna parviflora* being more similar between control plots, as well as, there being far fewer observations of *Othonna parviflora* plants in the survey.

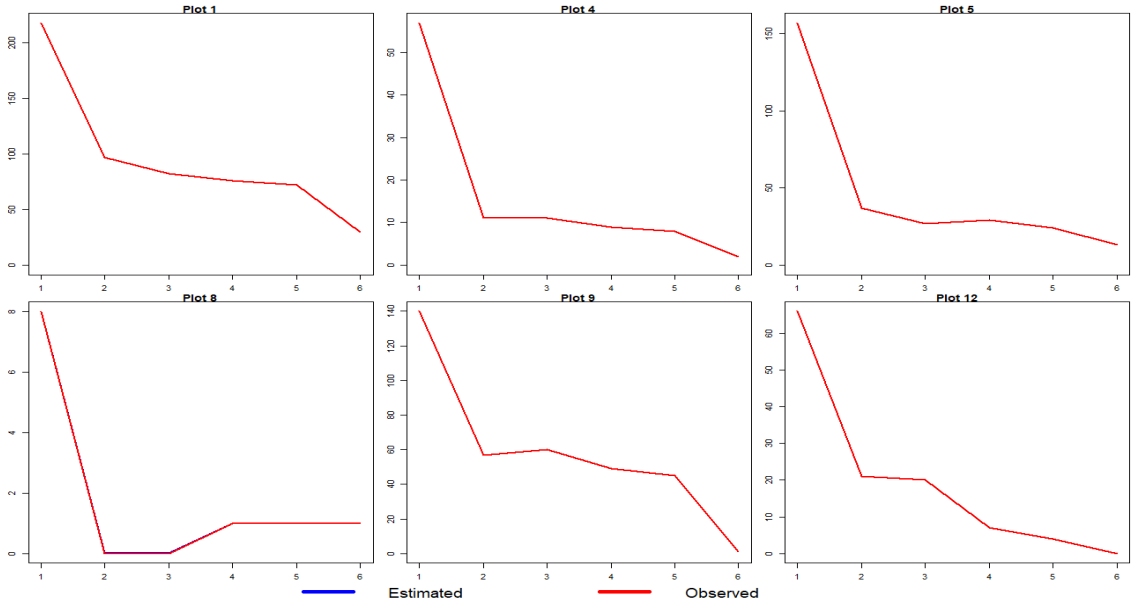

Figure 12: The population of *Othonna parviflora* plants, in six treatment plots, in the Renosterveld. The y-axis represents abundance of the population and the x-axis represents the time period.

Figure 12 shows the observed population of *Othonna parviflora* in the Renosterveld as well as the true states estimated by the SSM, in plots designated as treatment

plots. Again the SSM estimates of the true state of the population to be very close to the observed population of *Othonna parviflora*, with high certainty as the credibility intervals are very narrow. It is apparent that there are more observations in the treatment plots as compared to the control plots but are still relatively few. With more observations of the species models may become less precise and estimate the true state further away from observations to a higher probability of observation error.

	Plot	1	2	3	4	5
1	1	-0.81	-0.17	-0.08	-0.05	-0.88
2	4	-1.65	0.00	-0.20	-0.12	-1.39
3	5	-1.45	-0.32	0.07	-0.19	-0.61
4	8	-6.52	-0.81	5.25	0.00	-0.00
5	9	-0.90	0.05	-0.20	-0.09	-3.81
6	12	-1.15	-0.05	-1.05	-0.56	-7.53

Table 7: The estimates of growth rates, λ, of *Othonna parviflora*, in six treatment plots, over six periods.

Table 7 shows the intrinsic growth rates, $\lambda_{i,t}$, (at plot i and time t) of the population of *Othonna parviflora* in treatment plots over the six periods surveyed, estimated by the state-space model.

From Figure 12 and Table 7 it is apparent that just as with control plots there is a large decrease in the population within treatment plots after the first period. There is however a smaller decrease in the growth rate at subsequent time steps. Unlike the results for *Microdon polygaloides* in Section 5.1.1 there is not much if any recovery of *Othonna parviflora* after the first period in treatment plots.

	Coeffecient	sd	lower(2.5%)	upper(97.5%)
β_0	-3.66	1.53	-6.68	-0.51
β_1	2.18	1.99	-2.08	5.94

Table 8: Table of beta parameters estimated by the SSM.

Table 8 shows that the state-space model estimates the β_1 parameter to be 2.18. $X_{\text{treatment}}$ is a binary variable that is set as 1 if the plot in the model is a treatment plot and 0 otherwise. Therefore there is an increase of 2.18 in the mean of the intrinsic growth rate μ_λ when the plot modeled is a treatment plot.

By using the coefficients in the Equation 4, μ_λ can be calculated as: $\mu_\lambda = -3.66 + 2.18 = -1.48$ for treatment plots and $\mu_\lambda = -3.66 + 0 = -3.66$ for control plots. Thus it can be asserted that in treatment plots on average, every six months there

is a decrease of the *Othonna parviflora* population by 77.23% ($1 - e^{-1.48}$), whereas in control plots there is a decrease of 97.42%.

From this it can be asserted that the population *Othonna parviflora* benefits from the experimental treatment, of experiencing summer rainfall instead of winter rainfall.

Comparing these results to the analysis of *Microdon polygaloides* (another reseeder in the Renosterveld site), in Section 5.1.1 it is apparent that both species have benefited from the experimental treatment. The *Microdon polygaloides* population recording a decrease of 6.67% on average every six months in treatment plots a decrease of 22.1% in control plot, a difference of 15.43%. The *Othonna parviflora* population had a slightly higher benefit from the treatment recording a decrease of 77.23% on average every six months in treatment plots a decrease of 97.42% in control plot, a difference of 20.19%.

5.2.2 Interaction with *Thesium Strictum*

A state-space model as suggested in Section 3.4 is used to determine the effect of the presence of *Thesium strictum*, a parasite, on the growth of *Othonna parviflora* within a plot. The same prior distributions given in Section 5.1.2 are used in this model.

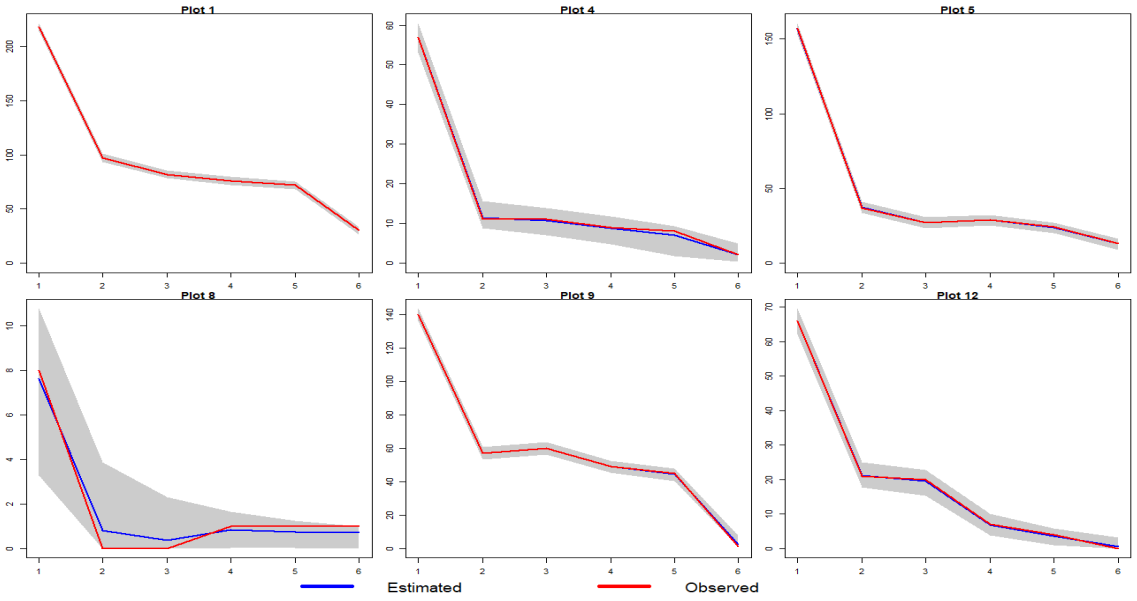

Figure 13: The population of *Othonna parviflora* plants in six treatment plots, in the Renosterveld, modeled with the effect of the population density of *Thesium strictum*. The y-axis represents abundance of the population and the x-axis represents the time period.

By comparison of Figures, 13 and 14 with Figures 11 and 12 it is apparent that adding complexity to the model has again negatively affected the precision of the model, although the model is still precise the increase of the with of the credibility intervals shows that the model has become less certain of the estimations particularly in plots 8, 2 and 11. With more data points, the effect of this may be reduced. The observation standard deviation $\sigma_{observation}$, estimated by the model was 5.2, whereas the process standard deviation $\sigma_{process}$, was estimated to be 1.8.

From the estimate for β_2 (Table 9), we see that there is a small negative effect of the abundance of *Thesium strictum* on the mean of the intrinsic growth rate of *Othonna parviflora* in control plots. The estimate for β_3 indicates that there is a small positive effect from the abundance of *Thesium strictum* in treatment plots.

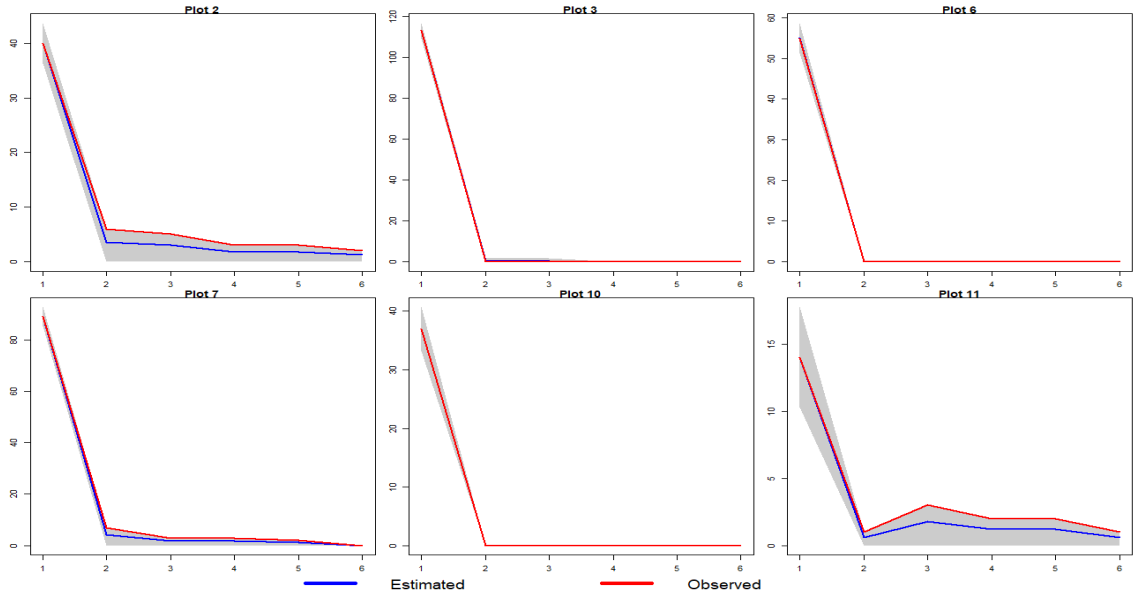

Figure 14: The population of *Othonna parviflora* plants in six control plots, in the Renosterveld, modeled with the effect of the population density of *Thesium strictum*. The y-axis represents abundance of the population and the x-axis represents the time period.

	mean	sd	2.5%	97.5%
β_0	-0.96	0.94	-2.73	0.92
β_1	0.03	0.93	-1.81	1.85
β_2	-0.08	0.17	-0.43	0.25
β_3	0.09	0.18	-0.25	0.44

Table 9: Table of beta parameters estimated by the SSM.

From it is apparent that the negative effect of the parasitic plant on the population of *Othonna parviflora* is reduced under experimental conditions. These are similar to the results of the interaction of *Microdon polygaloides* and *Thesium strictum* in Section 5.1.2.

5.3 *Elytropappus rhinocerotis*

Elytropappus rhinocerotis is a species of perennial woody shrub, with a growth form classified as a resprouter. *Elytropappus rhinocerotis* is present mainly in the Renosterveld site and the population will be modeled in this site only.

5.3.1 Normal Dynamic Linear Models

The population of *Elytropappus rhinocerotis* in the experiment plots over the six time periods of recording are modeled using the normal dynamic linear models described in Section 3.3

The same prior distributions given in Section 5.1.1 are used in modeling this species.

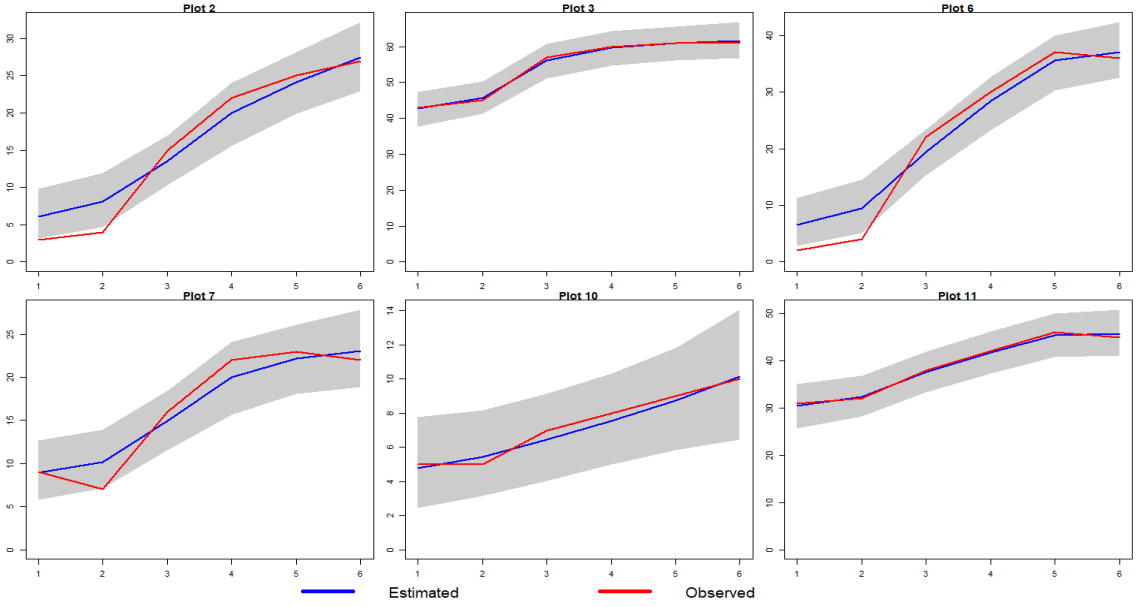

Figure 15: The population of *Elytropappus rhinocerotis* plants in six control plots, in the Renosterveld. The y-axis represents abundance of the population and the x-axis represents the time period. The grey bands represent a 95% credibility interval for the estimations.

Figure 15 shows the observed population of *Elytropappus rhinocerotis* in the Renosterveld as well as the true states estimated by the SSM, in plots designated as control plots. For these plots the estimations of the true state of the population, from the SSMs follow the same general trend as the observed population but show variations due to observation errors according to the model. The observation standard deviation $\sigma_{observation}$, estimated by the model was 2.54, whereas the process standard deviation $\sigma_{process}$, was estimated to be 0.19.

	Plot	1	2	3	4	5
1	2	0.30	0.54	0.39	0.19	0.13
2	3	0.07	0.21	0.06	0.02	0.01
3	6	0.39	0.74	0.38	0.23	0.04
4	7	0.14	0.39	0.29	0.10	0.04
5	10	0.15	0.18	0.16	0.15	0.15
6	11	0.06	0.15	0.11	0.09	0.00

Table 10: The estimates of growth rates, λ, of *Elytropappus rhinocerotis*, in six control plots over six periods.

Table 10 shows the intrinsic growth rates, $\lambda_{i,t}$, (at plot i and time t) of the population of *Elytropappus rhinocerotis* in control plots over the six periods surveyed, estimated by the state-space model.

Referring to Figure 15 and Table 10 it is apparent that in the population of *Elytropappus rhinocerotis* in control plots experience growth throughout all plots and in every time period. The largest growth generally takes place in the second time period, with plot 6 having an estimated growth of $\lambda = 0.74$ (a growth of 109.5%) in this period. It is also apparent that growth in control plots begins to plateau at later time periods (periods five and six), with all control plots experiencing almost no growth in period 6. This is very different to the reseeder species analysed in Sections 5.1.1 and 5.2.1 that experienced mainly negative growth rates, especially at the first period. Referring to Appendix 7.1, it is apparent that the credibility intervals in this model are again relatively wide. The credibility interval, $CI_{0.025}(\lambda)$, $CI_{0.975}(\lambda)$, for plot 6 at the second time period is (0.27, 1.42). This may be due to the influence of the growth of *Elytropappus rhinocerotis* in other control plots. The widest credibility intervals are estimated for the population in plot 10, where the most significantly different growth patterns occur.

Figure 16 shows the observed population of *Elytropappus rhinocerotis* in the Renosterveld as well as the true states estimated by the SSM, in plots designated as treatment plots. Again the SSM estimates of the true state of the population to follow the general trend of the observed population.

Table 11 shows the intrinsic growth rates, $\lambda_{i,t}$, (at plot i and time t) of the population of *Elytropappus rhinocerotis* in treatment plots over the six periods surveyed, estimated by the state-space model.

From Figure 16 and Table 11 it is apparent that, as with control plots there is a constant growth in the population throughout all plots. By comparison with the growth rates recorded in Table 10 it is apparent that most treatment plots (with the

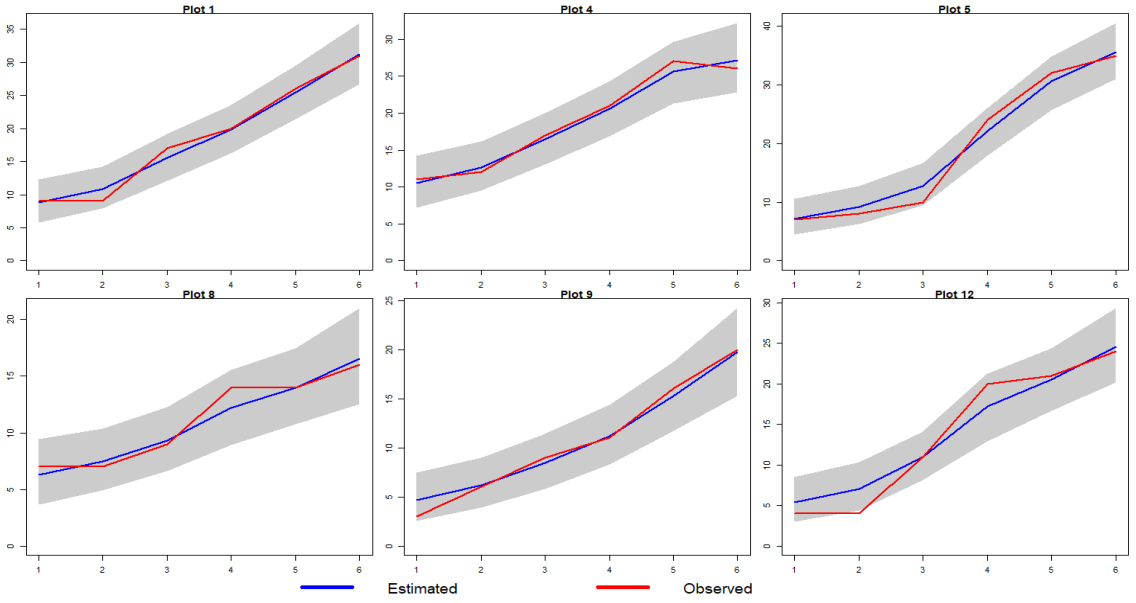

Figure 16: The population of *Elytropappus rhinocerotis* plants in six treatment plots, in the Renosterveld. The y-axis represents abundance of the population and the x-axis represents the time period. The grey bands represent a 95% credibility interval for the estimations.

exception of plot 4) do not experience the same reduction in growth rate at later periods. Unlike the species with reseeder growth forms analysed it seems that there is no apparent major change in growth patterns due to the effects of the experimental treatment.

Table 12 shows that the state-space model estimates the β_1 parameter to be 0.07. $X_{\text{treatment}}$ is a binary variable that is set as 1 if the plot in the model is a treatment plot and 0 otherwise. Therefore there is an increase of 0.07 in the mean of the intrinsic growth rate μ_λ when the plot modeled is a treatment plot.

By using the coefficients in the Equation 4, μ_λ can be calculated as: $\mu_\lambda = 0.19 + 0.07 = 0.26$ for treatment plots and $\mu_\lambda = 0.19 + 0 = 0.19$ for control plots. Thus it can be asserted that in treatment plots on average, every six months there is an increase of the *Elytropappus rhinocerotis* population by 29.69% ($e^{0.26} - 1$), whereas in control plots there is an increase by 20.92%.

There is a small difference in the average growth between treatment and control plots as compared to the difference experienced by species classified as reseeders in Sections 5.1.1 and 5.2.1. Therefore it can be asserted that, while there is a positive effect of the experimental treatment on the population of *Elytropappus rhinocerotis*

	Plot	1	2	3	4	5
1	1	0.21	0.37	0.24	0.25	0.20
2	4	0.19	0.27	0.23	0.22	0.06
3	5	0.25	0.33	0.56	0.32	0.15
4	8	0.18	0.23	0.27	0.14	0.17
5	9	0.31	0.32	0.28	0.31	0.26
6	12	0.29	0.45	0.45	0.18	0.18

Table 11: The estimates of growth rates, λ, of *Elytropappus rhinocerotis*, in six treatment plots over six periods.

	Coefficient	sd	lower(2.5%)	upper(97.5%)
β_0	0.19	0.05	0.10	0.30
β_1	0.07	0.07	-0.08	0.21

Table 12: Table of beta parameters estimated by the SSM.

it is less effective than the effect on reseeders in the same biome.

5.3.2 Interaction with *Thesium strictum*

A state-space model as suggested in Section 3.4 is used to determine the effect of the presence of *Thesium strictum*, a parasite, on the growth of *Elytropappus rhinocerotis* within a plot.

The same prior distributions given in Section 5.1.2 are used in modeling this species.

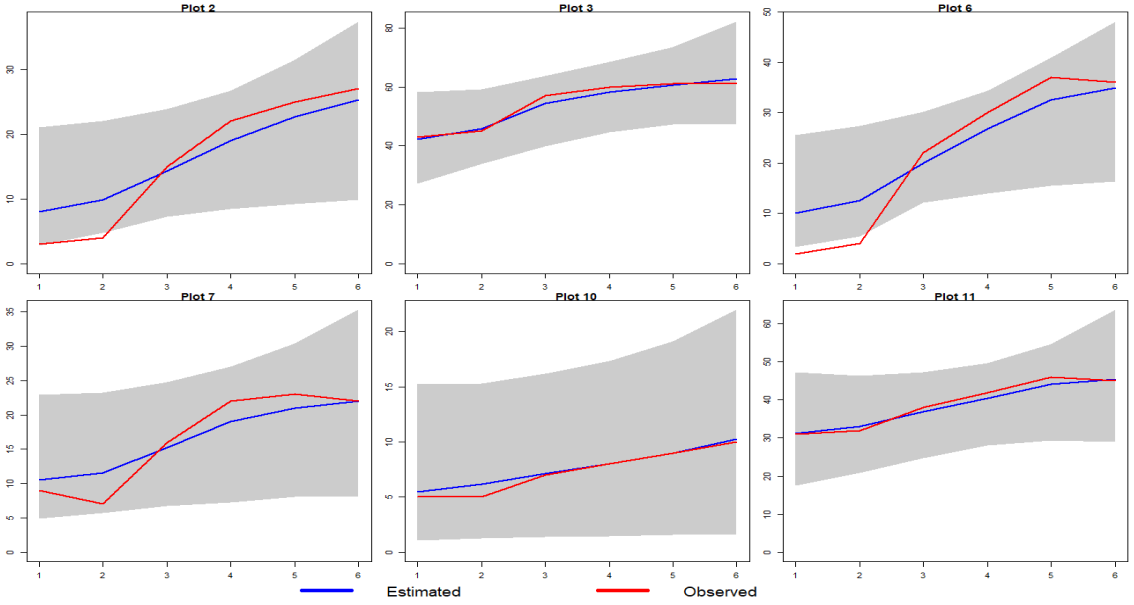

Figure 17: The population of *Elytropappus rhinocerotis* plants in six control plots in the Renosterveld, modeled with the effect of the population density of *Thesium strictum*. The y-axis represents abundance of the population and the x-axis represents the time period. The grey bands represent a 95% credibility interval for the estimations.

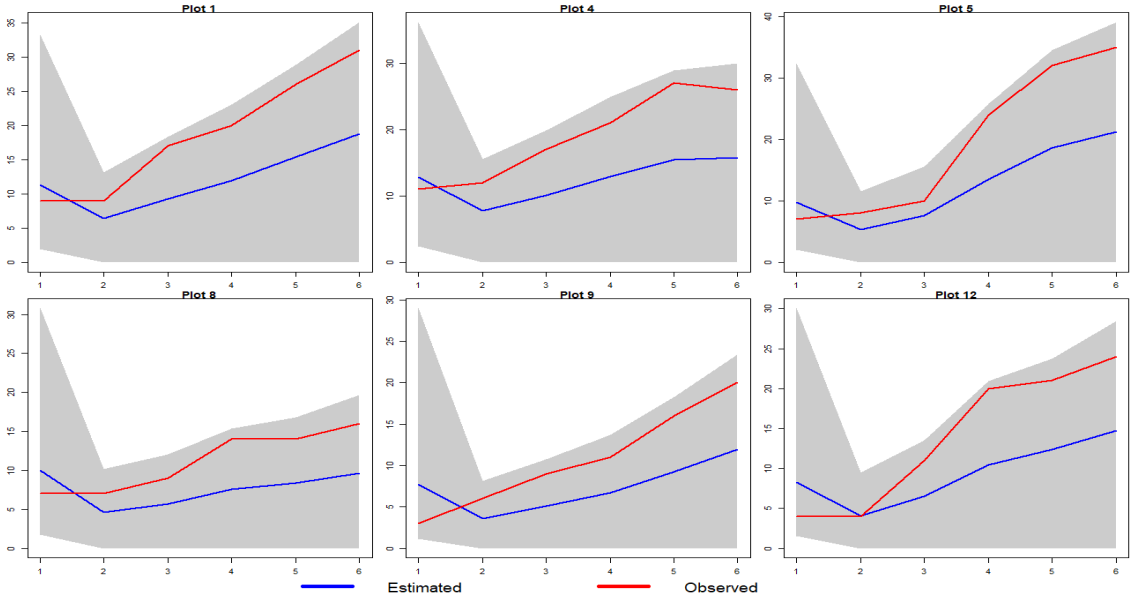

Figure 18: The population of *Elytropappus rhinocerotis* plants in six treatment plots in the Renosterveld, modeled with the effect of the population density of *Thesium strictum*. The y-axis represents abundance of the population and the x-axis represents the time period. The grey bands represent a 95% credibility interval for the estimations.

By comparison of Figures, 17 and 18 with Figures 15 and 16 it is apparent that adding complexity to the model has negatively affected the precision of the model. With more data points, the effect of this may be reduced. The observation standard deviation $\sigma_{observation}$, estimated by the model was 7.26, whereas the process standard deviation $\sigma_{process}$, was estimated to be 0.16.

	mean	sd	2.5%	97.5%
β_0	0.20	0.15	-0.09	0.51
β_1	-0.00	0.85	-1.78	1.94
β_2	-0.01	0.01	-0.04	0.01
β_3	-0.80	0.85	-2.13	0.03

Table 13: Table of beta parameters estimated by the SSM.

Table 13 shows the coefficient of interaction (β_3) has a strong, negative effect on the mean of the intrinsic growth rate of *Elytropappus rhinocerotis* and β_2 has a weak negative effect. From the credible interval it is apparent that the results are somewhat uncertain, as at the 97.5% level the effect is positive. It can therefore be asserted, with some uncertainty, that the presence parasitic plant has a negative effect on the population of *Elytropappus rhinocerotis* under experimental and controlled (normal) conditions. There is a far more significant negative impact on the mean growth rate under experimental conditions.

5.4 *Passerina obtusifolia*

Passerina obtusifolia is a species of perennial woody shrub, with a growth form classified as a resprouter. *Passerina obtusifolia* is present mainly in the Renosterveld site and the population will be modeled in this site only.

5.4.1 Normal Dynamic Linear Models

The population of *Passerina obtusifolia* in the experiment plots over the six time periods of recording are modeled using the normal dynamic linear models described in Section 3.3

The same prior distributions given in Section 5.1.1 are used in modeling this species.

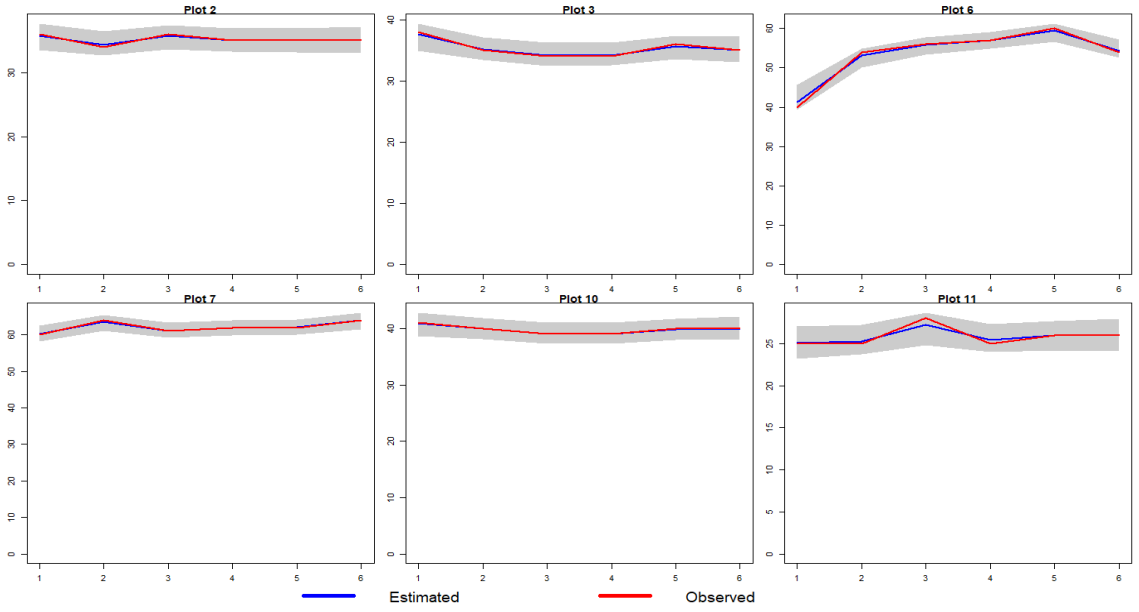

Figure 19: The population of *Passerina obtusifolia* plants in six control plots, in the Renosterveld. The y-axis represents abundance of the population and the x-axis represents the time period. The grey bands represent a 95% credibility interval for the estimations.

Figure 19 shows the observed population of *Passerina obtusifolia* in the Renosterveld as well as the true states estimated by the SSM, in plots designated as control plots. For these plots the estimates of the true state of the population, from the SSMs follow are very close to the the observed population but show small variations due to observation errors according to the model. The observation standard deviation $\sigma_{observation}$, estimated by the model was 0.92, whereas the process standard deviation $\sigma_{process}$, was estimated to be 0.076.

	Plot	1	2	3	4	5
1	2	-0.04	0.04	-0.02	-0.00	0.00
2	3	-0.07	-0.03	0.00	0.04	-0.02
3	6	0.26	0.05	0.02	0.04	-0.09
4	7	0.06	-0.04	0.01	0.00	0.03
5	10	-0.02	-0.02	-0.00	0.02	0.00
6	11	0.01	0.07	-0.07	0.02	0.00

Table 14: The estimates of growth rates, λ, of *Passerina obtusifolia* in six control plots, over six periods.

Table 14 shows the intrinsic growth rates, $\lambda_{i,t}$, (at plot i and time t) of the population of *Passerina obtusifolia* in control plots over the six periods surveyed, estimated by the state-space model.

Referring to Figure 19 and Table 14 it is apparent that in the population of *Passerina obtusifolia* in control plots experience almost no growth or decline throughout all plots and in every time period. There is no real significant period of growth, but plot 6 experiences the most growth relative to other plots. In the first period plot 6 experiences an estimated growth of a growth of 29.6% ($e^{0.26} - 1$). It is also the only plot to experience a negative growth rate in the last period. This is different from the control plots of the other resprouter in the Renosterveld *Elytropappus rhinocerotis*, which experienced constant growth.

Referring to the credibility intervals of the growth rates (Appendix 7.1), it is apparent that the credibility intervals are relatively small, as compared to other species models. It is noted that similar growth patterns occur in all plots, unlike other species that showed larger credibility intervals for growth rates.

Figure 20 shows the observed population of *Passerina obtusifolia* in the Renosterveld as well as the true states estimated by the SSM, in plots designated as treatment plots. The SSM estimates of the true state of the population to follow the general trend of the observed population and estimates it closely.

Table 14 shows the intrinsic growth rates, $\lambda_{i,t}$, (at plot i and time t) of the population of *Passerina obtusifolia* in treatment plots over the six periods surveyed, estimated by the state-space model.

From Figure 16 and Table 15 it is apparent that there is an initial period of growth in the population within treatment plots. However, after the first period the growth rates significantly reduce and population growth begin to plateau. This is again different from the population growth of *Elytropappus rhinocerotis*, which shows regular growth within treatment plots.

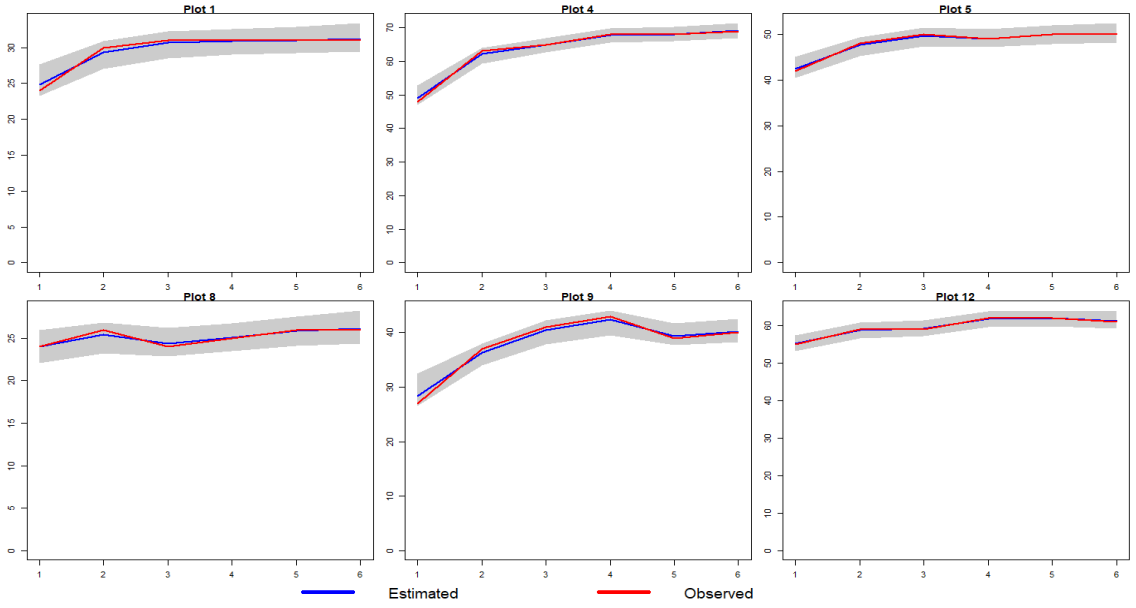

Figure 20: The population of *Passerina obtusifolia* plants in six treatment plots, in the Renosterveld. The y-axis represents abundance of the population and the x-axis represents the time period. The grey bands represent a 95% credibility interval for the estimations.

Table 16 shows that the state-space model estimates the β_1 parameter to be 0.03. $X_{\text{treatment}}$ is a binary variable that is set as 1 if the plot in the model is a treatment plot and 0 otherwise. Therefore there is an increase of 0.03 in the mean of the intrinsic growth rate μ_λ when the plot modeled is a treatment plot.

By using the coeffecients in the Equation 4, μ_λ can be calculated as: $\mu_\lambda = 0.01 + 0.03 = 0.4$ for treatment plots and $\mu_\lambda = 0.01 + 0 = 0.01$ for control plots. Thus it can be asserted that in treatment plots on average, every six months there is an increase of the *Passerina obtusifolia* population by 4.08% ($e^{0.04} - 1$), whereas in control plots there is an increase by 1%($e^{0.01} - 1$). This shows that although the growth rate is very small anyway there is a slight increase in the average growth rate as a result of the experimental treatment. Refering back to plot 20 and Table 15 it is apparent that the average is influenced heavily by the initial growth period as there is little growth in treatment plots afterward

Like with the analysis for the population of *Elytropappus rhinocerotis* (5.3.1), there is a small difference in the average growth between treatment and control plots as compared to the difference experienced by species classified as reseeders. Therefore it can be asserted that, while there is a small positive effect of the experimental treatment on the population of *Passerina obtusifolia* it is less effective than the

	Plot	1	2	3	4	5
1	1	0.17	0.04	0.01	0.00	0.01
2	4	0.24	0.04	0.04	0.00	0.02
3	5	0.12	0.04	-0.01	0.02	0.00
4	8	0.06	-0.04	0.03	0.03	0.01
5	9	0.25	0.11	0.04	-0.07	0.02
6	12	0.06	0.01	0.05	0.00	-0.01

Table 15: The estimates of growth rates, λ, of *Passerina obtusifolia* in six treatment plots over six periods.

	Coeffecient	sd	lower(2.5%)	upper(97.5%)
β_0	0.01	0.02	-0.02	0.04
β_1	0.03	0.02	-0.01	0.08

Table 16: Table of beta parameters estimated by the SSM.

effect on reseeders in the same Biome.

5.4.2 Interaction with *Thesium strictum*

A state-space model as suggested in Section 3.4 is used to determine the effect of the presence of *Thesium strictum*, a parasite, on the growth of *Passerina obtusifolia* within a plot. The same prior distributions given in Section 5.1.2 are used in modeling this species. The observation standard deviation $\sigma_{observation}$, estimated by the model was 1.5, whereas the process standard deviation $\sigma_{process}$, was estimated to be 0.076.

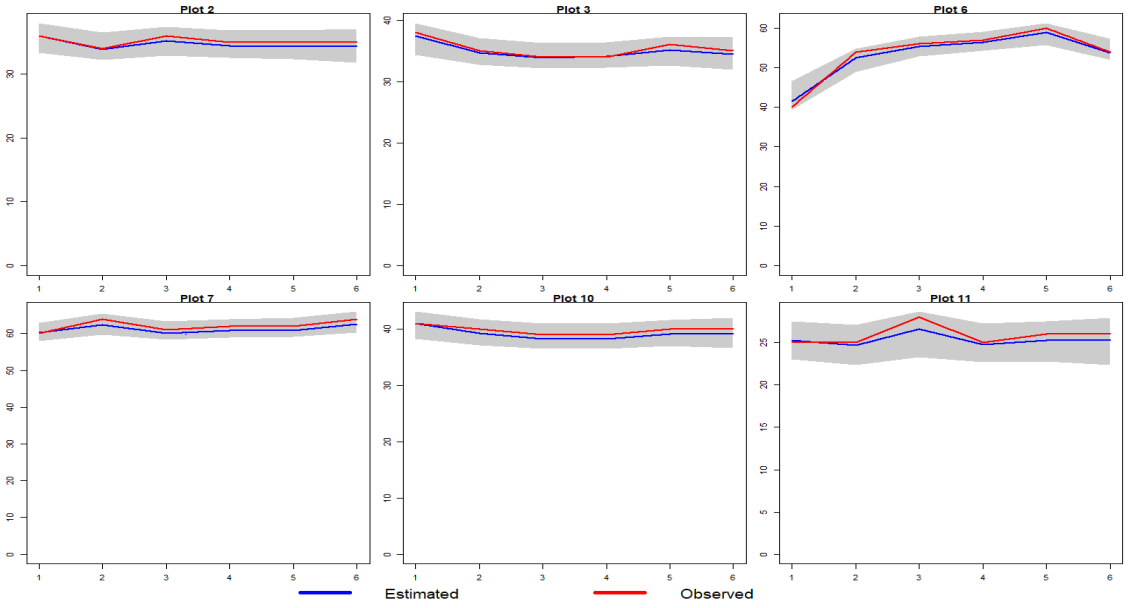

Figure 21: The population of *Passerina obtusifolia* plants, in six control plots, in the Renosterveld, modeled with the effect of the population density of *Thesium strictum*. The y-axis represents abundance of the population and the x-axis represents the time period.

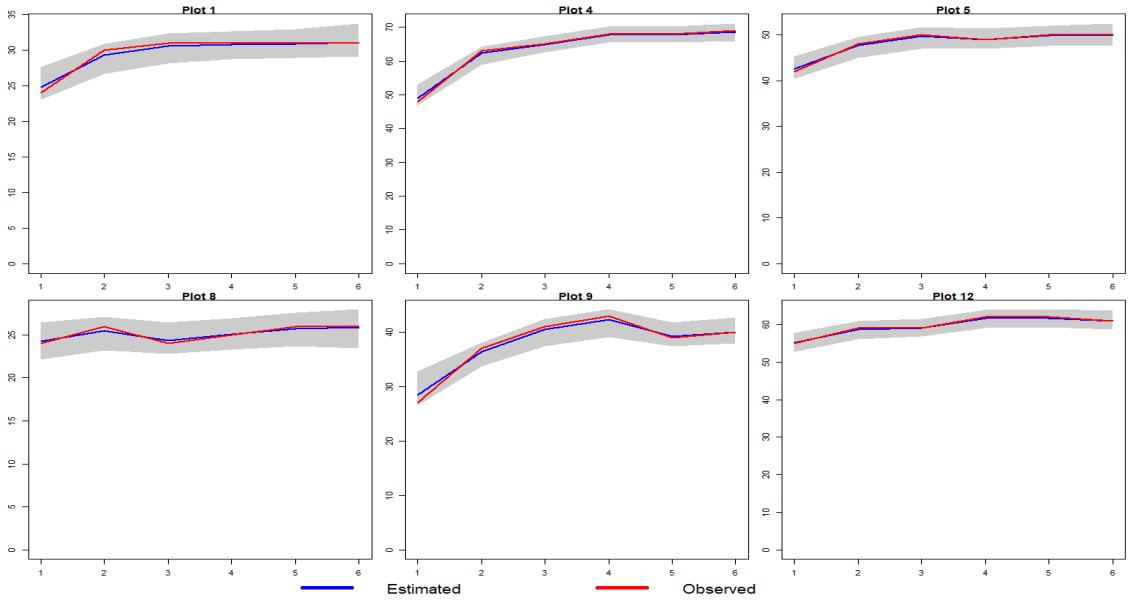

Figure 22: The population of *Passerina obtusifolia* plants, in six treatment plots in the Renosterveld, modeled with the effect of the population density of *Thesium strictum*. The y-axis represents abundance of the population and the x-axis represents the time period.

By comparison of Figures, 21 and 22 with Figures 19 and 20 it is apparent that adding complexity to the model has a slight negative effected on the precision of the model, although the model is still precise, there is a notable difference in the range of the credibility intervals of estimations. With more data points, the effect of this may be reduced (Warton et al., 2015b).

	mean	sd	2.5%	97.5%
β_0	0.00	0.11	-0.26	0.19
β_1	0.01	0.49	-1.53	0.89
β_2	0.00	0.02	-0.06	0.01
β_3	-0.47	0.94	-2.56	0.00

Table 17: Table of beta parameters estimated by the SSM.

Table 17 shows that the estimate for β_2 is zero and β_3 is -0.47. This indicates that the presence of $Thesium\,strictum$ has no effect on the mean of the intrinsic growth rate of $Passerina\,obtusifolia$ in control plots and a strong negative effect in treatment plots.

5.5 *Selago glabrata*

Selago glabrata is a species of perennial woody shrub, with a growth form classified as a reseeder. *Selago glabrata* is present mainly in the Fynbos site and the population will be modeled in this site only.

5.5.1 Normal Dynamic Linear Models

The population of *Selago glabrata* in the experiment plots over the six time periods of recording are modeled using the normal dynamic linear models described in Section 3.3

The same prior distributions given in Section 5.1.1 are used in modeling this species.

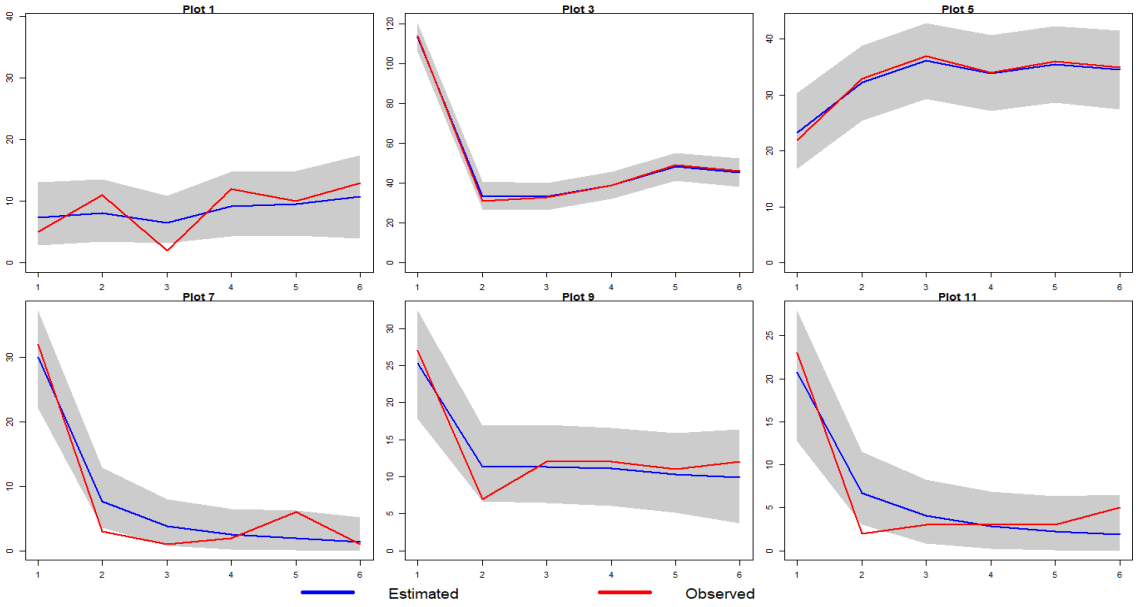

Figure 23: The population of *Selago glabrata* plants in six control plots, in the Fynbos. The y-axis represents abundance of the population and the x-axis represents the time period. The grey bands represent a 95% credibility interval for the estimations.

Figure 23 shows the observed population of *Selago glabrata* in the Fybnos site as well as the true states estimated by the SSM, in plots designated as control plots. For these plots the estimates of the true state of the population, from the SSMs follow the general trend of the observed population but show variations due to observation errors according to the model. The observation standard deviation $\sigma_{observation}$, estimated by the model was 3.56, whereas the process standard deviation $\sigma_{process}$, was estimated to be 0.44.

	Plot	1	2	3	4	5
1	1	0.10	-0.20	0.35	0.04	0.11
2	3	-1.23	-0.01	0.16	0.22	-0.06
3	5	0.33	0.12	-0.07	0.05	-0.03
4	7	-1.41	-0.79	-0.57	-0.50	-0.60
5	9	-0.82	0.00	-0.03	-0.08	-0.06
6	11	-1.16	-0.59	-0.47	-0.43	-0.41

Table 18: The estimates of growth rates, λ, of *Selago glabrata* in six control plots over six periods.

Table 18 shows the intrinsic growth rates, $\lambda_{i,t}$, (at plot i and time t) of the population of *Selago glabrata* in control plots over the six periods surveyed, estimated by the state-space model.

Referring to Figure 23 and Table 18 it is apparent that the population of *Selago glabrata* does not follow the same growth pattern in all control plots. Plots 1 and 5 in particular show grwoth patterns that deviate from other plots, most notably in the first time period, where they show growth rather than the sharp decline estimated in plots 3, 7, 9 and 11. Plot 5 shows the largest increase in population growth during the first period recording a growth of 39.01% ($e^{0.33} - 1$). The largest decline in population occurs in plot 7, recording a decline by 75.58% in the first period and a decline of 54.61% in the second period. In general the growth patterns of the population of *Selago glabrata* in control plots are similar to those of the other reseeders modeled in the Renosterveld plots, *Microdon polygaloides* (Section 5.1.1) and *Othonna parviflora* (Section 5.2.1).

Apendix 7.1, shows the credibility intervals for the estimates of the growth rates, λ. For example, the credibility interval, ($CI_{0.025}(\lambda)$, $CI_{0.975}(\lambda)$), for plot 5 at the first period is (-0.02, 0.68). This may be explained by the different growth patterns that occur in each plot, making the model less certain.

Figure 24 shows the observed population of *Selago glabrata* in the Fynbos site as well as the true states estimated by the SSM, in plots designated as treatment plots. The SSM estimates of the true state of the population to follow the general trend of the observed population but show variations from the observed data due to the observation errors modeled.

Table 19 shows the intrinsic growth rates, $\lambda_{i,t}$, (at plot i and time t) of the population of *Selago glabrata* in treatment plots over the six periods surveyed, estimated by the state-space model.

From Figure 24 and Table 19 it is apparent that, in all plots except plots 8 and 12

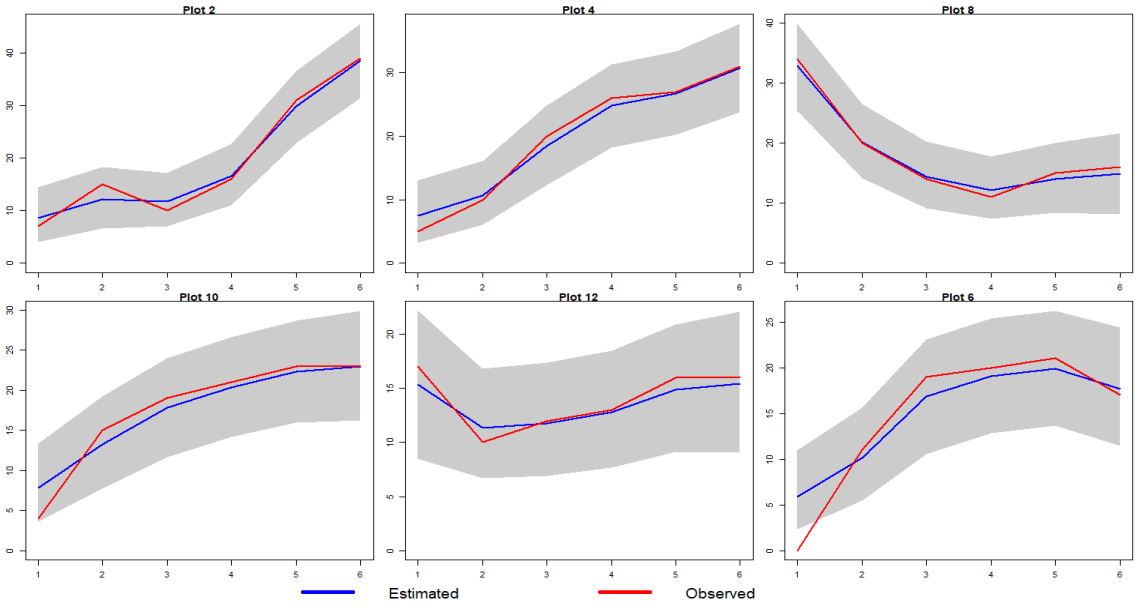

Figure 24: The population of *Selago glabrata* plants in six treatment plots in the Fynbos. The y-axis represents abundance of the population and the x-axis represents the time period. The grey bands represent a 95% credibility interval for the estimations.

there is an initial period of growth in the population within treatment plots. The population in plot 12 experiences an initial decline (by 25.9%) in the first period but experiences small but steady growth subsequently. The population in plot 8 is in decline until the fourth period, after which it experiences steady growth. These are the only plots that experiences similar growth to that of the reseeders in treatment plots at the Renosterveld site.

Table 16 shows that the state-space model estimates the β_1 parameter to be 0.42. $X_{\text{treatment}}$ is a binary variable that is set as 1 if the plot in the model is a treatment plot and 0 otherwise. Therefore there is an increase of 0.42 in the mean of the intrinsic growth rate μ_λ when the plot modeled is a treatment plot.

By using the coefficients in the Equation 4, μ_λ can be calculated as: $\mu_\lambda = -0.27 + 0.42 = 0.15$ for treatment plots and $\mu_\lambda = -0.27 + 0 = -0.27$ for control plots. Thus it can be asserted that in treatment plots on average, every six months there is an increase of the *Selago glabrata* population by 16.18% ($e^{0.15} - 1$), whereas in control plots there is a decrease by 23.6% ($1 - e^{-0.27}$). This shows that that there is a significant shift in growth patterns of *Selago glabrata* as a result of the experimental treatment.

	Plot	1	2	3	4	5
1	2	0.36	-0.04	0.36	0.60	0.26
2	4	0.38	0.57	0.30	0.08	0.14
3	8	-0.50	-0.34	-0.17	0.14	0.06
4	10	0.55	0.30	0.14	0.09	0.03
5	12	-0.30	0.04	0.09	0.15	0.04
6	6	0.58	0.52	0.13	0.04	-0.13

Table 19: The estimates of growth rates, λ, of *Selago glabrata* in six treatment plots, over 6 periods.

	mean	sd	2.5%	97.5%
β_0	-0.27	0.18	-0.69	0.02
β_1	0.42	0.23	0.02	0.95

Table 20: Table of beta parameters estimated by the SSM.

The effects of the experimental treatment are similar to the effect experienced by reseeders in the Renosterveld sites, however the effects of the treatment are much more profound on the population of *Selago glabrata* than that of *Microdon polygaloides* (Section 5.1.1) and *Othonna parviflora* (Section 5.2.1).

5.6 *Aspalathus shawii*

Aspalathus shawii is a species of perennial woody shrub, with a growth form classified as a reseeder. *Aspalathus shawii* is present mainly in the Fynbos site and the population will be modeled in this site only.

5.6.1 Normal Dynamic Linear Models

The population of *Aspalathus shawii* in the experiment plots over the six time periods of recording are modeled using the normal dynamic linear models described in Section 3.3

The same prior distributions and initial values in the Gibbs sampler, given in Section 5.5.1 are used in modeling this species.

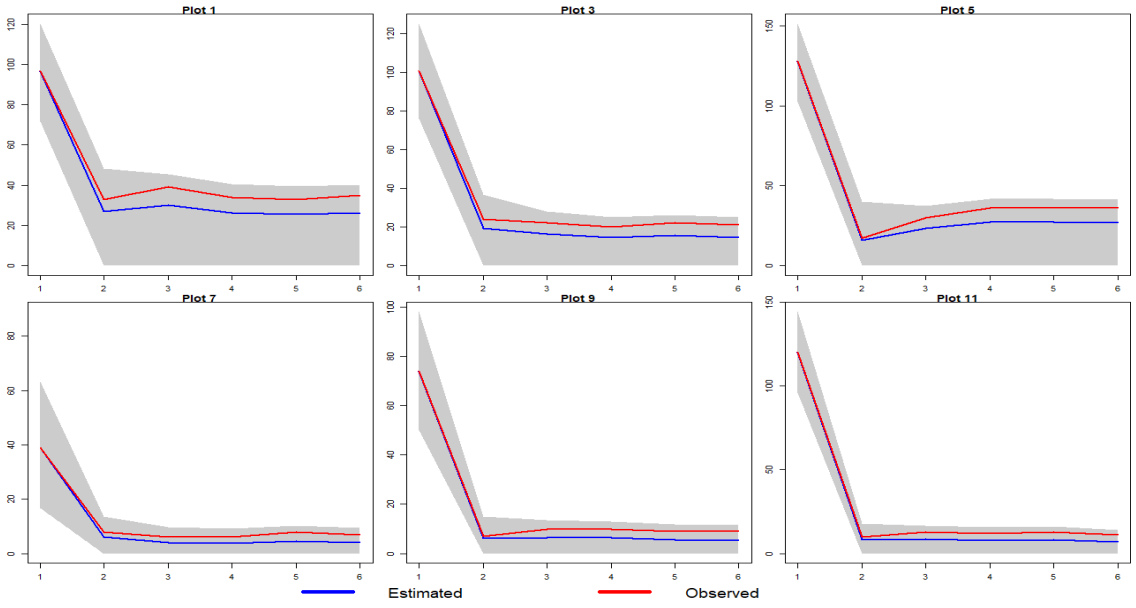

Figure 25: The population of *Aspalathus shawii* plants in six control plots in the Fynbos. The y-axis represents abundance of the population and the x-axis represents the time period. The grey bands represent a 95% credibility interval for the estimations.

Figure 25 shows the observed population of *Aspalathus shawii* in the Fybnos site as well as the true states estimated by the SSM, in plots designated as control plots. For these plots the estimations of the true state of the population, from the SSMs follow the general trend of the observed population but shows slight variations due to observation errors according to the model. The observation standard deviation

$\sigma_{observation}$, estimated by the model was 6.92, whereas the process standard deviation $\sigma_{process}$, was estimated to be 0.61.

	Plot	1	2	3	4	5
1	1	-5.31	-4.41	-4.61	-4.53	-4.48
2	3	-5.75	-4.82	-4.80	-4.68	-4.78
3	5	-5.99	-4.22	-4.40	-4.54	-4.55
4	7	-8.05	-7.31	-7.10	-6.96	-7.18
5	9	-8.37	-6.89	-6.95	-7.02	-6.99
6	11	-9.24	-7.62	-7.72	-7.64	-7.80

Table 21: The estimates of growth rates, λ, of *Aspalathus shawii* in six control plots, over 6 periods.

Table 21 shows the intrinsic growth rates, $\lambda_{i,t}$, (at plot i and time t) of the population of *Aspalathus shawii* in control plots over the six periods surveyed, estimated by the state-space model.

Referring to Figure 25 and Table 21 it is apparent that the population of *Aspalathus shawii* experiences declining population sizes in all control plots, at all time periods but particularly during the first time period. Plot 11 experiences the largest decline in population after the first time period, estimated to be by 99% ($1 - e^{-9.24}$). These results are very similar to those of reseeders in the Renosterveld site, particularly *Othonna parviflora* (Section 5.2.1).

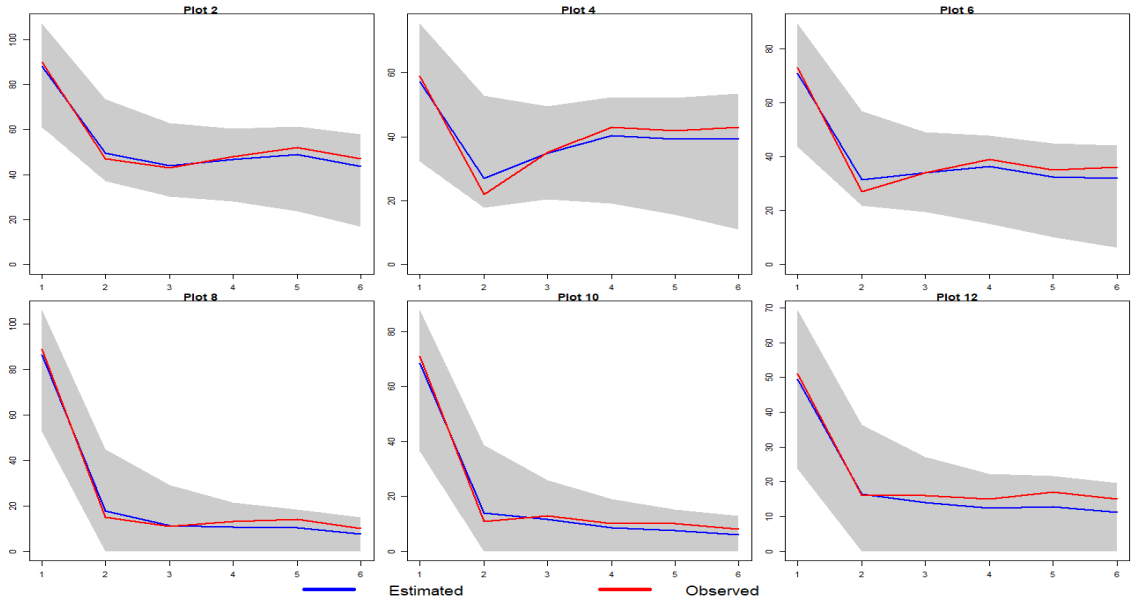

Figure 26: The population of *Aspalathus shawii* plants, in six treatment plots, in the Fynbos. The y-axis represents abundance of the population and the x-axis represents the time period. The grey bands represent a 95% credibility interval for the estimations.

Figure 26 shows the observed population of *Aspalathus shawii* in the Fynbos site as well as the true states estimated by the SSM, in plots designated as treatment plots. The SSM estimates of the true state of the population to follow the general trend of the observed population but show variations from the observed data due to the observation errors modeled.

	Plot	1	2	3	4	5
1	2	-0.58	-0.12	0.06	0.03	-0.12
2	4	-0.78	0.28	0.14	-0.04	-0.02
3	6	-0.83	0.09	0.06	-0.13	-0.05
4	8	-2.27	-1.28	-0.95	-1.00	-1.26
5	10	-3.57	-2.33	-2.51	-2.37	-2.50
6	12	-4.88	-4.13	-4.14	-4.02	-4.18

Table 22: The estimates of growth rates, λ, of *Aspalathus shawii* in six treatment plots, over 6 periods.

Table 22 shows the intrinsic growth rates, $\lambda_{i,t}$, (at plot i and time t) of the population of *Aspalathus shawii* in treatment plots over the six periods surveyed, estimated by the state-space model.

From Figure 26 and Table 22 it is apparent that, in all plots the population of *Aspalathus shawii* experiences a sharp decline after the initial period, however unlike the control plots there is some recovery in the population in some plots (plots 2, 4 and 6) after the initial period. These results are similar to the analysis of reseeders in treatment plots in the Renosterveld site.

	mean	sd	2.5%	97.5%
β_0	-6.04	10.08	-33.07	-0.08
β_1	4.58	10.15	-6.88	32.55

Table 23: Table of beta parameters estimated by the SSM.

Table 23 shows that the state-space model estimates the β_1 parameter to be 4.58. $X_{\text{treatment}}$ is a binary variable that is set as 1 if the plot in the model is a treatment plot and 0 otherwise. Therefore there is an increase of 4.58 in the mean of the intrinsic growth rate μ_λ when the plot modeled is a treatment plot.

By using the coefficients in the Equation 4, μ_λ can be calculated as: $\mu_\lambda = -6.04 + 4.58 = -1.46$ for treatment plots and $\mu_\lambda = -6.04 + 0 = -6.04$ for control plots. Thus it can be asserted that in treatment plots on average, every six months there is a decrease of the *Selago glabrata* population by 76.78% $(1 - e^{-1.46})$, whereas in control plots there is a decrease by 99.7% $(1 - e^{-6.04})$. This shows that there is a reduction of the declining growth in the population of *Aspalathus shawii* as a result of the experimental treatment.

The effects of the experimental treatment are similar to the effect experienced by reseeders in the Renosterveld sites.

5.7 *Wahlenbergia nodosa*

Wahlenbergia nodosa is a species of perennial woody shrub, with a growth form classified as a resprouter. *Wahlenbergia nodosa* is present mainly in the Fynbos site and the population will be modeled in this site only.

5.7.1 Normal Dynamic Linear Models

The population of *Wahlenbergia nodosa* in the experiment plots over the six time periods of recording are modeled using the normal dynamic linear models described in Section 3.3

The same prior distributions and initial values in the Gibbs sampler, given in Section 5.5.1 are used in modeling this species.

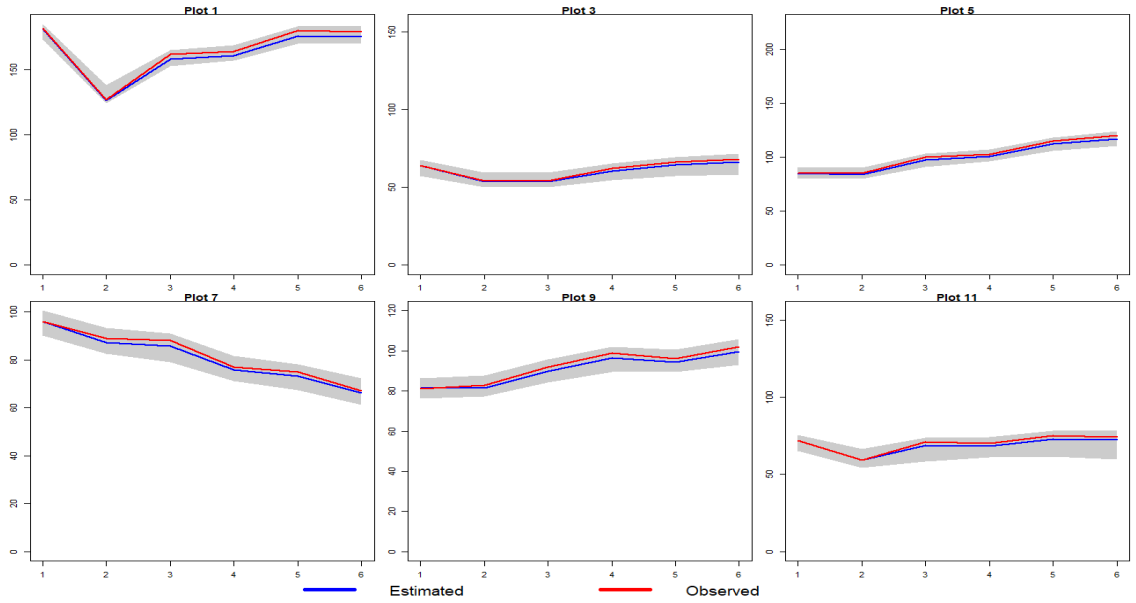

Figure 27: The population of *Wahlenbergia nodosa* plants, in six control plots in the Fynbos. The y-axis represents abundance of the population and the x-axis represents the time period. The grey bands represent a 95% credibility interval for the estimations.

Figure 27 shows the observed population of *Wahlenbergia nodosa* in the Fybnos site as well as the true states estimated by the SSM, in plots designated as control plots. For these plots the estimations of the true state of the population, from the SSMs are very close to the observed population and shows very slight variations due to observation errors according to the model. The observation standard deviation $\sigma_{observation}$, estimated by the model was 1.54, whereas the process standard deviation

$\sigma_{process}$, was estimated to be 0.1. This is reflected by the estimations being relatively close to the observations and the credibility intervals being relatively narrow.

	Plot	1	2	3	4	5
1	1	-0.34	0.23	0.02	0.09	-0.00
2	3	-0.14	-0.00	0.12	0.06	0.03
3	5	0.01	0.15	0.04	0.11	0.04
4	7	-0.07	-0.02	-0.13	-0.03	-0.10
5	9	0.03	0.10	0.07	-0.02	0.06
6	11	-0.16	0.15	-0.00	0.06	-0.01

Table 24: The estimates of growth rates, λ, of *Wahlenbergia nodosa* in six control plots, over six periods.

Table 24 shows the intrinsic growth rates, $\lambda_{i,t}$, (at plot i and time t) of the population of *Wahlenbergia nodosa* in control plots over the six periods surveyed, estimated by the state-space model.

Referring to Figure 27 and Table 24 it is apparent that the population of *Wahlenbergia nodosa* experiences growth during most time periods in every plot with the exception of plot 7 where the population experiences a constant decline. Plots 1, 3 and 11 also experience an decline in population after the first period (by 28.88%, 13.06% and 14.7% respectively), but these declines are offset by growth in the subsequent period (for example, in the following period the population in plot one experiences growth by 25.8%). These growth patterns are similar to those of the population of *Elytropappus rhinocerotis*, a resprouter found in the Renosterveld (Section 5.3.1), particularly in control plots. From Appendix 7.1, it is apparent that the model predicts much smaller credibility intervals as compared to other species models.

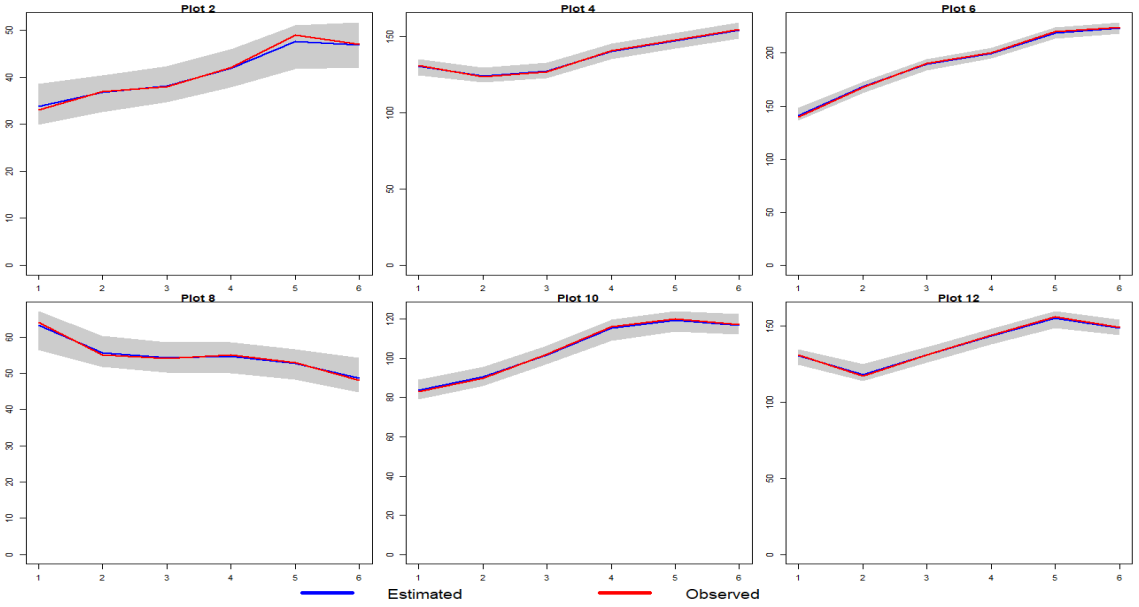

Figure 28: The population of *Wahlenbergia nodosa* plants, in six treatment plots in the Fynbos. The y-axis represents abundance of the population and the x-axis represents the time period. The grey bands represent a 95% credibility interval for the estimations.

Figure 28 shows the observed population of *Wahlenbergia nodosa* in the Fynbos site as well as the true states estimated by the SSM, in plots designated as treatment plots. The SSM estimates of the true state of the population to be very close to that of the observed population but show slight variations from the observed data due to the observation errors modeled.

	Plot	1	2	3	4	5
1	2	0.09	0.04	0.10	0.13	-0.02
2	4	-0.05	0.02	0.10	0.05	0.05
3	6	0.18	0.12	0.05	0.09	0.02
4	8	-0.13	-0.02	0.01	-0.04	-0.08
5	10	0.08	0.12	0.13	0.03	-0.02
6	12	-0.10	0.11	0.09	0.08	-0.04

Table 25: The estimates of growth rates, λ, of *Wahlenbergia nodosa* in six treatment plots, over six periods.

Table 25 shows the intrinsic growth rates, $\lambda_{i,t}$, (at plot i and time t) of the population of *Wahlenbergia nodosa* in treatment plots over the six periods surveyed, estimated by the state-space model.

From Figure 26 and Table 22 it is apparent that, the population in three of the plots (4, 8 and 12) experience a decline in the first period (4.8%, 12.2% and 9.5% respectively), but to a smaller extent to that of the decline experienced in control plots. After the first period the population in nearly all plots with the exception of plot 8 experience mostly growth periods. These results are similar to the analysis of resprouters in treatment plots in the Renosterveld site. It is apparent that the credibility intervals in plots 2 and 8 are broader than that of other plots modeled. This may be attributed to growth in these plots most significantly differing from growth in other plots.

	mean	sd	2.5%	97.5%
β_0	0.01	0.02	-0.02	0.04
β_1	0.02	0.02	-0.02	0.06

Table 26: Table of beta parameters estimated by the SSM.

Table 26 shows that the state-space model estimates the β_1 parameter to be 0.02. $X_{\text{treatment}}$ is a binary variable that is set as 1 if the plot in the model is a treatment plot and 0 otherwise. Therefore there is an increase of 0.02 in the mean of the intrinsic growth rate μ_λ when the plot modeled is a treatment plot.

By using the coeffecients in the Equation 4, μ_λ can be calculated as: $\mu_\lambda = 0.01 + 0.02 = 0.03$ for treatment plots and $\mu_\lambda = 0.01 + 0 = 0.01$ for control plots. Thus it can be asserted that in treatment plots on average, every six months there is an increase of the *Wahlenbergia nodosa* population by 3.04% ($e^{0.03} - 1$), whereas in control plots there is an increase by 1% ($e^{0.01} - 1$). This shows that the experimental treatment has a positive effect on the growth of the population of *Wahlenbergia nodosa*.

The effects of the experimental treatment are similar to the effect experienced by resprouters in the Renosterveld sites.

5.8 *Agathosma capensis*

Agathosma capensis is a species of perennial woody shrub, with a growth form classified as a resprouter. *Agathosma capensis* is present mainly in the Fynbos site and the population will be modeled in this site only.

5.8.1 Normal Dynamic Linear Models

The population of *Agathosma capensis* in the experiment plots over the six time periods of recording are modeled using the normal dynamic linear models described in Section 3.3

The parameters and hyperparameters are given the following prior distributions:

1. $N_{i,0} \sim U(0, 10000)$
2. $\beta_0 \sim N(0, 1000)$
3. $\beta_1 \sim N(0, 1000)$
4. $\sigma^2_{\text{process}} \sim U(0, 5000)$
5. $\sigma^2_{\text{plot}} \sim U(0, 5000)$
6. $\sigma^2_{\text{observation}} \sim U(0, 5000)$

For this model the prior distribution are changed as a larger range for the priors of the variances are required for the parameters of the model to converge.

Figure 27 shows the observed population of *Agathosma capensis* in the Fybnos site as well as the true states estimated by the SSM, in plots designated as control plots. For these plots the estimations of the true state of the population, from the SSMs are very close to the observed population and shows slight variations due to observation errors according to the model. The observation standard deviation $\sigma_{observation}$, estimated by the model was 1.58, whereas the process standard deviation $\sigma_{process}$, was estimated to be 0.09.

Table 27 shows the intrinsic growth rates, $\lambda_{i,t}$, (at plot i and time t) of the population of *Agathosma capensis* in control plots over the six periods surveyed, estimated by the state-space model.

Referring to Figure 29 and Table 27 it is apparent that the population of *Agathosma capensis* remains almost constant within control plots, with the exception of plot 5 which experiences growth throughout the all periods. The highest period of growth of the population in plot 5 is recorded after the first period, recording a growth in population by 24.6% ($e^{0.22} - 1$). The largest credibility intervals estimated in the model

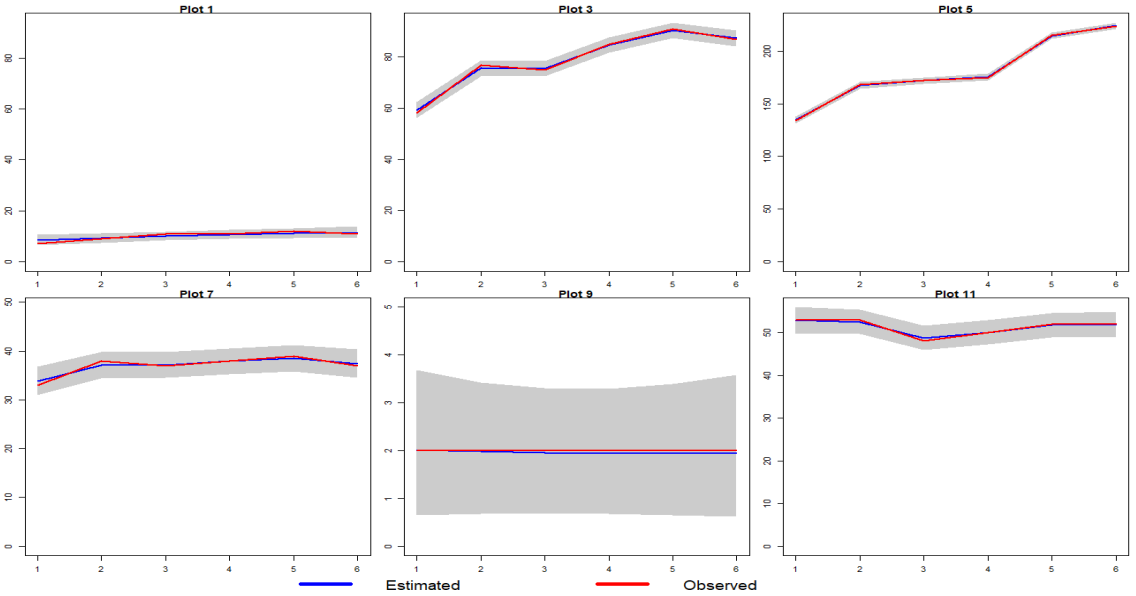

Figure 29: The population of *Agathosma capensis* plants, in six control plots, in the Fynbos. The y-axis represents abundance of the population and the x-axis represents the time period. The grey bands represent a 95% credibility interval for the estimations.

occur at plot 9 where there is no growth throughout the experimental period and a very small population.

	Plot	1	2	3	4	5
1	1	0.08	0.09	0.06	0.05	0.02
2	3	0.25	-0.00	0.12	0.07	-0.04
3	5	0.22	0.03	0.02	0.20	0.04
4	7	0.09	0.00	0.02	0.02	-0.03
5	9	-0.01	-0.01	-0.01	-0.01	-0.00
6	11	-0.01	-0.08	0.03	0.03	0.00

Table 27: The estimates of growth rates, λ, of *Agathosma capensis* in six control plots, over six periods.

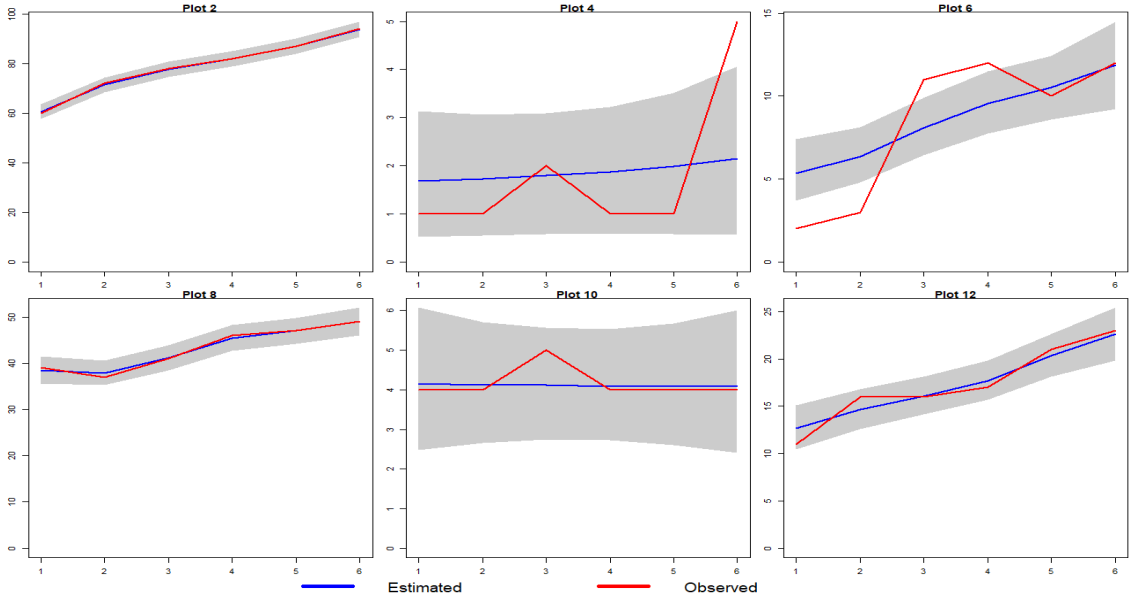

Figure 30: The population of *Agathosma capensis* plants, in six treatment plots, in the Fynbos. The y-axis represents abundance of the population and the x-axis represents the time period. The grey bands represent a 95% credibility interval for the estimations.

Figure 30 shows the observed population of *Agathosma capensis* in the Fynbos site as well as the true states estimated by the SSM, in plots designated as treatment plots. The estimations of the true state of the population, from the SSMs, are close to the observed population within plots 2 and 8 and follow the general trend of the population in plot 12. The model does not seem to follow the observations in plots 4, 6 and 10 instead estimating a very general trend. This is probably due to the very small numbers of observations recorded in this plot as opposed to other plots within the site, causing a small disparity in the population to be have a very large

growth rate.

	Plot	1	2	3	4	5
1	2	0.17	0.08	0.05	0.06	0.08
2	4	0.04	0.04	0.04	0.05	0.06
3	6	0.17	0.25	0.17	0.09	0.12
4	8	-0.02	0.08	0.10	0.03	0.04
5	10	-0.00	0.00	-0.01	-0.00	-0.00
6	12	0.15	0.09	0.10	0.14	0.11

Table 28: The estimates of growth rates, λ, of *Agathosma capensis* in six treatment plots, over six periods.

Table 28 shows the intrinsic growth rates, $\lambda_{i,t}$, (at plot i and time t) of the population of *Agathosma capensis* in treatment plots over the six periods surveyed, estimated by the state-space model.

From Figure 26 and Table 22 it is apparent that, the population of *Agathosma capensis* within plots 2, 6,8 and 12 shows significant growth through every period, whereas plots 2 and 10 show almost no growth throughout the period. This is similar to the results for *Passerina obtusifolia*, a resprouter found in the Renosterveld site (Section 5.4.1).

	mean	sd	2.5%	97.5%
β_0	0.0098	0.01	-0.01	0.03
β_1	0.0062	0.01	-0.01	0.03

Table 29: Table of beta parameters estimated by the SSM.

Table 26 shows that the state-space model estimates the β_1 parameter to be 0.0062. $X_{\text{treatment}}$ is a binary variable that is set as 1 if the plot in the model is a treatment plot and 0 otherwise. Therefore there is an increase of 0.0062 in the mean of the intrinsic growth rate μ_λ when the plot modeled is a treatment plot.

By using the coeffecients in the Equation 4, μ_λ can be calculated as: $\mu_\lambda = 0.0098 + 0.0062 = 0.016$ for treatment plots and $\mu_\lambda = 0.0098 + 0 = 0.0098$ for control plots. Thus it can be asserted that in treatment plots on average, every six months there is an increase of the *Wahlenbergia nodosa* population by 1.61% ($e^{0.016} - 1$), whereas in control plots there is an increase by 0.98% ($e^{0.0098} - 1$). This shows that the experimental treatment has a very marginal positive effect on the growth of the population of *Wahlenbergia nodosa*. The credibility intervals of the β parameters both overlap through zero, therefore it is evident that there is not much certainty that the effect of treatment has a significant effect on growth of the population.

The effects of the experimental treatment are similar to the effect experienced by *Passerina obtusifolia* in the Renosterveld sites.

5.9 Multivariate Auto-regressive State-Space Models

A MARSS model is constructed (as described in Section 3.6), and applied to the species prevalent in both the Renosterveld and Fynbos sites. Two species of re-sprouters and reseeders are included in a model for each site.

The parameters for the models are estimated in a Bayesian framework using a Gibbs sampler in R. Gaussian prior distributions are used for the **B** and **Z** matrices and uniform priors are selected for **Q** and **R** the variance of error terms **w** and **v**.

5.9.1 Renosterveld MARSS model

As in the univariate analysis, the growth of four species of woody shrubs are modeled in the Renosterveld site namely, *Microdon polygaloides*, *Othonna parviflora*, *Elytropappus rhinocerotis* and *Passerina obtusifolia*. The densities of all these species are included in the MARSS model.

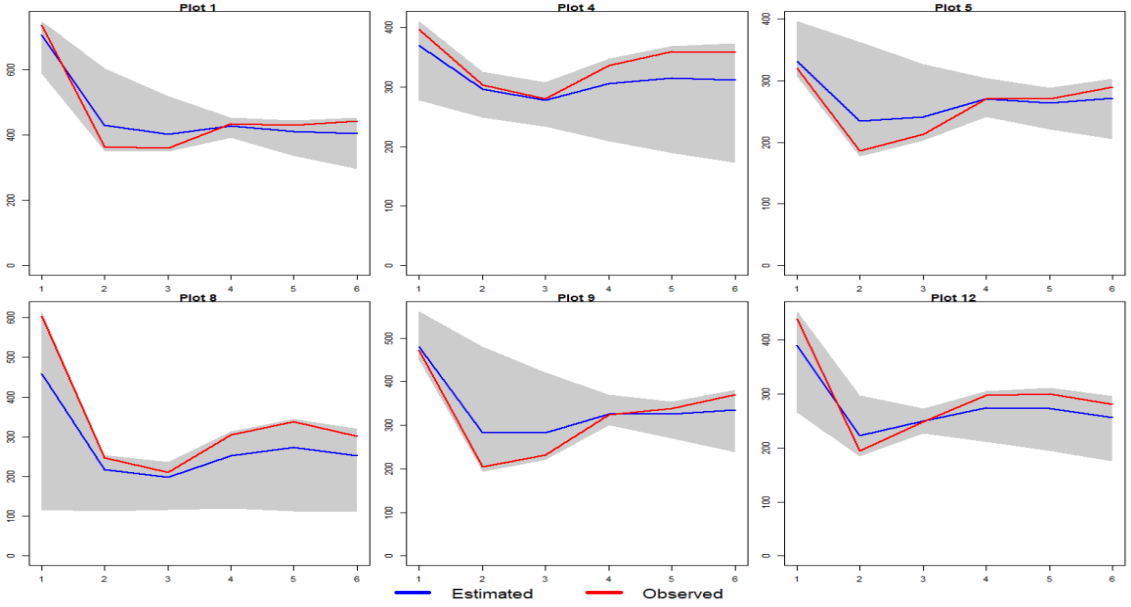

Figure 31: The population of *Microdon polygaloides* plants in six treatment plots in the Renosterveld, with estimates from a multivariate model. The y-axis represents abundance of the population and the x-axis represents the time period. The grey bands represent a 95% credibility interval for the estimations.

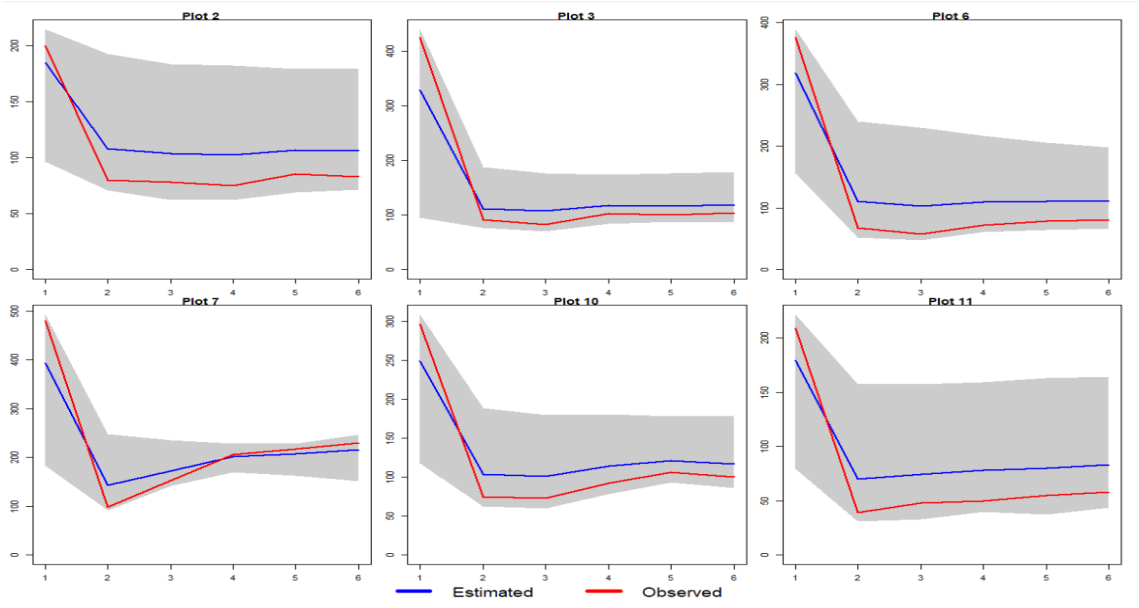

Figure 32: The population of *Microdon polygaloides* plants, in six control plots in the Renosterveld, with estimates from a multivariate model. The y-axis represents abundance of the population and the x-axis represents the time period. The grey bands represent a 95% credibility interval for the estimations.

Figures 31 and 32 show the observed and estimated densities of plants of the *Microdon polygaloides* species in the Rensosterveld. By inspection, it is apparent that the estimations from the multivariate models follow the observed data less precisely than in univariate models, but still follow the general trend of the observations. The graphs showing the densities of other species in the Renosterveld are included in Appendix 7.3.1. In comparison with the univariate analysis it is apparent that confidence intervals for predictions are much wider, this may be due to the use of a more complex model with no new data modeled (Warton et al., 2015b).

The main purpose in fitting a multivariate model to this ecological data is to investigate the interactions between species in a given plot (Zuur et al., 2003b). The **B** matrix in the state process is the interaction matrix that gives inference on the effect of state variables on other state variables. The diagonal elements of **B** indicate the strength of density dependence, values near 1 indicate no density dependence and those near 0 indicate strong density dependence. The off diagonal elements show represent the effect of one species on the per-capita growth rate of another (Holmes et al., 2012).

Table 30 shows the elements of the **B** matrix of the Renosterveld MARSS model

	MP	OP	ER	PO
MP	0.75	0.01	0.02	0.39
OP	0.06	0.28	-0.19	-0.25
ER	-0.07	0.04	0.47	0.09
PO	-0.06	-0.04	0.10	0.54

Table 30: The **B** matrix of the MARSS model, applied to species in the Renosterveld.

where MP represents *Microdon polygaloides*, OP is *Othonna parviflora*, ER is *Elytropappus rhinocerotis* and PO is *Passerina obtusifolia*. It is read as the effect that the species in column j has on that of row i.

Table 30 shows that *Microdon polygaloides* has relatively weak density dependence and only *Othonna parviflora* shows relatively strong density dependence. Both resprouters, *Elytropappus rhinocerotis* and *Passerina obtusifolia* show density dependence that is not as strong but still significant.

Both Reseeders *Microdon polygaloides* and *Othonna parviflora* seem to have little effect on the growth of other species in the Renosterveld. *Elytropappus rhinocerotis* has a negative effect on the growth of *Othonna parviflora* (-0.19 per-capita) and a slight positive effect on the growth of *Passerina obtusifolia* (0.1). *Passerina obtusifolia* has more effect on the growth of other species than any other species in the Renosterveld. It has a relatively strong positive effect on the growth of *Microdon polygaloides* (0.39) and a negative effect on *Othonna parviflora* (-0.25) . This shows that the presence of resprouters seem to have a more significant effect on the growth of reseeders in the Renosterveld. The presence of resprouter species has an especially strong negative effect on the growth of *Othonna parviflora*, this may be due to a competition for resources post-fire.

5.9.2 Fynbos MARSS model

Four species of parenial woody shrubs are included in the multivariate model at the Fynbos site. They are: *Selago glabrata*, *Aspalathus shawii*, *Agathosma capensis* and *Wahlenbergia nodosa*.

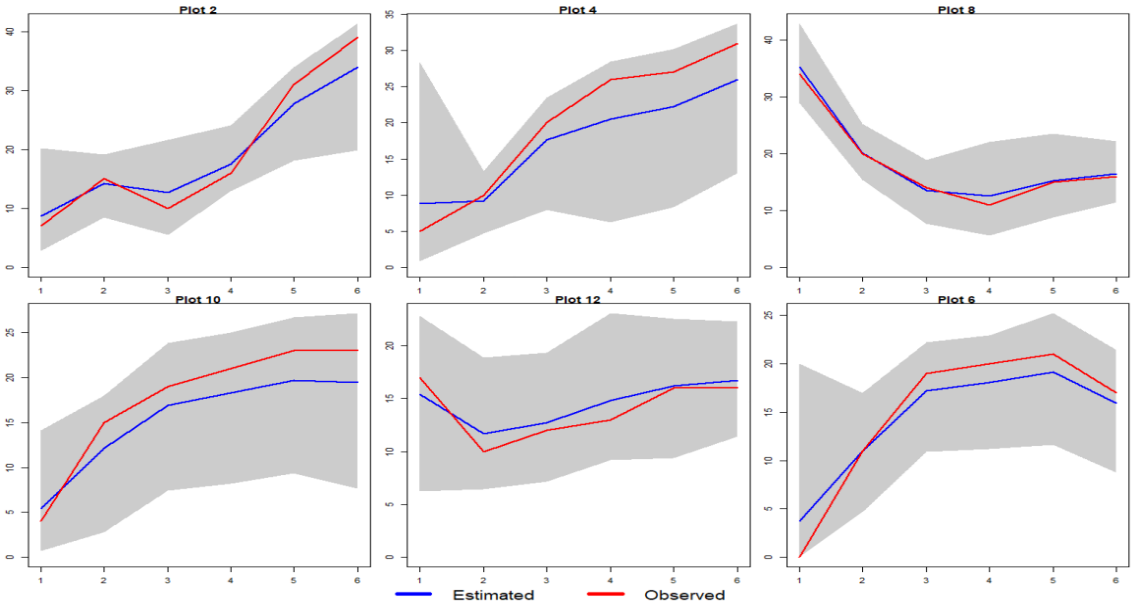

Figure 33: The population of *Selago glabrata* plants, in six treatment plots in the Renosterveld, with estimates from a multivariate model. The y-axis represents abundance of the population and the x-axis represents the time period.

Figures 33 and 33 show the density of *Selago glabrata* in Fynbos plots and the predicted density from the MARSS model. Again it is apparent that the predictions from the MARSS model follow the observed data less precisely than in the univariate case, owing to the increase in the complexity of the model.

	SG	AS	AC	WN
SG	0.46	-0.13	0.10	0.01
AS	-0.34	0.14	0.15	0.11
AC	0.04	0.05	1.05	-0.03
WN	-0.09	-0.09	-0.00	1.00

Table 31: The **B** matrix of the MARSS model, applied to species in the Fynbos.

Table 31 shows the elements of the **B** matrix of the Fynbos MARSS model where SG represents *Selago glabrata*, AS is *Aspalathus shawii*, AC is *Agathosma capensis* and WN is *Wahlenbergia nodosa*.

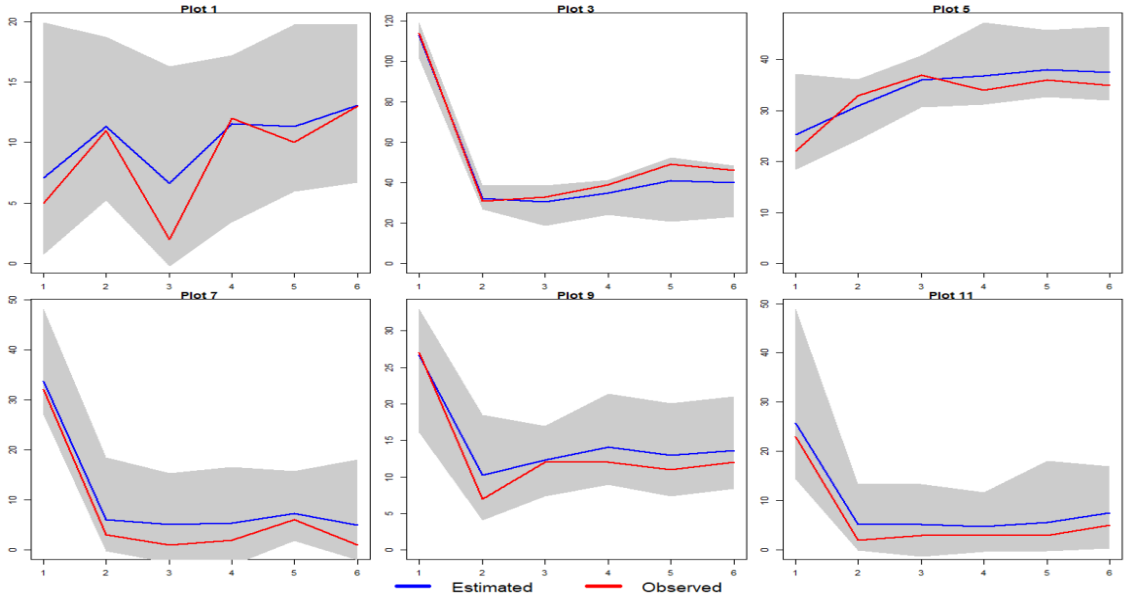

Figure 34: The population of *Selago glabrata* plants, in six control plots in the Renosterveld, with estimates from a multivariate model. The y-axis represents abundance of the population and the x-axis represents the time period.

From Table 31 it is apparent that the reseeder, *Selago glabrata* shows significant density dependence whereas the other reseeder, *Aspalathus shawii*, shows very strong density dependence. The resprouter species *Agathosma capensis* and *Wahlenbergia nodosa* show extremely weak density depence in the Fynbos. *Selago glabrata* has a strong negative effect on the growth of *Aspalathus shawii* (-0.34). *Aspalathus shawii* also has a moderate negative effect on both *Selago glabrata* and *Wahlenbergia nodosa*. It is apparent that the reseeder species in the Fynbos have a more significant, negative, effect on the growth of other reseeders as apposed to resprouters. The presence of resprouters seems to have a small positive effect on the growth of reseeders in the Fynbos.

6 Discussion

State-space modeling is a powerful tool for population dynamics modeling, allowing for the consideration of observation errors in modeling a population. The survey data analysed had only six periods of observations, making modeling and analysis of models difficult at times. The experiment from which the data was taken would benefit from a longer period of observations as this would make models more reliable and robust. Such an instance where more data would have been useful, is in the attempt to forecast populations two time steps ahead using the state-space model (5.1.3). It showed that while forecasted population sizes followed the trend of the population intervals, the credibility intervals of the forecasted variables was too large for them to be useful.

The species of perennial woody shrubs modeled in the Renosterveld and Fynbos site experienced either higher growth rates or no significant impact on growth as a result of the experimental treatment of changing rainfall seasonality as opposed to their controls. None of the species modeled showed a decline in population as a result of experimental treatment.

From this analysis of experimental data it is apparent that a changing rainfall seasonality in the Cape Floristic Region does have a significant effect on the growth of some vegetation in the region. The difference in growth is somewhat significant and may have an impact on other life inhabiting this region. This impact may require further study to be better understood. The findings align with those of Dr. Van Blerk (Van Blerk, 2021), whereby the the influence of the first period of experimentation has a significant effect on the growth of a species in subsequent periods. It is noted in that study that the "bottom-up" effect observed in early post-fire environments may have significant effects in mortality in the long-term and may lead to drastic changes in long-term trends in community structures.

The analysis shows that the populations of reseeder species benefit significantly from changing rainfall seasonality experiencing growth or reduction in negative growth. The population of resprouter species, however, experienced little benefit from a change in rainfall seasonality resulting in small increases to their growth rates.

The reseeders in the Renosterveld and Fynbos site experienced a decrease in population after the first survey. This is probably due to young seedlings failing to reach maturity between the first and second survey. The first survey is conducted in a winter period and the second during a summer period, in an area that usually experiences a rainy season during winter. Under experimental conditions the rainfall seasonality is swapped. These species experienced more growth (or a reduction in negative population growth) under experimental conditions than controlled condi-

tions after the second period. This may be due to seedlings receiving more rainfall during a crucial time in their growth cycle. A longer time series may give more insight into the long term effects of changing rainfall seasonality (Warton et al., 2015b).

The growth of populations of reeseders show similar patterns within the Renosterveld and Fynbos site and show similar responses to the experimental treatment, as do the populations of resprouters. This shows that the site that a particular growth form inhabits has little effect its growth patterns or its response to a changing rainfall pattern.

By analysing the effect of the pressence of *Thesium strictum* on populations of reseeders and resprouters in the Renosterveld, it was shown that the presence of the parasitic plant *Thesium strictum* had a negative effect on the population growth of both reseeders and resprouters in the Renosterveld site. This effect was reduced for reseeders as a result of changing rainfall patterns, whereas resprouter populations showed that the effect had little impact or was exacerbated by changing rainfall patterns.

Multivariate stat-space models in this research was used primarily to to investigate the relationship of the abundance of certain species on the growth of other species. Such analysis are popular in the space of ecology (Holmes et al., 2012). There are other useful tools pertaining to multivariate state-space models such as dimension reduction (Hinrichsen and Holmes, 2009).

From the analysis it was apparent that in the Renosterveld, the presence of reseeders have little effect on the growth of resprouters, wheras he presence of resprouters can have significant effects on the growth of reseeders. In the Fynbos we saw that reseeders discourage the growth of other reseeders but not resprouters. The presence of resprouters also encourage the growth of reseeders in the Fynbos.

The data for this research was recorded over a relatively short period of time for a time series analysis. It is noted that several aspects of this analysis would benefit from a longer time series, such as the ability to forecast more accurately. Using replicated plots has given more certainty of the reliability of results, but a longer period of recording would have been beneficial to many aspects of modeling as noted on several instances throughout this research.

There are other potential pitfalls in the use of SSMs for ecological applications. Some of these are noted in the paper "State-space models' dirty little secrets: even simple linear Gaussian models can have estimation problems" (Auger-Méthé et al., 2016). From that research it is noted that linear Gaussian SSMs may have parameter- and state-estimation problems that can effect biological inferences. It is noted that

estimation problems are more frequent when the measurement error is much larger than the process stochasticity. This is concerning as SSMs are most needed when there is a large measurement error as compared to the process stochasticity. By fixing error values and selection of prior distributions this effect is mitigated in this research but it should be noted that in larger studies with more significant error in measurement even these methods may prove to be less effective.

It is also noted in Auger-Méthé et al. (2016) that, as with other models, parameter estimatability becomes more unreliable with more complexity in hierarchical models as compared to the information content. This is observed in the application with multivariate SSMs in this study as compared to simpler univariate models. This should also be noted for other studies that may wish to include more ecological determinants such as climate and environmental data.

References

M. Auger-Méthé, K. Newman, D. Cole, F. Empacher, R. Gryba, A. King, V. Leos-Barajas, J. Flemming, A. Nielsen, G. Petris, and L. Thomas. A guide to state-space modeling of ecological time series. *Ecological Monographs*, 91:1834–1846.

M. Auger-Méthé, C. Field, C. M. Albertsen, A. E. Derorcher, M. A. Lewes, I. D. Jonsen, and J. M. Flemming. State-space models' dirty little secrets: even simple linear gaussian models can have estimation problems. *Scientific Reports*, 6:1 – 10, 2016. doi: https://doi.org/10.1038/srep26677.

M. Auger-Méthé, K. Newman, D. Cole, F. Empacher, R. Gryba, A. King, V. Leos-Barajas, J. Flemming, A. Nielsen, G. Petris, and L. Thomas. An introduction to state-space modeling of ecological time series. *ArXiv*, 2020. doi: https://doi.org/10.48550/arXiv.2002.02001.

B. Bolker. *Ecological Models and Data in R*. Princeton University Press, 2007.

J. Born, P. Linder, and P. Desmet. The Greater Cape Floristic Region. *Journal of Biogeography*, 34:147 – 162, 2006. doi: 10.1111/j.1365-2699.2006.01595.x.

M. Cramer. *Fynbos: ecology, evolution, and conservation of a megadiverse region*, pages 248–272. Oxford University Press, 2014.

A. Dafni, D. Cohen, and I. Noy-Mier. Life-cycle variation in geophytes. *Annals of the Missouri Botanical Garden*, 68, 1981. doi: https://doi.org/10.2307/2398893.

D. Dail and L. Madsen. Models for estimating abundance from repeated counts of an open metapopulation. *Biometrics*, 67:577–87, 2011. doi: 10.1111/j.1541-0420.2010.01465.x.

W. R. J. Dean and S. Milton. *The Karoo: Ecological Patterns and Processes*. Cambridge University Press, 1999.

L. M. Dupont, X. Zhao, C. Charles, J. T. Faith, and D. Braun. Continuous vegetation record of the Greater Cape Floristic Region (South Africa) covering the past 300 000 years. *Climate of the Past*, 18:1–21, 2022. doi: 10.5194/cp-18-1-2022. URL `https://cp.copernicus.org/articles/18/1/2022/`.

A. Gelfand. Gibbs sampling. *Journal of the American Statistical Association*, 95:1300–1304, 2000. doi: 10.2307/2669775.

R. Hinrichsen and E. Holmes. Using multivariate state-space models to study spatial structure and dynamics. *Spatial Ecology*, 8:144–165, 2009. doi: 10.1201/9781420059861.ch8.

E. Holmes, E. Ward, and K. Wills. Marss: Multivariate autoregressive state-space models for analyzing time-series data. *The R Journal*, 4:11–19, 2012. doi: 10.32614/RJ-2012-002.

A. Ives, B. Dennis, K. L. Cottingham, and S. Carpenter. Estimating community stability and ecological interactions from time-series data. *Ecological Monographs*, 73:301–330, 2003.

M. Kery and M. Schaub. *Bayesian Population Analysis using WinBUGS. A hierarchical perspective*. Academic Press, 2011.

H. Lopes, R. McCulloch, and R. Tsay. Parsimony inducing priors for large scale state–space models. *Journal of Econometrics*, 230:39–61, 2021. doi: 10.1016/j.jeconom.2021.11.005.

A. Nielsen and C. Berg. Estimation of time-varying selectivity in stock assessments using state-space models. *Fisheries Research*, 158:96–101, 2014. doi: 10.1016/j.fishres.2014.01.014.

M. Plummer. *rjags: Bayesian Graphical Models using MCMC*, 2023. URL `https://CRAN.R-project.org/package=rjags`. R package version 4-15.

R Core Team. *R: A Language and Environment for Statistical Computing*. R Foundation for Statistical Computing, Vienna, Austria, 2021. URL `https://www.R-project.org/`.

S. Riga and J. Knape. A toolbox to explore the composition of species dynamics behind multi-species indices. *Methods in Ecology and Evolution*, 14:1821–1832, 2022. doi: 10.1111/2041-210X.14117.

Y.-S. Su and M. Yajima. *R2jags: Using R to Run 'JAGS'*, 2021. URL `https://CRAN.R-project.org/package=R2jags`. R package version 0.7-1.

J. J. Van Blerk. The effect of altered rainfall seasonality on post-fire recovery of fynbos and renosterveld shrublands in the cape floristic region [doctoral thesis, university of cape town]. *University of Cape Town, Faculty of Science, Department of Biological Sciences.*, pages 2–176, 2021. doi: http://hdl.handle.net/11427/33950.

J. J. van Blerk, A. G. West, R. Altwegg, and M. Hoffman. Post-fire summer rainfall differentially affects reseeder and resprouter population recovery in fire-prone shrublands of south africa. *Science of the Total Environment*, 788:147699, 2021. doi: https://doi.org/10.1016/j.scitotenv.2021.147699.

D. Warton, S. Foster, G. De'ath, J. Stoklosa, and P. Dunstan. Model-based thinking for community ecology. *Plant Ecology*, 216:669–682, 2015a. doi: 10.1007/s11258-014-0366-3.

D. I. Warton, F. G. Blanchet, R. B. O'Hara, O. Ovaskainen, S. Taskinen, S. C. Walker, and F. K. C. Hui. So many variables: Joint modeling in community ecology. *Trends in Ecology and Evolution; evolution*, 30:766—779, 2015b. doi: 10.1016/j.tree.2015.09.007.

A. Zuur, R. Fryer, I. Jolliffe, R. Dekker, and J. Beukema. Estimating common trends in multivariate time series using dynamic factor analysis. *Environmetrics*, 14:665 – 685, 2003a. doi: 10.1002/env.611.

A. Zuur, I. Tuck, and N. Bailey. Dynamic factor analysis to estimate common trends in fisheries time series. *Canadian Journal of Fisheries and Aquatic Sciences*, 60: 542–552, 2003b. doi: 10.1139/f03-030.

7 Appendix

7.1 Credibility intervals of growth rates for univariate models

The credibility intervals for all growth rates $\lambda_{i,t}$ are tabulated below. $\lambda_{i,t}$ is noted in the form lam[i,t] for plot i at time period t

7.1.0.1 *Microdon polygaloides*

	mean	2.5%	97.5%
lam[1,1]	-0.70	-0.81	-0.58
lam[1,2]	-0.02	-0.19	0.11
lam[1,3]	0.19	0.07	0.33
lam[1,4]	-0.01	-0.12	0.11
lam[1,5]	0.03	-0.09	0.14
lam[2,1]	-0.84	-1.17	-0.39
lam[2,2]	-0.11	-0.60	0.29
lam[2,3]	-0.05	-0.56	0.39
lam[2,4]	0.09	-0.43	0.57
lam[2,5]	-0.06	-0.63	0.40
lam[3,1]	-1.43	-1.67	-1.05
lam[3,2]	-0.18	-0.66	0.17
lam[3,3]	0.15	-0.32	0.54
lam[3,4]	-0.01	-0.44	0.41
lam[3,5]	-0.00	-0.51	0.44
lam[4,1]	-0.27	-0.43	-0.12
lam[4,2]	-0.07	-0.22	0.11
lam[4,3]	0.17	-0.00	0.31
lam[4,4]	0.07	-0.06	0.23
lam[4,5]	-0.00	-0.15	0.13
lam[5,1]	-0.51	-0.69	-0.29
lam[5,2]	0.11	-0.13	0.32
lam[5,3]	0.24	0.03	0.43
lam[5,4]	-0.00	-0.18	0.17
lam[5,5]	0.07	-0.10	0.25
lam[6,1]	-1.54	-1.86	-1.07
lam[6,2]	-0.27	-0.79	0.12
lam[6,3]	0.12	-0.47	0.53
lam[6,4]	0.07	-0.49	0.55
lam[6,5]	-0.02	-0.57	0.47

Table 32: λ credibility intervals

	mean	2.5%	97.5%
lam[7,1]	-1.46	-1.71	-1.07
lam[7,2]	0.31	-0.14	0.58
lam[7,3]	0.29	0.02	0.56
lam[7,4]	0.06	-0.17	0.28
lam[7,5]	0.05	-0.17	0.27
lam[8,1]	-0.87	-0.99	-0.71
lam[8,2]	-0.17	-0.36	0.03
lam[8,3]	0.35	0.13	0.52
lam[8,4]	0.11	-0.05	0.28
lam[8,5]	-0.12	-0.27	0.03
lam[9,1]	-0.82	-0.99	-0.60
lam[9,2]	0.11	-0.12	0.34
lam[9,3]	0.32	0.12	0.49
lam[9,4]	0.05	-0.10	0.22
lam[9,5]	0.09	-0.06	0.23
lam[10,1]	-1.25	-1.57	-0.81
lam[10,2]	-0.12	-0.66	0.30
lam[10,3]	0.17	-0.39	0.65
lam[10,4]	0.12	-0.37	0.54
lam[10,5]	-0.08	-0.56	0.35
lam[11,1]	-1.35	-1.76	-0.70
lam[11,2]	-0.08	-0.78	0.36
lam[11,3]	-0.02	-0.64	0.52
lam[11,4]	0.01	-0.68	0.59
lam[11,5]	-0.03	-0.74	0.55
lam[12,1]	-0.80	-1.00	-0.57
lam[12,2]	0.22	-0.01	0.45
lam[12,3]	0.18	0.00	0.36
lam[12,4]	0.01	-0.16	0.18
lam[12,5]	-0.07	-0.24	0.09

Table 33: λ credibility intervals

7.1.0.2 *Othonna parviflora*

	mean	2.5%	97.5%
lam[1,1]	-0.81	-0.81	-0.81
lam[1,2]	-0.17	-0.17	-0.17
lam[1,3]	-0.08	-0.08	-0.08
lam[1,4]	-0.05	-0.05	-0.05
lam[1,5]	-0.88	-0.88	-0.88
lam[2,1]	-1.90	-1.90	-1.90
lam[2,2]	-0.18	-0.18	-0.18
lam[2,3]	-0.51	-0.51	-0.51
lam[2,4]	0.00	-0.00	0.00
lam[2,5]	-0.40	-0.41	-0.40
lam[3,1]	-12.61	-20.12	-9.69
lam[3,2]	-10.10	-20.24	-2.21
lam[3,3]	-10.09	-19.96	-1.74
lam[3,4]	-10.08	-20.16	-1.68
lam[3,5]	-10.05	-19.69	-1.74
lam[4,1]	-1.64	-1.65	-1.64
lam[4,2]	0.00	-0.00	0.00
lam[4,3]	-0.20	-0.20	-0.20
lam[4,4]	-0.12	-0.12	-0.12
lam[4,5]	-1.39	-1.39	-1.38
lam[5,1]	-1.45	-1.45	-1.45
lam[5,2]	-0.32	-0.32	-0.32
lam[5,3]	0.07	0.07	0.07
lam[5,4]	-0.19	-0.19	-0.19
lam[5,5]	-0.61	-0.61	-0.61
lam[6,1]	-11.92	-18.98	-9.01
lam[6,2]	-9.59	-18.91	-1.89
lam[6,3]	-9.56	-18.93	-1.62
lam[6,4]	-9.54	-18.93	-1.43
lam[6,5]	-9.55	-18.94	-1.46

Table 34: λ credibility intervals

	mean	2.5%	97.5%
lam[7,1]	-2.54	-2.54	-2.54
lam[7,2]	-0.85	-0.85	-0.84
lam[7,3]	0.00	-0.00	0.00
lam[7,4]	-0.40	-0.41	-0.40
lam[7,5]	-7.02	-9.72	-5.45
lam[8,1]	-6.52	-6.81	-6.02
lam[8,2]	-0.81	-1.44	-0.38
lam[8,3]	5.25	4.83	6.03
lam[8,4]	0.00	-0.01	0.01
lam[8,5]	-0.00	-0.01	0.01
lam[9,1]	-0.90	-0.90	-0.90
lam[9,2]	0.05	0.05	0.05
lam[9,3]	-0.20	-0.20	-0.20
lam[9,4]	-0.08	-0.08	-0.08
lam[9,5]	-3.81	-3.81	-3.80
lam[10,1]	-11.79	-20.71	-8.67
lam[10,2]	-9.62	-20.34	-1.62
lam[10,3]	-9.61	-20.22	-1.36
lam[10,4]	-9.57	-20.70	-1.00
lam[10,5]	-9.61	-20.07	-1.14
lam[11,1]	-2.64	-2.65	-2.63
lam[11,2]	1.10	1.09	1.11
lam[11,3]	-0.40	-0.41	-0.40
lam[11,4]	0.00	-0.00	0.00
lam[11,5]	-0.69	-0.70	-0.68
lam[12,1]	-1.14	-1.15	-1.14
lam[12,2]	-0.05	-0.05	-0.05
lam[12,3]	-1.05	-1.05	-1.05
lam[12,4]	-0.56	-0.56	-0.56
lam[12,5]	-7.53	-9.96	-6.06

Table 35: λ credibility intervals

7.1.0.3 *Elytropappus rhinocerotis*

	mean	2.5%	97.5%
lam[1,1]	0.21	-0.12	0.53
lam[1,2]	0.37	0.09	0.70
lam[1,3]	0.24	0.01	0.48
lam[1,4]	0.25	0.04	0.46
lam[1,5]	0.20	0.01	0.39
lam[2,1]	0.30	-0.03	0.68
lam[2,2]	0.54	0.16	1.10
lam[2,3]	0.39	0.13	0.66
lam[2,4]	0.19	-0.02	0.42
lam[2,5]	0.13	-0.08	0.34
lam[3,1]	0.07	-0.07	0.21
lam[3,2]	0.21	0.07	0.34
lam[3,3]	0.06	-0.05	0.17
lam[3,4]	0.02	-0.08	0.13
lam[3,5]	0.01	-0.09	0.12
lam[4,1]	0.19	-0.11	0.50
lam[4,2]	0.26	0.01	0.53
lam[4,3]	0.23	-0.00	0.46
lam[4,4]	0.22	0.01	0.43
lam[4,5]	0.06	-0.15	0.28
lam[5,1]	0.25	-0.09	0.59
lam[5,2]	0.33	0.04	0.64
lam[5,3]	0.56	0.25	0.91
lam[5,4]	0.32	0.13	0.53
lam[5,5]	0.15	-0.02	0.35
lam[6,1]	0.39	0.06	0.80
lam[6,2]	0.74	0.27	1.42
lam[6,3]	0.38	0.18	0.62
lam[6,4]	0.23	0.05	0.40
lam[6,5]	0.04	-0.13	0.25

Table 36: λ credibility intervals

	mean	2.5%	97.5%
lam[7,1]	0.14	-0.21	0.46
lam[7,2]	0.39	0.08	0.78
lam[7,3]	0.29	0.04	0.55
lam[7,4]	0.10	-0.12	0.33
lam[7,5]	0.04	-0.19	0.27
lam[8,1]	0.18	-0.17	0.53
lam[8,2]	0.23	-0.08	0.55
lam[8,3]	0.27	-0.02	0.58
lam[8,4]	0.14	-0.14	0.41
lam[8,5]	0.17	-0.10	0.43
lam[9,1]	0.31	-0.05	0.71
lam[9,2]	0.32	-0.00	0.67
lam[9,3]	0.28	-0.01	0.59
lam[9,4]	0.31	0.05	0.59
lam[9,5]	0.26	0.01	0.51
lam[10,1]	0.14	-0.22	0.52
lam[10,2]	0.18	-0.16	0.54
lam[10,3]	0.16	-0.17	0.49
lam[10,4]	0.15	-0.17	0.47
lam[10,5]	0.15	-0.17	0.46
lam[11,1]	0.06	-0.11	0.24
lam[11,2]	0.15	-0.01	0.31
lam[11,3]	0.10	-0.04	0.25
lam[11,4]	0.09	-0.05	0.22
lam[11,5]	0.00	-0.13	0.14
lam[12,1]	0.29	-0.06	0.66
lam[12,2]	0.45	0.13	0.89
lam[12,3]	0.45	0.16	0.77
lam[12,4]	0.18	-0.06	0.43
lam[12,5]	0.18	-0.05	0.40

Table 37: λ credibility intervals

7.1.0.4 *Passerina obtusifolia*

	mean	2.5%	97.5%
lam[1,1]	0.17	0.03	0.24
lam[1,2]	0.04	-0.02	0.12
lam[1,3]	0.01	-0.06	0.08
lam[1,4]	0.00	-0.06	0.08
lam[1,5]	0.01	-0.06	0.08
lam[2,1]	-0.04	-0.10	0.04
lam[2,2]	0.04	-0.04	0.10
lam[2,3]	-0.02	-0.08	0.05
lam[2,4]	-0.00	-0.07	0.06
lam[2,5]	0.00	-0.07	0.07
lam[3,1]	-0.07	-0.13	0.02
lam[3,2]	-0.03	-0.09	0.04
lam[3,3]	0.00	-0.06	0.07
lam[3,4]	0.04	-0.04	0.10
lam[3,5]	-0.02	-0.08	0.06
lam[4,1]	0.24	0.14	0.29
lam[4,2]	0.04	0.00	0.10
lam[4,3]	0.04	0.00	0.08
lam[4,4]	0.00	-0.04	0.05
lam[4,5]	0.02	-0.03	0.06
lam[5,1]	0.12	0.04	0.17
lam[5,2]	0.04	-0.01	0.10
lam[5,3]	-0.01	-0.06	0.05
lam[5,4]	0.02	-0.04	0.07
lam[5,5]	0.00	-0.05	0.06
lam[6,1]	0.26	0.12	0.31
lam[6,2]	0.05	0.00	0.11
lam[6,3]	0.02	-0.02	0.07
lam[6,4]	0.04	-0.01	0.08
lam[6,5]	-0.09	-0.13	-0.01

Table 38: λ credibility intervals

	mean	2.5%	97.5%
lam[7,1]	0.06	-0.00	0.10
lam[7,2]	-0.04	-0.08	0.01
lam[7,3]	0.01	-0.04	0.06
lam[7,4]	0.00	-0.04	0.05
lam[7,5]	0.03	-0.02	0.07
lam[8,1]	0.06	-0.04	0.13
lam[8,2]	-0.04	-0.11	0.06
lam[8,3]	0.03	-0.05	0.10
lam[8,4]	0.03	-0.05	0.11
lam[8,5]	0.01	-0.06	0.10
lam[9,1]	0.25	0.09	0.33
lam[9,2]	0.11	0.04	0.17
lam[9,3]	0.04	-0.02	0.10
lam[9,4]	-0.07	-0.13	0.02
lam[9,5]	0.02	-0.05	0.08
lam[10,1]	-0.02	-0.08	0.04
lam[10,2]	-0.02	-0.08	0.04
lam[10,3]	-0.00	-0.06	0.06
lam[10,4]	0.02	-0.04	0.08
lam[10,5]	0.00	-0.06	0.07
lam[11,1]	0.01	-0.07	0.09
lam[11,2]	0.07	-0.03	0.14
lam[11,3]	-0.07	-0.14	0.04
lam[11,4]	0.02	-0.07	0.09
lam[11,5]	0.00	-0.08	0.08
lam[12,1]	0.06	0.01	0.11
lam[12,2]	0.00	-0.04	0.06
lam[12,3]	0.04	-0.01	0.09
lam[12,4]	0.00	-0.04	0.05
lam[12,5]	-0.01	-0.06	0.04

Table 39: λ credibility intervals

7.1.0.5 *Selago glabrata*

	mean	2.5%	97.5%
lam[1,1]	0.10	-0.60	0.82
lam[1,2]	-0.20	-0.90	0.51
lam[1,3]	0.35	-0.35	1.04
lam[1,4]	0.04	-0.60	0.67
lam[1,5]	0.11	-0.58	0.73
lam[2,1]	0.36	-0.27	1.02
lam[2,2]	-0.04	-0.62	0.57
lam[2,3]	0.36	-0.13	0.87
lam[2,4]	0.60	0.20	1.01
lam[2,5]	0.26	-0.01	0.56
lam[3,1]	-1.23	-1.45	-1.00
lam[3,2]	-0.01	-0.29	0.26
lam[3,3]	0.16	-0.10	0.42
lam[3,4]	0.22	-0.00	0.44
lam[3,5]	-0.06	-0.27	0.15
lam[4,1]	0.38	-0.25	1.07
lam[4,2]	0.57	0.04	1.12
lam[4,3]	0.30	-0.09	0.72
lam[4,4]	0.08	-0.26	0.43
lam[4,5]	0.14	-0.18	0.46
lam[5,1]	0.33	-0.02	0.68
lam[5,2]	0.12	-0.15	0.40
lam[5,3]	-0.07	-0.33	0.20
lam[5,4]	0.05	-0.23	0.32
lam[5,5]	-0.03	-0.30	0.24
lam[6,1]	-1.41	-2.17	-0.76
lam[6,2]	-0.79	-1.85	-0.00
lam[6,3]	-0.57	-1.82	0.38
lam[6,4]	-0.50	-1.83	0.57
lam[6,5]	-0.60	-1.86	0.42

Table 40: λ credibility intervals

	mean	2.5%	97.5%
lam[7,1]	-0.50	-0.86	-0.14
lam[7,2]	-0.34	-0.80	0.10
lam[7,3]	-0.17	-0.69	0.33
lam[7,4]	0.14	-0.40	0.68
lam[7,5]	0.06	-0.49	0.58
lam[8,1]	-0.82	-1.37	-0.30
lam[8,2]	0.00	-0.57	0.57
lam[8,3]	-0.03	-0.61	0.55
lam[8,4]	-0.08	-0.68	0.50
lam[8,5]	-0.06	-0.76	0.57
lam[9,1]	0.55	-0.09	1.27
lam[9,2]	0.30	-0.19	0.82
lam[9,3]	0.14	-0.28	0.58
lam[9,4]	0.09	-0.30	0.49
lam[9,5]	0.03	-0.36	0.42
lam[10,1]	-1.16	-1.97	-0.47
lam[10,2]	-0.59	-1.63	0.20
lam[10,3]	-0.47	-1.65	0.42
lam[10,4]	-0.43	-1.67	0.53
lam[10,5]	-0.41	-1.68	0.63
lam[11,1]	-0.30	-0.86	0.28
lam[11,2]	0.04	-0.52	0.59
lam[11,3]	0.08	-0.46	0.63
lam[11,4]	0.15	-0.36	0.68
lam[11,5]	0.04	-0.49	0.55
lam[12,1]	0.58	-0.12	1.37
lam[12,2]	0.52	-0.03	1.10
lam[12,3]	0.13	-0.31	0.60
lam[12,4]	0.04	-0.38	0.47
lam[12,5]	-0.12	-0.58	0.32

Table 41: λ credibility intervals

7.1.0.6 *Aspalathus shawii*

	mean	2.5%	97.5%
lam[1,1]	0.17	0.03	0.24
lam[1,2]	0.04	-0.02	0.12
lam[1,3]	0.01	-0.06	0.08
lam[1,4]	0.00	-0.06	0.08
lam[1,5]	0.01	-0.06	0.08
lam[2,1]	-0.04	-0.10	0.04
lam[2,2]	0.04	-0.04	0.10
lam[2,3]	-0.02	-0.08	0.05
lam[2,4]	-0.00	-0.07	0.06
lam[2,5]	0.00	-0.07	0.07
lam[3,1]	-0.07	-0.13	0.02
lam[3,2]	-0.03	-0.09	0.04
lam[3,3]	0.00	-0.06	0.07
lam[3,4]	0.04	-0.04	0.10
lam[3,5]	-0.02	-0.08	0.06
lam[4,1]	0.24	0.14	0.29
lam[4,2]	0.04	0.00	0.10
lam[4,3]	0.04	0.00	0.08
lam[4,4]	0.00	-0.04	0.05
lam[4,5]	0.02	-0.03	0.06
lam[5,1]	0.12	0.04	0.17
lam[5,2]	0.04	-0.01	0.10
lam[5,3]	-0.01	-0.06	0.05
lam[5,4]	0.02	-0.04	0.07
lam[5,5]	0.00	-0.05	0.06
lam[6,1]	0.26	0.12	0.31
lam[6,2]	0.05	0.00	0.11
lam[6,3]	0.02	-0.02	0.07
lam[6,4]	0.04	-0.01	0.08
lam[6,5]	-0.09	-0.13	-0.01

Table 42: λ credibility intervals

	mean	2.5%	97.5%
lam[7,1]	0.06	-0.00	0.10
lam[7,2]	-0.04	-0.08	0.01
lam[7,3]	0.01	-0.04	0.06
lam[7,4]	0.00	-0.04	0.05
lam[7,5]	0.03	-0.02	0.07
lam[8,1]	0.06	-0.04	0.13
lam[8,2]	-0.04	-0.11	0.06
lam[8,3]	0.03	-0.05	0.10
lam[8,4]	0.03	-0.05	0.11
lam[8,5]	0.01	-0.06	0.10
lam[9,1]	0.25	0.09	0.33
lam[9,2]	0.11	0.04	0.17
lam[9,3]	0.04	-0.02	0.10
lam[9,4]	-0.07	-0.13	0.02
lam[9,5]	0.02	-0.05	0.08
lam[10,1]	-0.02	-0.08	0.04
lam[10,2]	-0.02	-0.08	0.04
lam[10,3]	-0.00	-0.06	0.06
lam[10,4]	0.02	-0.04	0.08
lam[10,5]	0.00	-0.06	0.07
lam[11,1]	0.01	-0.07	0.09
lam[11,2]	0.07	-0.03	0.14
lam[11,3]	-0.07	-0.14	0.04
lam[11,4]	0.02	-0.07	0.09
lam[11,5]	0.00	-0.08	0.08
lam[12,1]	0.06	0.01	0.11
lam[12,2]	0.00	-0.04	0.06
lam[12,3]	0.04	-0.01	0.09
lam[12,4]	0.00	-0.04	0.05
lam[12,5]	-0.01	-0.06	0.04

Table 43: λ credibility intervals

7.1.0.7 *Agathosma capensis*

	mean	2.5%	97.5%
lam[1,1]	0.08	-0.08	0.26
lam[1,2]	0.09	-0.07	0.25
lam[1,3]	0.06	-0.09	0.21
lam[1,4]	0.05	-0.10	0.20
lam[1,5]	0.02	-0.14	0.18
lam[2,1]	0.17	0.10	0.23
lam[2,2]	0.08	0.03	0.14
lam[2,3]	0.05	0.00	0.10
lam[2,4]	0.06	0.01	0.11
lam[2,5]	0.08	0.03	0.12
lam[3,1]	0.25	0.17	0.31
lam[3,2]	-0.00	-0.06	0.06
lam[3,3]	0.12	0.06	0.17
lam[3,4]	0.07	0.02	0.11
lam[3,5]	-0.04	-0.08	0.01
lam[4,1]	0.04	-0.19	0.26
lam[4,2]	0.04	-0.18	0.27
lam[4,3]	0.04	-0.18	0.27
lam[4,4]	0.05	-0.18	0.28
lam[4,5]	0.06	-0.17	0.30
lam[5,1]	0.22	0.19	0.25
lam[5,2]	0.03	0.00	0.05
lam[5,3]	0.02	-0.00	0.05
lam[5,4]	0.20	0.18	0.22
lam[5,5]	0.04	0.02	0.06
lam[6,1]	0.17	-0.01	0.37
lam[6,2]	0.25	0.06	0.47
lam[6,3]	0.17	0.00	0.34
lam[6,4]	0.10	-0.08	0.26
lam[6,5]	0.12	-0.05	0.28

Table 44: λ credibility intervals

	mean	2.5%	97.5%
lam[7,1]	0.09	-0.01	0.20
lam[7,2]	0.00	-0.09	0.09
lam[7,3]	0.02	-0.07	0.11
lam[7,4]	0.02	-0.07	0.10
lam[7,5]	-0.03	-0.12	0.06
lam[8,1]	-0.02	-0.11	0.08
lam[8,2]	0.08	-0.00	0.17
lam[8,3]	0.10	0.02	0.18
lam[8,4]	0.03	-0.04	0.11
lam[8,5]	0.04	-0.04	0.12
lam[9,1]	-0.01	-0.23	0.21
lam[9,2]	-0.01	-0.23	0.21
lam[9,3]	-0.01	-0.23	0.21
lam[9,4]	-0.00	-0.23	0.21
lam[9,5]	-0.00	-0.23	0.21
lam[10,1]	-0.00	-0.20	0.20
lam[10,2]	0.00	-0.19	0.20
lam[10,3]	-0.01	-0.20	0.18
lam[10,4]	-0.00	-0.20	0.19
lam[10,5]	-0.00	-0.20	0.20
lam[11,1]	-0.01	-0.08	0.07
lam[11,2]	-0.07	-0.15	0.00
lam[11,3]	0.03	-0.05	0.10
lam[11,4]	0.03	-0.04	0.11
lam[11,5]	0.00	-0.07	0.08
lam[12,1]	0.15	-0.00	0.32
lam[12,2]	0.09	-0.05	0.23
lam[12,3]	0.10	-0.03	0.23
lam[12,4]	0.14	0.01	0.27
lam[12,5]	0.10	-0.02	0.23

Table 45: λ credibility intervals

7.1.0.8 *Wahlenbergia Nodosa*

	mean	2.5%	97.5%
lam[1,1]	-0.34	-0.37	-0.27
lam[1,2]	0.23	0.16	0.26
lam[1,3]	0.02	-0.01	0.06
lam[1,4]	0.09	0.06	0.12
lam[1,5]	-0.00	-0.03	0.03
lam[2,1]	0.09	-0.03	0.19
lam[2,2]	0.04	-0.05	0.15
lam[2,3]	0.10	-0.00	0.19
lam[2,4]	0.13	0.02	0.21
lam[2,5]	-0.02	-0.10	0.10
lam[3,1]	-0.14	-0.21	-0.03
lam[3,2]	-0.00	-0.08	0.07
lam[3,3]	0.12	0.02	0.19
lam[3,4]	0.06	-0.01	0.14
lam[3,5]	0.03	-0.04	0.10
lam[4,1]	-0.05	-0.09	-0.00
lam[4,2]	0.02	-0.02	0.06
lam[4,3]	0.10	0.06	0.14
lam[4,4]	0.05	0.01	0.09
lam[4,5]	0.05	0.01	0.08
lam[5,1]	0.01	-0.04	0.07
lam[5,2]	0.15	0.08	0.20
lam[5,3]	0.04	-0.01	0.09
lam[5,4]	0.11	0.05	0.15
lam[5,5]	0.04	-0.00	0.09
lam[6,1]	0.18	0.13	0.21
lam[6,2]	0.12	0.09	0.15
lam[6,3]	0.05	0.03	0.08
lam[6,4]	0.09	0.07	0.12
lam[6,5]	0.02	-0.01	0.04

Table 46: λ credibility intervals

	mean	2.5%	97.5%
lam[7,1]	-0.07	-0.12	-0.01
lam[7,2]	-0.02	-0.08	0.03
lam[7,3]	-0.12	-0.18	-0.05
lam[7,4]	-0.03	-0.10	0.02
lam[7,5]	-0.10	-0.16	-0.02
lam[8,1]	-0.13	-0.19	-0.02
lam[8,2]	-0.02	-0.11	0.05
lam[8,3]	0.01	-0.08	0.08
lam[8,4]	-0.04	-0.12	0.04
lam[8,5]	-0.08	-0.16	0.02
lam[9,1]	0.03	-0.03	0.09
lam[9,2]	0.10	0.04	0.15
lam[9,3]	0.07	0.01	0.12
lam[9,4]	-0.02	-0.07	0.04
lam[9,5]	0.06	-0.00	0.10
lam[10,1]	0.08	0.02	0.14
lam[10,2]	0.12	0.07	0.17
lam[10,3]	0.13	0.07	0.17
lam[10,4]	0.04	-0.01	0.08
lam[10,5]	-0.02	-0.06	0.03
lam[11,1]	-0.16	-0.22	-0.04
lam[11,2]	0.15	0.03	0.21
lam[11,3]	-0.00	-0.06	0.08
lam[11,4]	0.06	-0.01	0.12
lam[11,5]	-0.01	-0.07	0.06
lam[12,1]	-0.10	-0.14	-0.05
lam[12,2]	0.11	0.06	0.14
lam[12,3]	0.09	0.05	0.13
lam[12,4]	0.08	0.04	0.11
lam[12,5]	-0.04	-0.07	-0.00

Table 47: λ credibility intervals

7.2 Trace Plots

Examples of trace plots are added from the NDLM of the population of *Microdon polygaloides*. Considering the number of parameters it would not be feasible to show evidence of convergence in all parameters. From the smooth, overlaying Markov Chains, showing no apparent trend, it can be concluded that convergence was achieved for these parameters. Estimates of other models have similarly reached convergence.

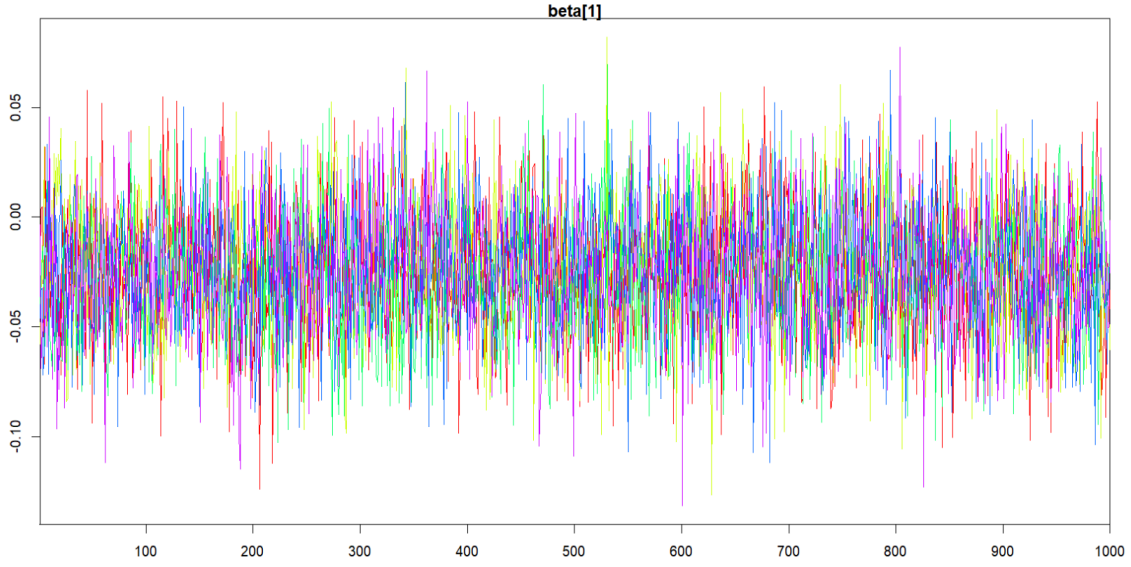

Figure 35: The trace plot of β_1 parameter from the NDLM of the population of *Microdon polygaloides* plants.

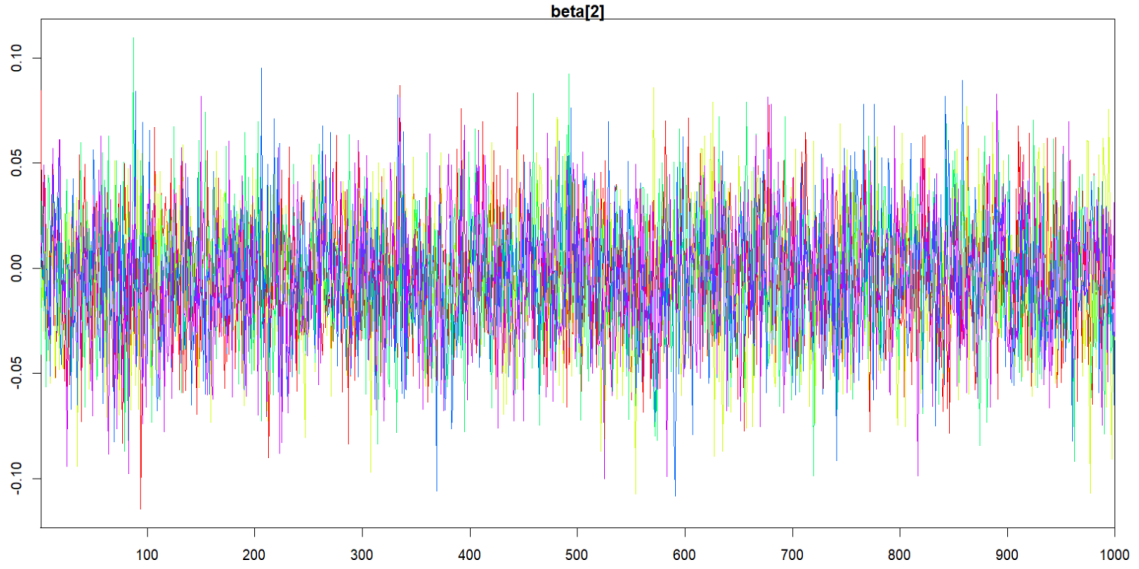

Figure 36: The trace plot of β_2 parameter from the NDLM of the population of *Microdon polygaloides* plants.

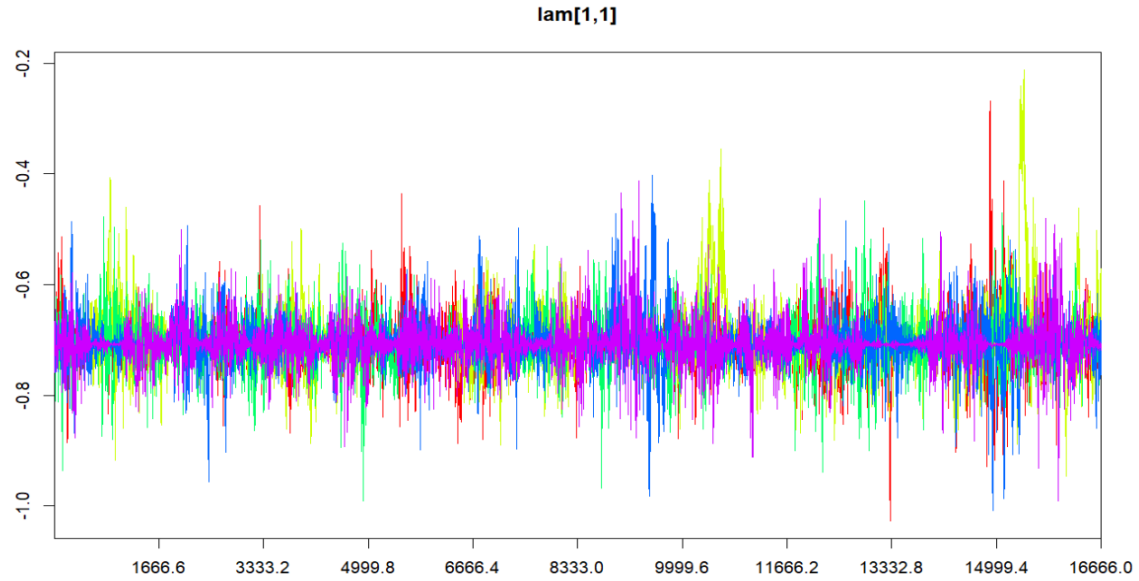

Figure 37: The trace plot of $\lambda_{1,1}$ parameter from the NDLM of the population of *Microdon polygaloides* plants.

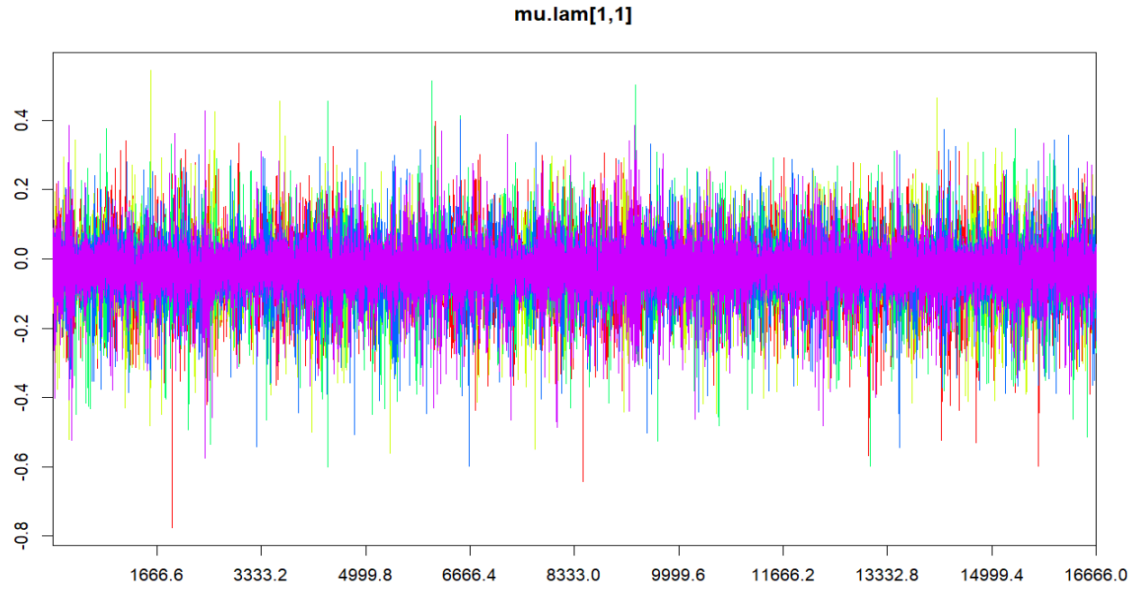

Figure 38: The trace plot of $\mu_{\lambda_{1,1}}$ parameter from the NDLM of the population of *Microdon polygaloides* plants.

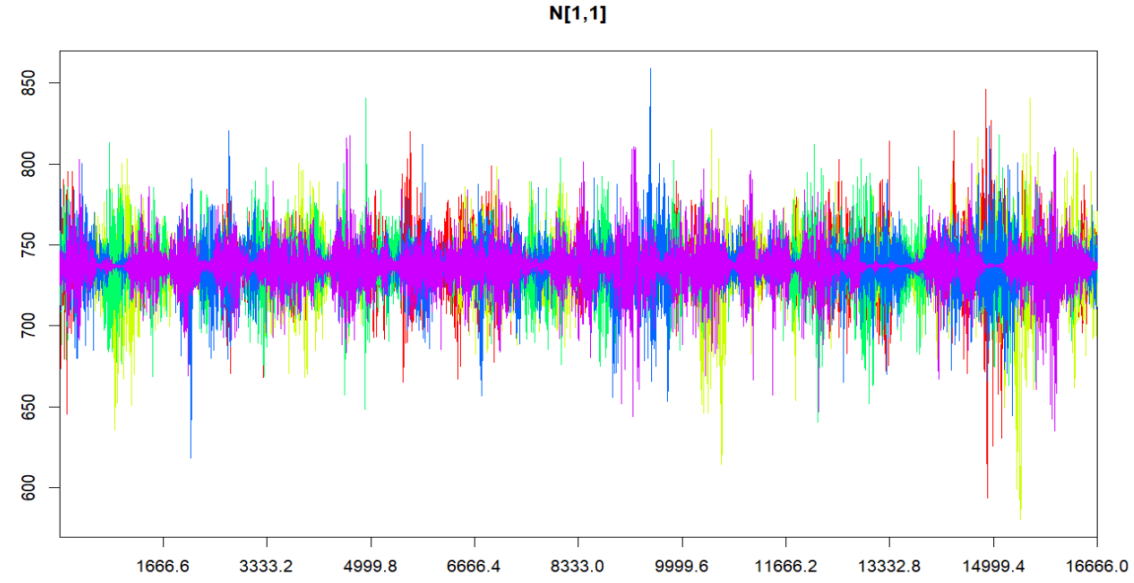

Figure 39: The trace plot of $_{1,1}$ estimate, (Population estimate for plot 1 in period 1), from the NDLM of the population of *Microdon polygaloides* plants.

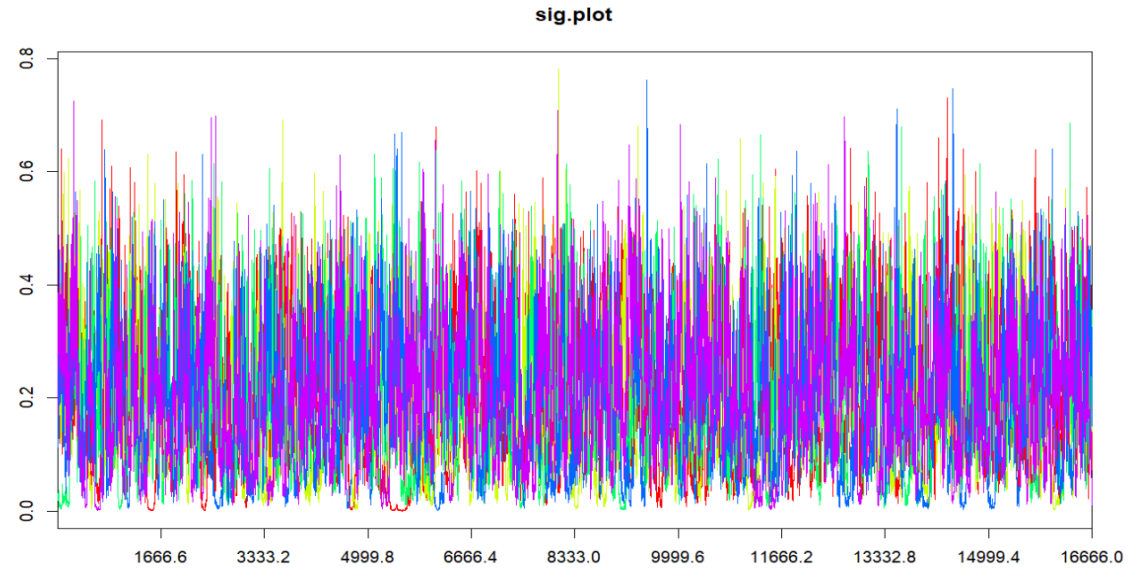

Figure 40: The trace plot of σ_{plot}, (The variance captured between plots), parameter from the NDLM of the population of *Microdon polygaloides* plants.

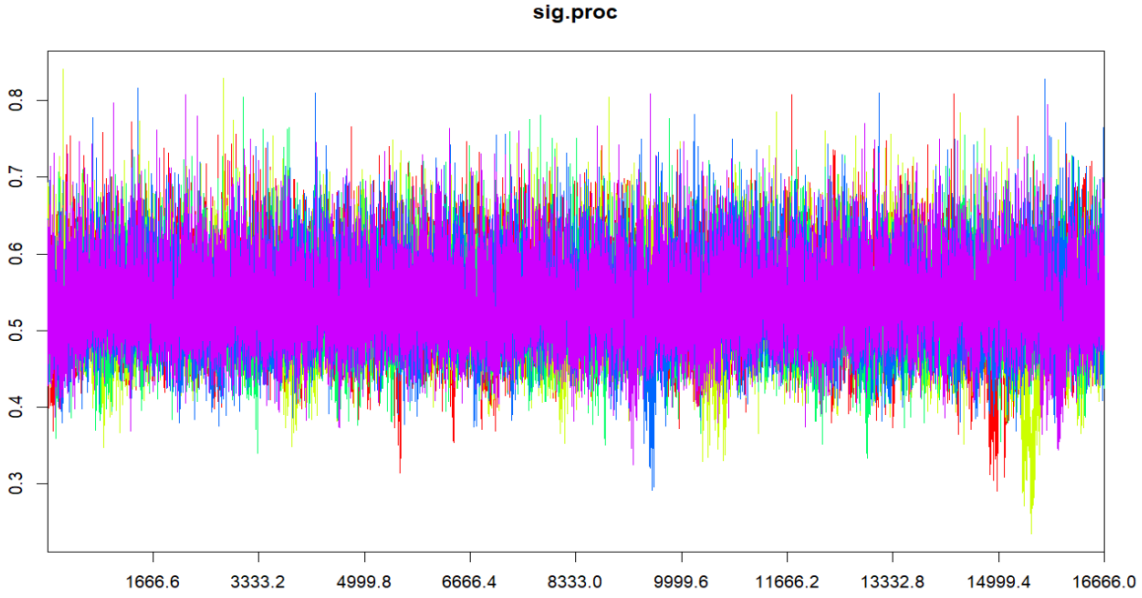

Figure 41: The trace plot of $\sigma_{process}$, (The variance in growth rate captured in the process equation), parameter from the NDLM of the population of *Microdon polygaloides* plants.

7.3 MARSS Plots

7.3.1 Renosterveld Plots

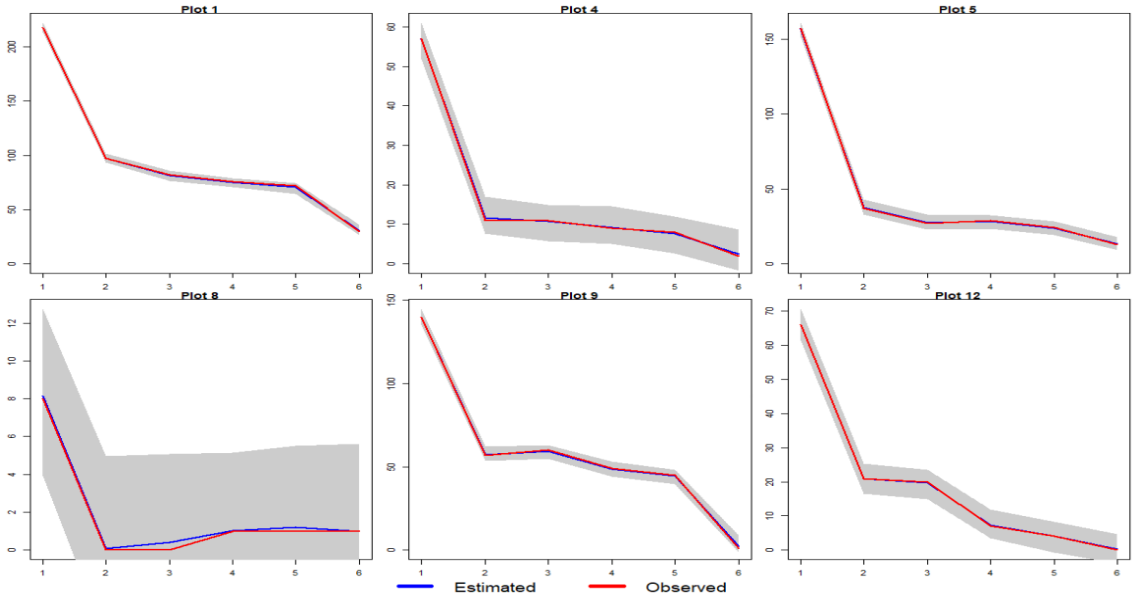

Figure 42: Population densities of *Othonna parviflora* in treatment plots in the Renosterveld with estimates from a multivariate model. The y-axis represents abundance of the population and the x-axis represents the time period.

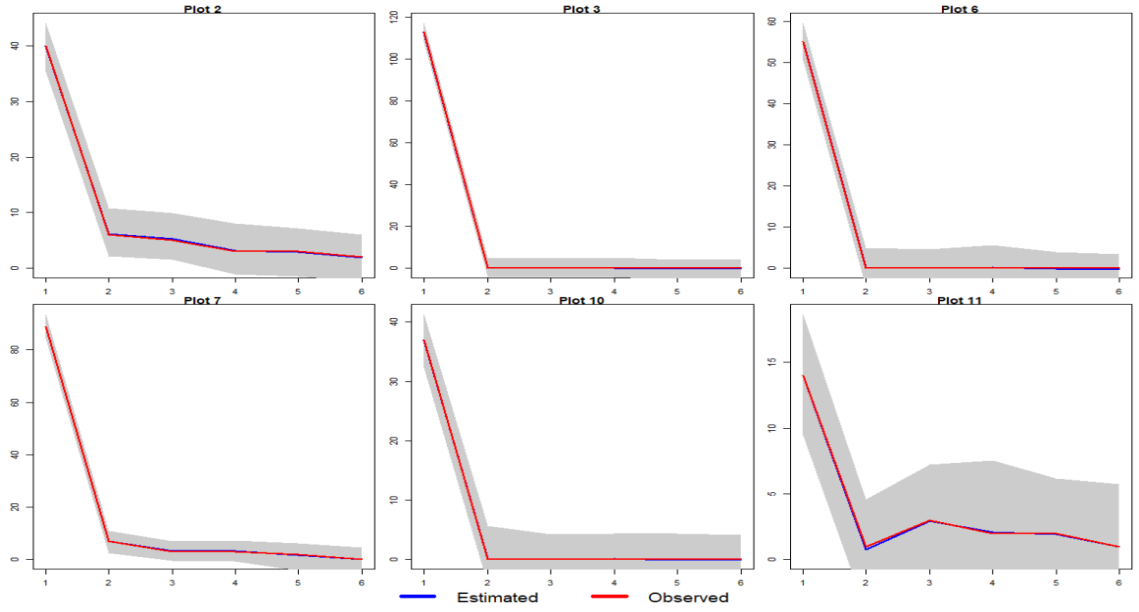

Figure 43: Population densities of *Othonna parviflora* in control plots in the Renosterveld with estimates from a multivariate model. The y-axis represents abundance of the population and the x-axis represents the time period.

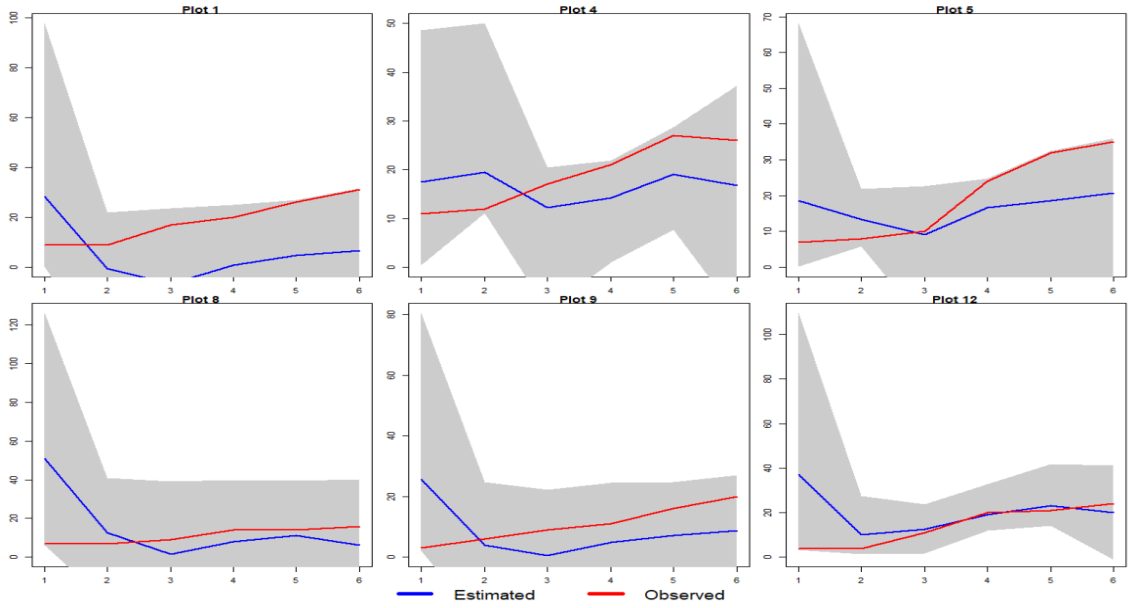

Figure 44: Population densities of *Elytropappus rhinocerotis* in treatment plots in the Renosterveld with estimates from a multivariate model. The y-axis represents abundance of the population and the x-axis represents the time period.

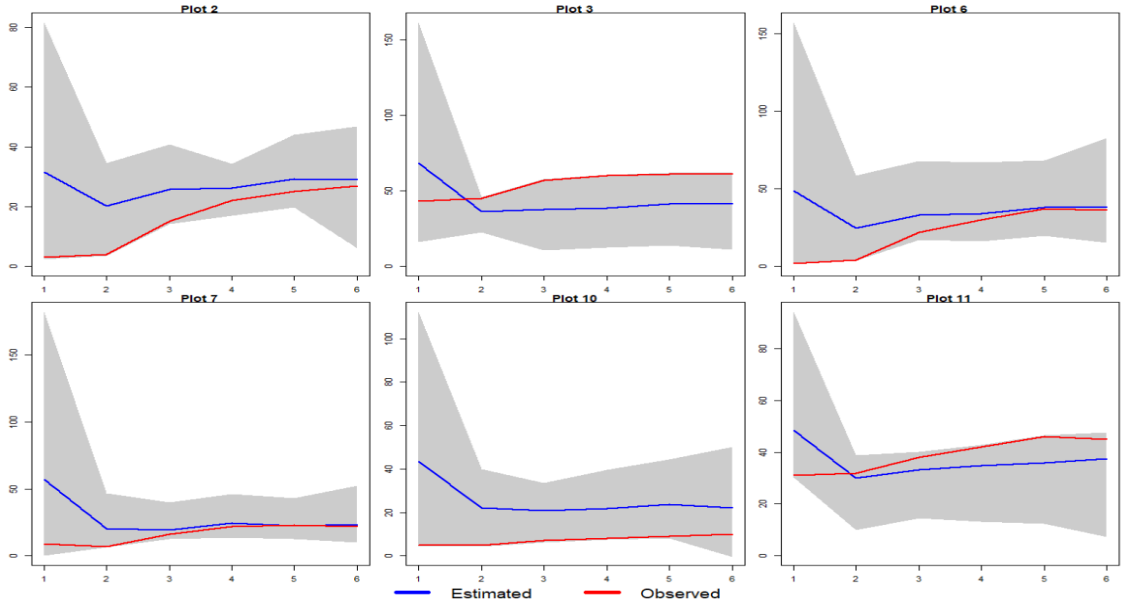

Figure 45: Population densities of *Elytropappus rhinocerotis* in control plots in the Renosterveld with estimates from a multivariate model. The y-axis represents abundance of the population and the x-axis represents the time period.

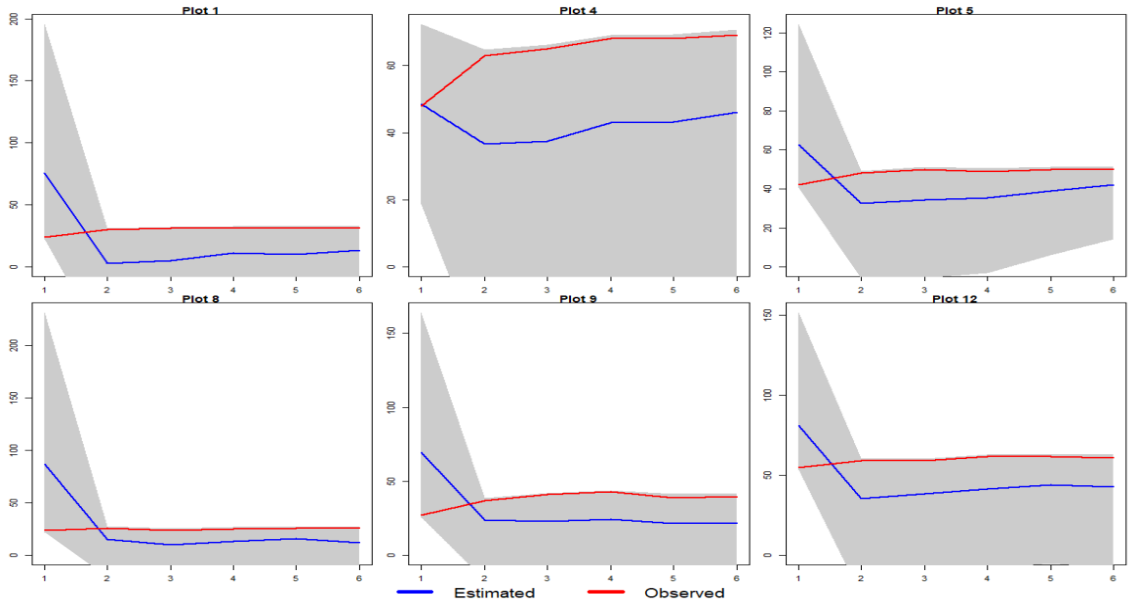

Figure 46: Population densities of *Passerina obtusifolia* in treatment plots in the Renosterveld with estimates from a multivariate model. The y-axis represents abundance of the population and the x-axis represents the time period.

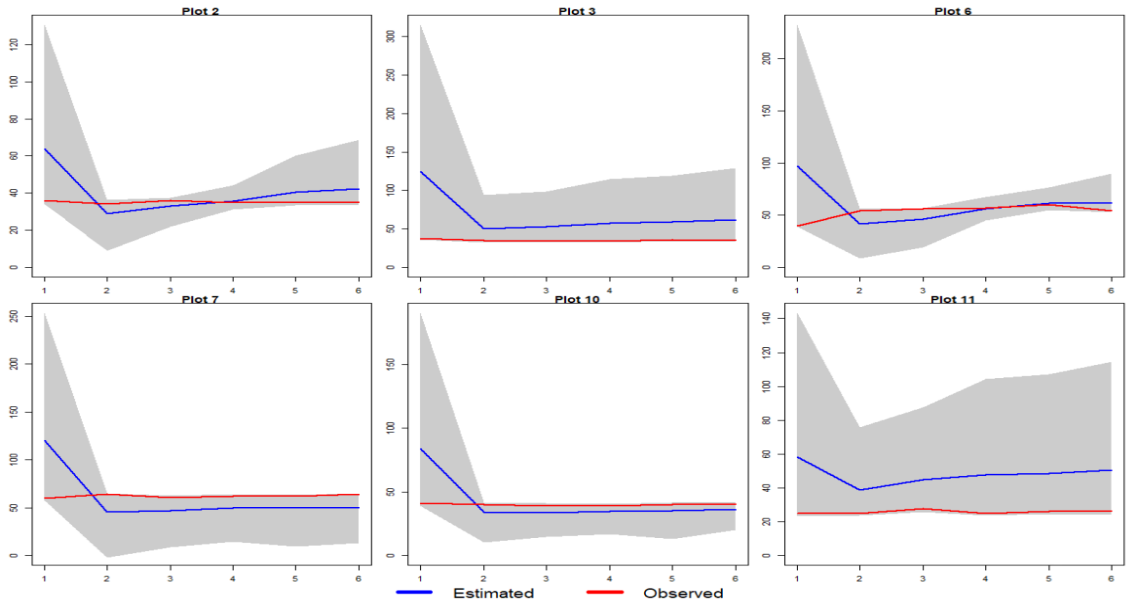

Figure 47: Population densities of *Passerina obtusifolia* in control plots in the Renosterveld with estimates from a multivariate model. The y-axis represents abundance of the population and the x-axis represents the time period.

7.3.2 Fynbos Plots

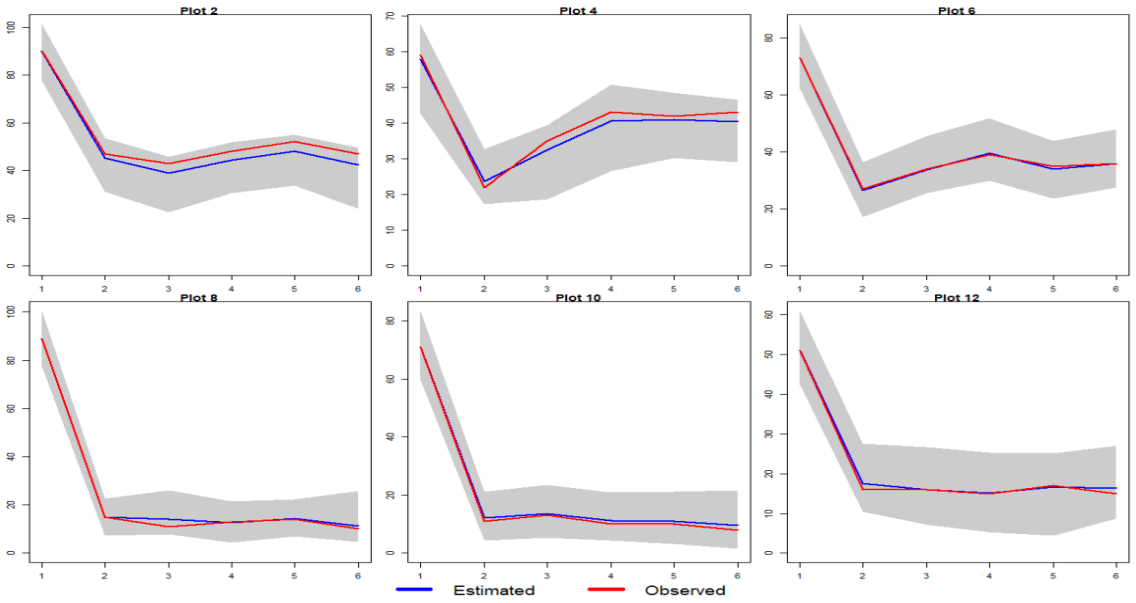

Figure 48: Population densities of *Aspalathus shawii* in treatment plots in the Fynbos with estimates from a multivariate model. The y-axis represents abundance of the population and the x-axis represents the time period.

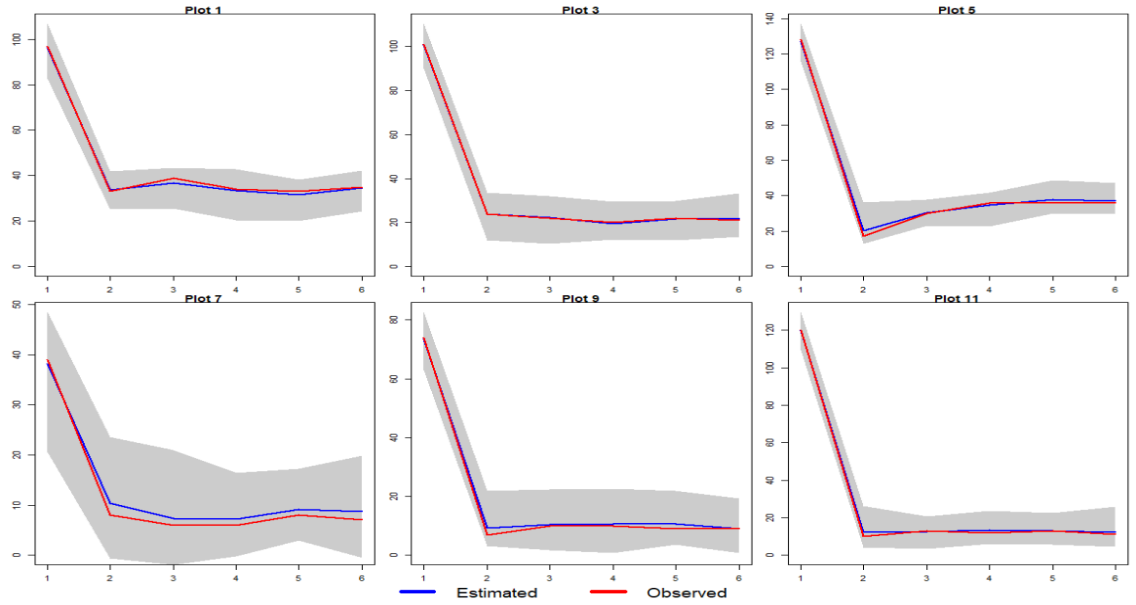

Figure 49: Population densities of *Aspalathus shawii* in control plots in the Fynbos with estimates from a multivariate model. The y-axis represents abundance of the population and the x-axis represents the time period.

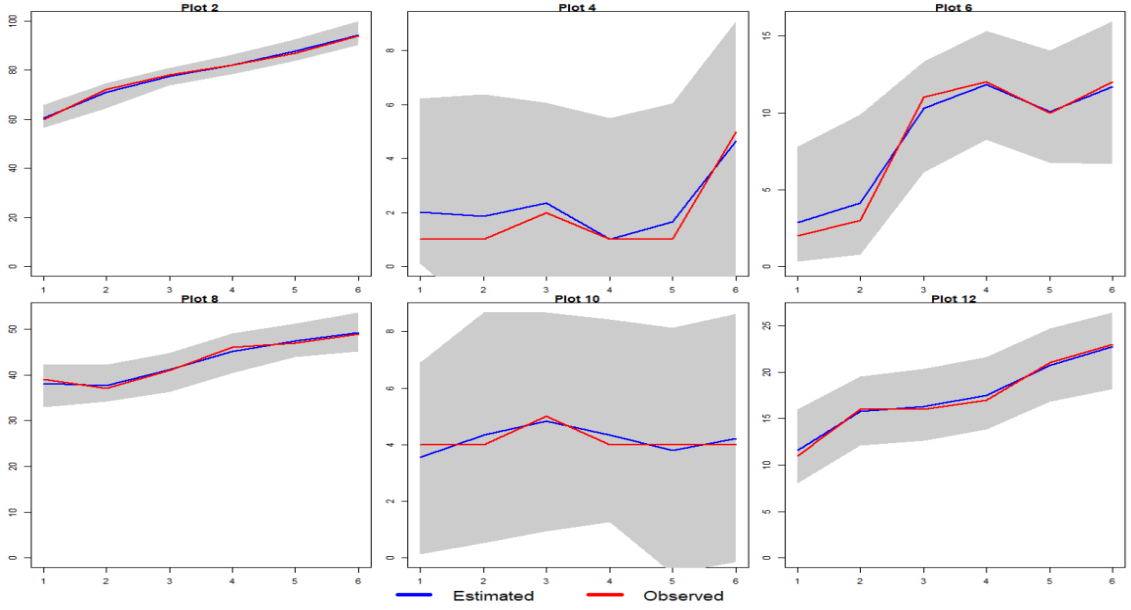

Figure 50: Population densities of *Agathosma capensis* in treatment plots in the Fynbos with estimates from a multivariate model. The y-axis represents abundance of the population and the x-axis represents the time period.

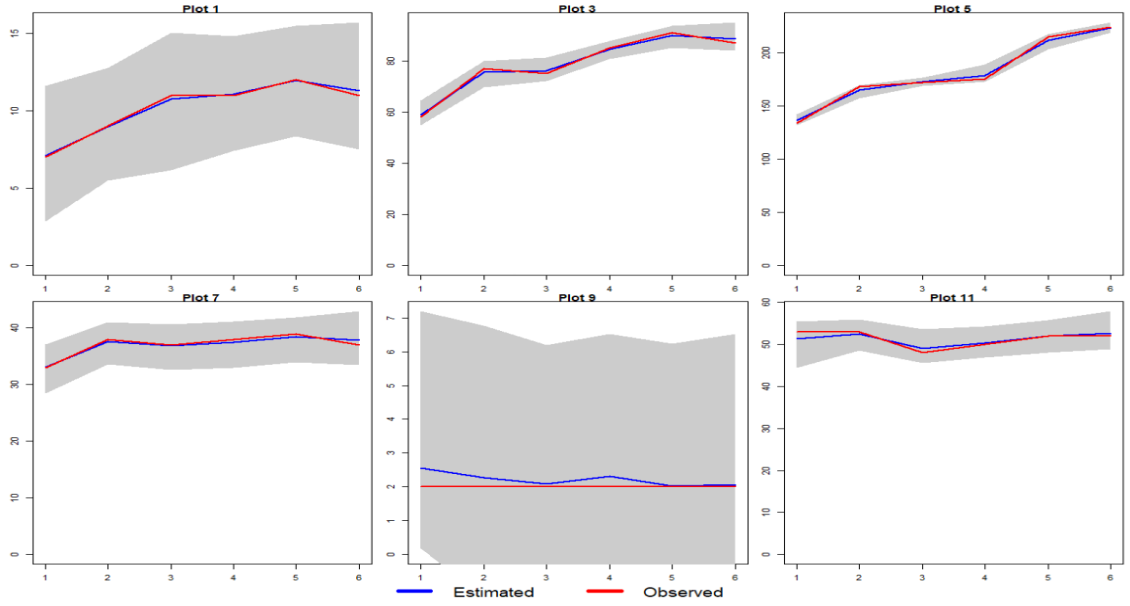

Figure 51: Population densities of *Agathosma capensis* in control plots in the Fynbos with estimates from a multivariate model. The y-axis represents abundance of the population and the x-axis represents the time period.

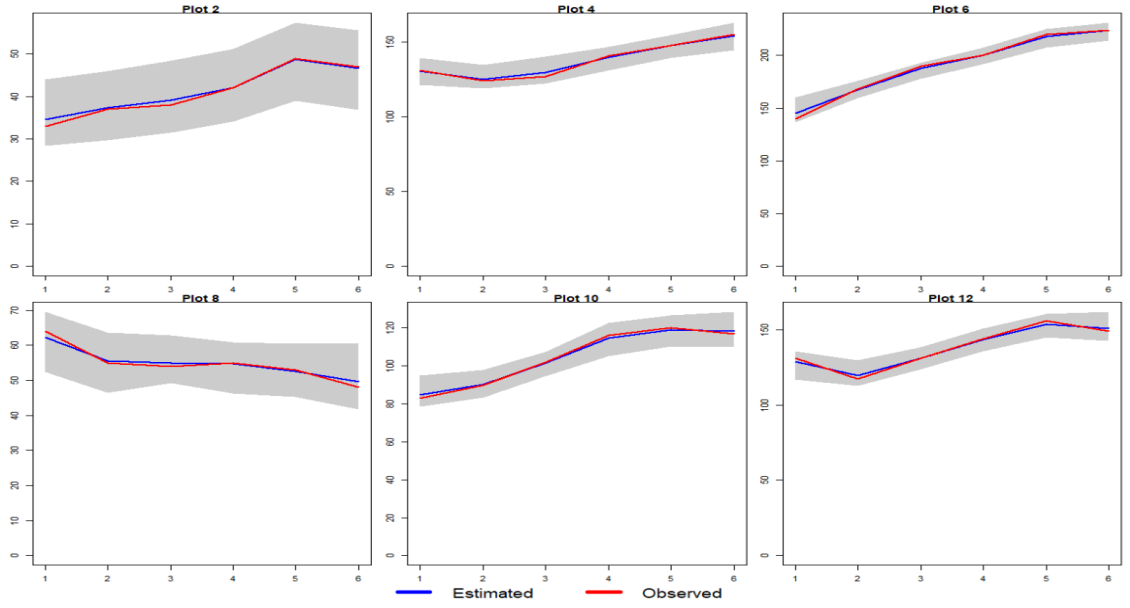

Figure 52: Population densities of *Wahlenbergia nodosa* in treatment plots in the Fynbos with estimates from a multivariate model. The y-axis represents abundance of the population and the x-axis represents the time period.

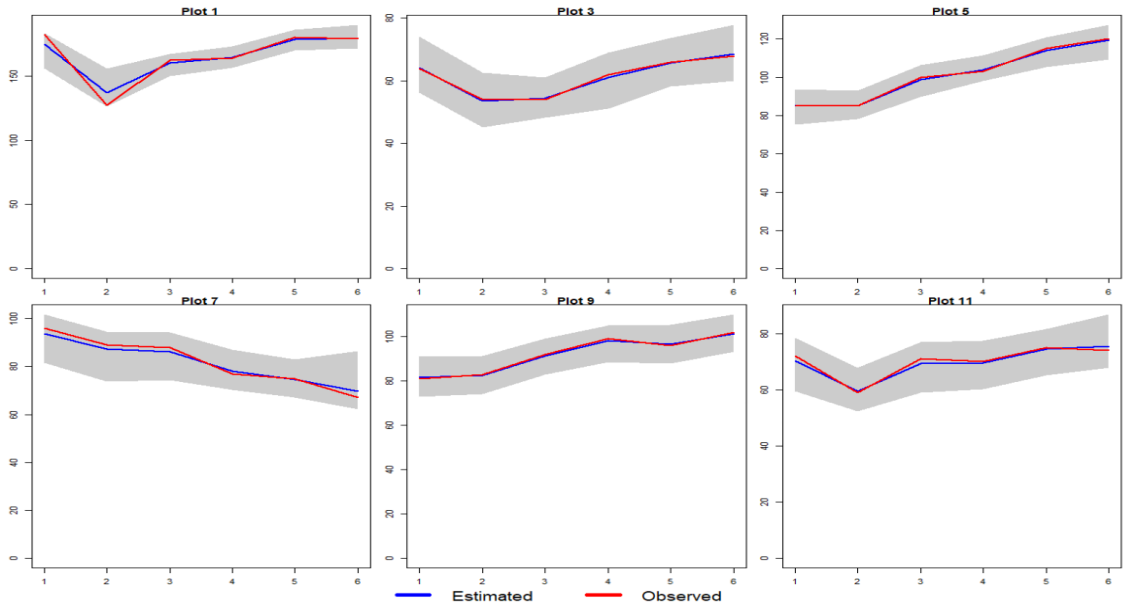

Figure 53: Population densities of *Wahlenbergia nodosa* in control plots in the Fynbos with estimates from a multivariate model. The y-axis represents abundance of the population and the x-axis represents the time period.

7.4 Box Plots

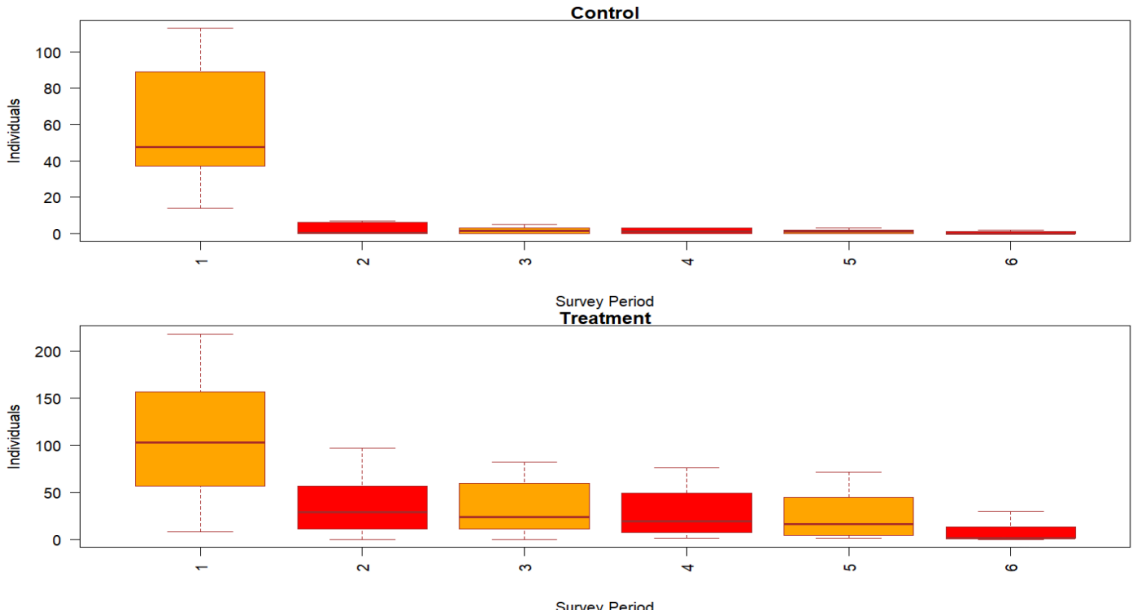

Figure 54: Two box plots showing the dispersion of *Othonna parviflora* plants in both treatment and control plots in the Renosterveld. The y-axis represents the abundance of the population in the biome and the x-axis represents the time period.

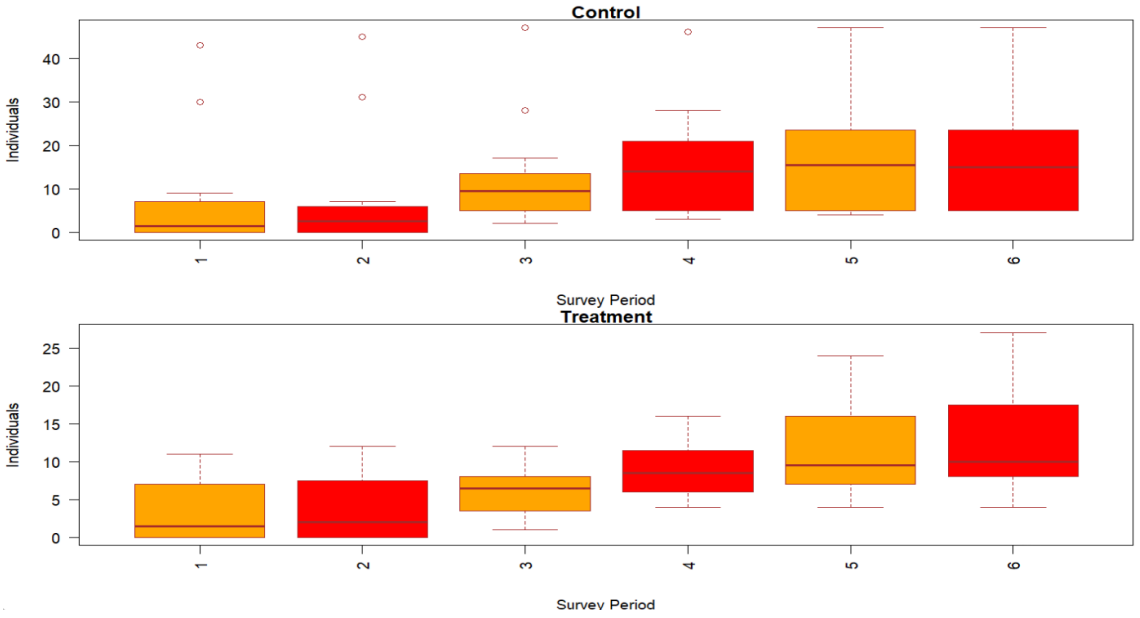

Figure 55: Two box plots showing the dispersion of *Elytropappus rhinocerotis* plants in both treatment and control plots in the Renosterveld. The y-axis represents the abundance of the population in the biome and the x-axis represents the time period.

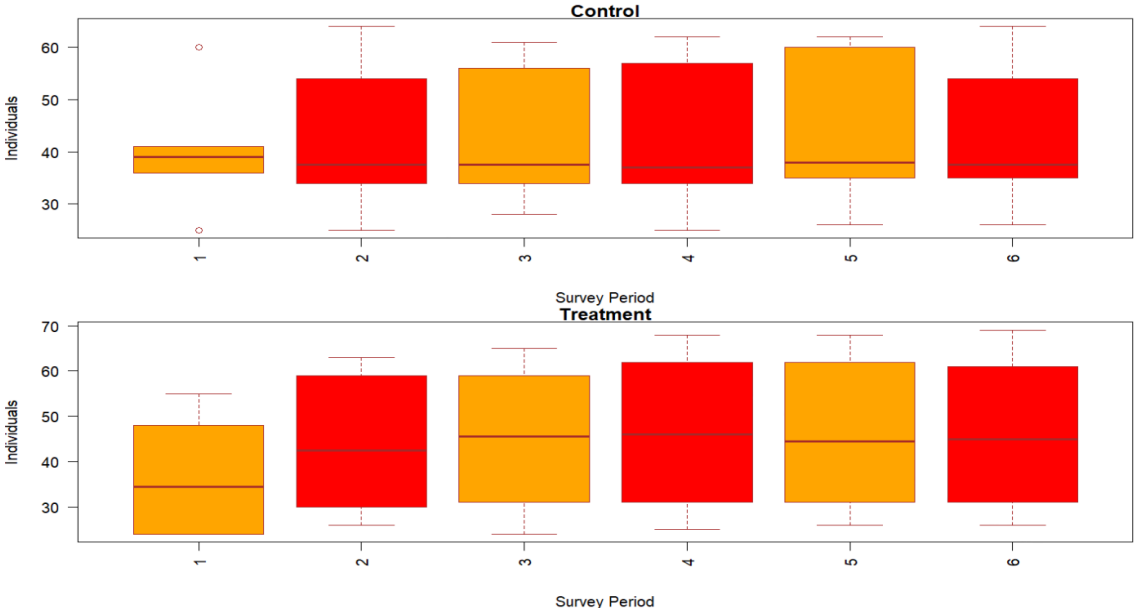

Figure 56: Two box plots showing the dispersion of *Passerina obtusifolia* plants in both treatment and control plots in the Renosterveld. The y-axis represents the abundance of the population in the biome and the x-axis represents the time period.

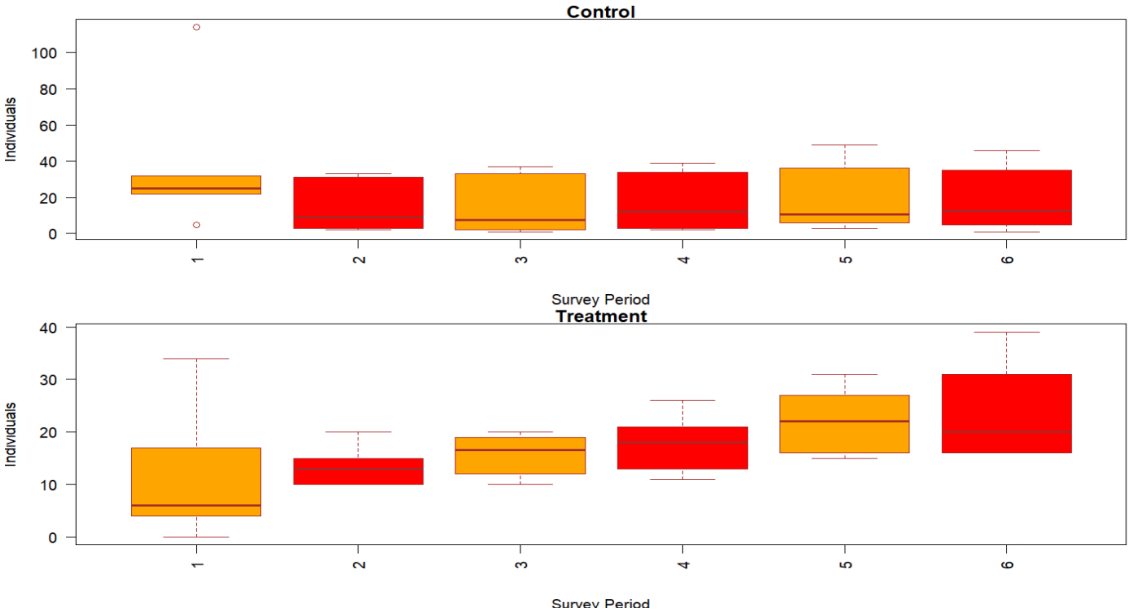

Figure 57: Two box plots showing the dispersion of *Selago glabrata* plants in both treatment and control plots in the Fynbos. The y-axis represents the abundance of the population in the biome and the x-axis represents the time period.

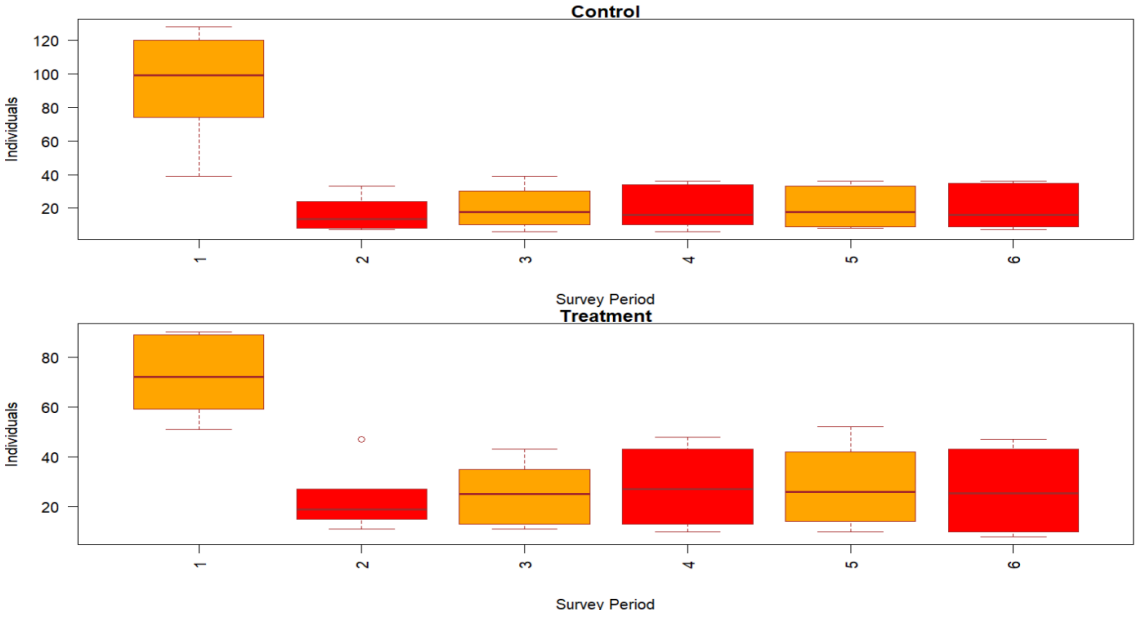

Figure 58: Two box plots showing the dispersion of *Aspalathus shawii* plants in both treatment and control plots in the Fynbos. The y-axis represents the abundance of the population in the biome and the x-axis represents the time period.

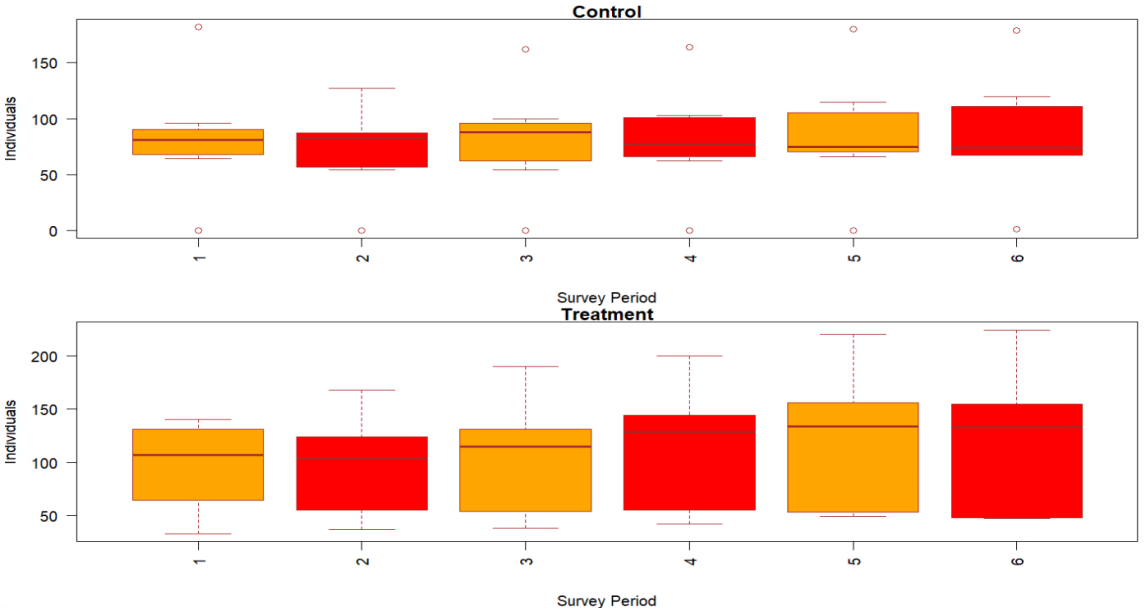

Figure 59: Two box plots showing the dispersion of *Wahlenbergia nodosa* plants in both treatment and control plots in the Fynbos. The y-axis represents the abundance of the population in the biome and the x-axis represents the time period.

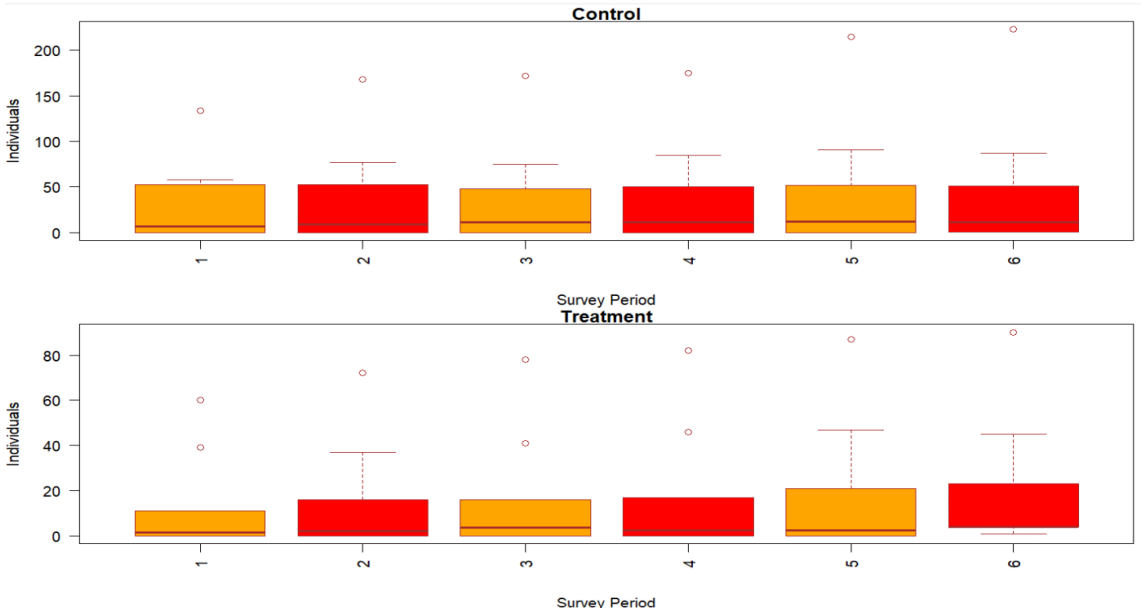

Figure 60: Two box plots showing the dispersion of *Agathosma capensis* plants in both treatment and control plots in the Fynbos. The y-axis represents the abundance of the population in the biome and the x-axis represents the time period.

7.5 Code

R code is presented for the model of the population of one species (*Microdon polygaloides*), and it's interaction with *Thesium strictum*, as an example of the code used to model all other species. The parameters for priors, and the sites where they are modeled, may vary as described in the research.

7.6 Code for Single species models

This code includes code to model a forecast period but this can be set to zero to run the normal state-space model.

```
library(tidyverse)
#Load In data
setwd("C:/Users/Serayen/Research Work/Data")
load("MicrodonDat_Plot_C.RData")
load("ClimDatRenV2.RData")
setwd("C:/Users/Serayen/Research Work/Code")

#Set Fynbos to 1 and Renostoveld as 0
dat <- data.Microdon.C %>% ungroup(by = "Site") %>%
    mutate(Site = ifelse(Site == "Fynbos",1,0))
#Set Treatment to 1 and control as 0
dat <- dat  %>% ungroup(by = "CT") %>% mutate(CT = ifelse(CT == "Treatment",1,0))

#data grouped by site
dat_fyn <- dat %>% filter(Site == 1)
#dat_fyn£seq_plotNo <- seq(1:12)
dat_ren <- dat %>% filter(Site == 0)
#Data grouped by treatment/control
dat_T <- dat %>% filter(CT == 1)
dat_C <- dat %>% filter(CT == 0)
#Data grouped by site and treatment/control
dat_T_fyn <- dat_fyn %>% filter(CT == 1)
dat_C_fyn <- dat_fyn %>% filter(CT == 0)
dat_T_Ren <- dat_T %>% filter(Site == 0)
dat_C_Ren <- dat_C %>% filter(Site == 0)

sink("Microdon2.jag")
cat("
    model {
```

```
# Priors

for(i in 1:x) #Loop trough each plot
{
#mu.lam[i,1] ~ dunif(0,10)
N[i,1] ~ dunif(0, 40000)

}
#Priors
sig.proc ~ dunif(0,500)
sig2.proc <- pow(sig.proc,2)
tau.proc <- pow(sig.proc, -2)

sig.obs ~ dunif(0,500)
sig2.obs <- pow(sig.obs, 2)
tau.obs <- pow(sig.obs, -2)


sig.plot ~ dunif(0,500)
sig2.plot <- pow(sig.plot , 2)
tau.plot <- pow(sig2.plot, -2)

beta[1] ~ dnorm(0, 0.001) #intercept
beta[2] ~ dnorm(0, 0.001) #B Treatmment

# Likelihood
for(i in 1:(x)){

#State Process
eps.plot[i] ~ dnorm(0,tau.plot)
#For each time step, after the first modeling each plot seperately
for(t in 1:(T-1))
{


mu.lam[i,t] = beta[1] + beta[2]*z1[i] + eps.plot[i]
lam[i,t] ~ dnorm(mu.lam[i,t], tau.proc)

N[i,(t+1)] = N[i,(t)] * exp(lam[i,t])
```

```
    }#end t


    #Observation Process

    for(t in 1:(T))
    {
    y[i,t]  ~ dnorm(N[i,t], tau.obs)
    }#end t

    }#end i

    #Forecasting
      for(i in 1:(x))
      {


        #State Process
        for(t in 1:fp)
        {
          #mean growth rate for ith plot
          mu.lam[i,T+t] = beta[1]+ beta[2] *z1[i] +  eps.plot[i]
          lam[i,T+t] ~ dnorm(mu.lam[i,T+t], tau.proc)
          N[i, T+t] = N[i,T+(t-1)] * exp(lam[i,T+t])

        }#end t


    }#end i



    }#end model



    ",fill = TRUE)#end cat
sink()

#Setting up Variables for JAGS function in R
```

```
Y = as.matrix(dat[, c(8:13)])  #Observed volume of population

#Site and treatment as categorical varibles
treat = as.matrix(dat[,7])


#Number of periods to forecast to
for_per = 0

#JAGS data to model
jags.data <- list(y = Y, T=6, x = dim(Y)[1], fp = for_per, z1 = as.numeric(treat))

# Function to generate starting values
inits <- function()
{
  list(sig.proc = runif(1, 0, 5),sig.plot=runif(1, 0, 5),
     beta =runif(2,0,1),  sig.obs = runif(1, 0, 10),
        N=  matrix(c(runif(dim(Y)[1],0,5000),
        rep(NA,(dim(Y)[2]-1+(for_per))*dim(Y)[1])),
  nrow=dim(Y)[1]))
}


# Parameters to be estimated
parameters <- c("lam", "beta", "mu.lam", "sig.obs", "sig.proc", "N","sig.plot")


# MCMC settings
nc <- 5 # Number of chains
ni <- 100000 # Number of draws from posterior (for each chain)
nb <- 50000 # Number of draws to discard as burn in
nt <- 3 # Thinning rate


#Start Gibbs sampler: Run model in JAGS and save results in object called ssm
#***Useful Data is saved in objects so it is not necessary to run this to check th
ssm2 <- jags(jags.data, inits, parameters,
    "Microdon2.jag", n.chains = nc, n.thin = nt, n.iter = ni, n.burnin = nb)

ssm2 <- autojags(ssm2, n.iter=1000)
```

```
setwd("C:/Users/Serayen/Research Work/Data")
#save(ssm2, file = "MicrodonR_SSM.RData")
#load("MicrodonR_SSM.RData")
setwd("C:/Users/Serayen/Research Work/Code")

#Estimations of population size
N.out <- ssm2$BUGSoutput$mean$N
#Predicted Data
tmp <- as_tibble(N.out)
tmp <-
    rename(tmp, "1" = "V1", "2" = "V2" , "3" ="V3",
                "4" = "V4", "5" = "V5", "6" = "V6")
preds <- as_tibble(cbind(dat[,1:7],tmp))
preds_T <- preds %>% filter(CT == 1)
preds_C <- preds %>% filter(CT == 0)

N.out_T <- as.matrix(preds_T[, c(8:(13+for_per))])
N.out_C <- as.matrix(preds_C[, c(8:(13+for_per))])

Y_T = as.matrix(dat_T[, c(8:13)])
Y_C = as.matrix(dat_C[, c(8:13)])

#Summary stats of estimations population volumes
N.sum <- ssm2$BUGSoutput$summary

#Graph for inspection purposes
N1.sum <- N.sum[seq(1,196, by = 12),]
N1.sum <- N1.sum[1:(6+for_per),]

plot(N.out[1,], type = 'l', ylim = c(0, max(N1.sum[,7])),
    ylab = "Volume", xlab = "Time Step" ,
    main = "Estimated and \n Observed Population at \n Plot 1 Control")

polygon(c(seq(1:6),rev(seq(1:6))),c(N1.sum[,3],rev(N1.sum[,7])),
    col = "grey80", border = FALSE)

lines(N.out[1,], type = 'l', col = 'blue')
lines(Y[1,], type ='l', col = 'red')
```

```
#Summary stats of estimations population volumes
period <- (6+for_per)
nBeta <- 2
#Number of plots there were recordings in
nPlots <-12
N.sum <- ssm2$BUGSoutput$summary
# mu.lam + lam + N + deviance
No_entries = (2*12*(period-1)) + 12*period +1 + nBeta
deviance.sum <- N.sum[((12*period)+2),]
N.sum<- rbind(N.sum[1:((12*period+2)),], N.sum[((12*period)+4):No_entries,])
No_entries = (2*12*(period-1)) + 12*period  + nBeta
#Summary Statistics for Confidence intervals By Plot Number
N_sum <- vector("list")
for(i in 1:12)
{

  Ni.sum <-N.sum[seq(i,No_entries, by = 12),]
  N_sum[[i]] <- Ni.sum[1:period,]
}

Add_legend <- function()
{
  par(fig = c(0, 1, 0, 1), oma = c(0, 0, 0, 0), mar = c(0, 0, 0, 0), new = TRUE)
  plot(0, 0, type = 'l', bty = 'n', xaxt = 'n', yaxt = 'n')
  legend('bottom',legend =
    c("Estimated", "Observed"), col = c("blue", "red"),
    lwd = 5, xpd = TRUE, horiz = TRUE, cex = 1.8, seg.len=1.4, bty = 'n')
}

#Graphs for Renosterveld Treatment Plots
par(oma = c(4,1,1,1), mfrow = c(2, 3), mar = c(2, 2, 1, 1))
for(i in 1:6)
{
  plotNo <- as.numeric(dat_T[i,14])

  title= paste( "Plot", toString(as.numeric(dat_T[i,1])) )


  plot(N.out_T[i,], type = 'l', col = 'blue',
    ylim = c(0, max(c(N_sum[[plotNo]][1:6,7],Y_T[i,])) ) , ylab = "Volume",
```

```
        xlab = "Time Step",  main = title, cex.main = 1.3)
    polygon(c(seq(1:period),rev(seq(1:period))),
        c(N_sum[[plotNo]][,3],rev(N_sum[[plotNo]][,7])),
    col = "grey80", border = FALSE)
    lines(N.out_T[i,], type = 'l', col = 'blue', lwd = 2)
    lines(Y_T[i,], type ='l', col = 'red', lwd = 2)
}
Add_legend()


#Graphs for Renosterveld Control Plots
par(oma = c(4,1,1,1), mfrow = c(2, 3), mar = c(2, 2, 1, 1))
for(i in 1:6)
{
  plotNo <- as.numeric(dat_C[i,14])

  title= paste( "Plot", toString(as.numeric(dat_C[i,1])) )

  plot(N.out_C[i,], type = 'l', col = 'blue',
  ylim = c(0, max(c(N_sum[[plotNo]][1:6,7],Y_C[i,])) ) ,
  ylab = "Volume", xlab = "Time Step",  main = title, cex.main = 1.3)
  polygon(c(seq(1:period),
  rev(seq(1:period))),c(N_sum[[plotNo]][,3],
    rev(N_sum[[plotNo]][,7])),col = "grey80", border = FALSE)
  lines(N.out_C[i,], type = 'l', col = 'blue', lwd = 2)
  lines(Y_C[i,], type ='l', col = 'red', lwd = 2)
}
Add_legend()

###############################################
#--------------Get Stats--------------------#

#Put summary into list
Nplots <- nrow(dat)
nBeta <- 2
#Summary stats of estimations population volumes
period <- (6+for_per)
N.sum <- ssm2$BUGSoutput$summary
No_entries = (2*Nplots*(period-1)) + Nplots*period +1
deviance.sum <- N.sum[((Nplots*period)+1+nBeta),]
```

```
beta.out <- N.sum[((Nplots*period)+1):((Nplots*period)+nBeta),]
N.sum<- rbind(N.sum[1:((Nplots*period)),],
              N.sum[((Nplots*period)+nBeta+2):No_entries,])
No_entries = (2*Nplots*(period-1)) + Nplots*period - nBeta
#Summary Statistics for Confidence intervals By Plot Number
N_sum <- vector("list")
for(i in 1:Nplots)
{

  Ni.sum <-N.sum[seq(i,No_entries, by = Nplots),]
  N_sum[[i]] <- Ni.sum
}



#Lambdas
lams <- ssm2$BUGSoutput$mean$lam

lams_mat <- cbind(dat[,7], dat[,1], as.matrix(lams))

lams_T <- lams_mat %>% filter(CT ==1)
lams_T <- lams_T[,-1]

lams_C <- lams_mat %>% filter(CT ==0)
lams_C <- lams_C[,-1]

#mu_lamdas
mu.lams <- ssm2$BUGSoutput$mean$mu.lam

mu.lams_mat <- cbind(dat[,7], dat[,1], as.matrix(mu.lams))


mu.lams_T <- mu.lams_mat %>% filter(CT ==1)
mu.lams_T <- mu.lams_T[,-1]

mu.lams_C <- mu.lams_mat %>% filter(CT ==0)
mu.lams_C <- mu.lams_C[,-1]

#Betas
beta_tab <- beta.out[,c(1,2,3,7)]
```

7.7 Interaction Models

```
library(tidyverse)
#Load In data
setwd("C:/Users/Serayen/Research Work/Data")
load("MicrodonDat_Plot_C.RData")
load("ClimDatRenV2.RData")
load("Thesium_Plot_C.RData")
setwd("C:/Users/Serayen/Research Work/Code")
#Set Fynbos to 1 and Renostoveld as 0
dat <- data.Microdon.C %>% ungroup(by = "Site") %>%
            mutate(Site = ifelse(Site == "Fynbos",1,0))
#Set Treatment to 1 and control as 0
dat <- dat  %>% ungroup(by = "CT") %>% mutate(CT = ifelse(CT == "Treatment",1,0))


#Thesium data
dat.th <- data.Thesium.C %>%
    ungroup(by = "Site") %>% mutate(Site = ifelse(Site == "Fynbos",1,0))
dat.th <- dat.th  %>% ungroup(by = "CT") %>%
    mutate(CT = ifelse(CT == "Treatment",1,0))
dat.th_ren <- dat.th %>% filter(Site == 0)
dat.th_fyn <- dat.th %>% filter(Site == 1)


#data grouped by site
dat_fyn <- dat %>% filter(Site == 1)
#dat_fyn£seq_plotNo <- seq(1:12)
dat_ren <- dat %>% filter(Site == 0)
#Data grouped by treatment/control
dat_T <- dat %>% filter(CT == 1)
dat_C <- dat %>% filter(CT == 0)
#Data grouped by site and treatment/control
dat_T_fyn <- dat_fyn %>% filter(CT == 1)
dat_C_fyn <- dat_fyn %>% filter(CT == 0)
dat_T_Ren <- dat_T %>% filter(Site == 0)
dat_C_Ren <- dat_C %>% filter(Site == 0)
```

```
sink("Microdon_Th_R.jag")
cat("
    model {
    # Priors

    for(i in 1:x) #Loop trough each plot
    {
    #mu.lam[i,1] ~ dunif(0,10)
    N[i,1] ~ dunif(0, 100000)

    }
    #Priors
    sig.proc ~ dunif(0,500)
    sig2.proc <- pow(sig.proc,2)
    tau.proc <- pow(sig.proc, -2)

    sig.obs ~ dunif(0,500)
    sig2.obs <- pow(sig.obs, 2)
    tau.obs <- pow(sig.obs, -2)


    sig.plot ~ dunif(0,500)
    sig2.plot <- pow(sig.plot , 2)
    tau.plot <- pow(sig2.plot, -2)

    beta[1] ~ dnorm(0, 1000) #intercept
    beta[2] ~ dnorm(0, 1000) #B Treatmment
    beta[3] ~ dnorm(0, 500) #B Thesium Treatment
    beta[4] ~ dnorm(0, 500) #B Thesium Control


    # Likelihood
    for(i in 1:(x)){

    #State Process
    eps.plot[i] ~ dnorm(0,tau.plot)
    #For each time step after the first modeling each plot seperately
    for(t in 1:(T-1))
    {
```

```
    mu.lam[i,t] = beta[1] + beta[2]*z1[i] +
                    beta[3]*z2[i,t] + beta[4]*z3[i,t] + eps.plot[i]
    lam[i,t] ~ dnorm(mu.lam[i,t], tau.proc)

    N[i,(t+1)] = N[i,(t)] * exp(lam[i,t])

    }#end t


    #Observation Process

    for(t in 1:(T))
    {
    y[i,t]  ~ dnorm(N[i,t], tau.obs)
    }#end t

    }#end i



    }#end model



    ",fill = TRUE)#end cat
sink()

#Renosterveld SSM
dat <- dat_ren
dat <-dat %>% add_column(seq_plotNo = seq(1,nrow(dat)))
#Data grouped by treatment/control
dat_T <- dat %>% filter(CT == 1)
dat_C <- dat %>% filter(CT == 0)

#Setting up Variables for JAGS function in R
Y = as.matrix(dat[, c(8:13)])  #Observed volume of population

#site = as.matrix(dat[,2]) #Site and treatment as categorical varibles
treat = as.matrix(dat[,7])
```

```
#Data for thesium in treatment plots, control plots set to zero
X_T <- dat.th_ren %>% mutate(Count.A = ifelse(CT== 0,0, Count.A) ) %>%
        mutate(Count.B = ifelse(CT== 0,0, Count.B) ) %>%
        mutate(Count.C = ifelse(CT== 0,0, Count.C) ) %>%
        mutate(Count.D = ifelse(CT== 0,0, Count.D) ) %>%
        mutate(Count.E = ifelse(CT== 0,0, Count.E) ) %>%
        mutate(Count.F = ifelse(CT== 0,0, Count.F) )

#Data for thesium in control plots, treatment plots set to zero
X_C <- dat.th_ren %>% mutate(Count.A = ifelse(CT== 1,0, Count.A) ) %>%
        mutate(Count.B = ifelse(CT== 1,0, Count.B) ) %>%
        mutate(Count.C = ifelse(CT== 1,0, Count.C) ) %>%
        mutate(Count.D = ifelse(CT== 1,0, Count.D) ) %>%
        mutate(Count.E = ifelse(CT== 1,0, Count.E) ) %>%
        mutate(Count.F = ifelse(CT== 1,0, Count.F) )


#Number of periods to forecast to
for_per = 0


#Setup JAGS data
jags.data <- list(y = Y, T=6, x = dim(Y)[1],
    fp = for_per, z1 = as.numeric(treat),
    z2 = as.matrix(dat.th_ren[,8:13]))
# Function to generate starting values
inits <- function()
{
  list(sig.proc = runif(1, 0, 5),sig.plot=runif(1, 0, 5),
    beta =runif(4,0,1),  sig.obs = runif(1, 0, 10),
    N=  matrix(c(runif(dim(Y)[1],0,5000),
    rep(NA,(dim(Y)[2]-1+(for_per))*dim(Y)[1])), nrow=dim(Y)[1]))
}


# Parameters to be estimated
parameters <- c("lam", "beta", "mu.lam", "sig.obs", "sig.proc", "N","sig.plot")
```

```
# MCMC settings
nc <- 5 # Number of chains
ni <- 150000 # Number of draws from posterior (for each chain)
nb <- 50000 # Number of draws to discard as burn in
nt <- 3 # Thinning rate


#Start Gibbs sampler: Run model in JAGS and save results in object called ssm
#***Useful Data is saved in objects so it is not necessary to run this to check th
ssm2 <- jags(jags.data, inits, parameters,
        "Microdon_Th_R.jag", n.chains = nc,
        n.thin = nt, n.iter = ni, n.burnin = nb)

ssm2 <- autojags(ssm2, n.iter=10000)


setwd("C:/Users/Serayen/Research Work/Data")
#save(ssm2, file = "Microdon_Th_R_SSM.RData")
#load("Microdon_Th_R_SSM.RData")
setwd("C:/Users/Serayen/Research Work/Code")

#Predicted Population sizes
N.out <- ssm2$BUGSoutput$mean$N
tmp <- as_tibble(N.out)
tmp <- rename(tmp, "1" = "V1", "2" = "V2" , "3" ="V3",
                "4" = "V4", "5" = "V5", "6" = "V6")
preds <- as_tibble(cbind(dat[,1:7],tmp))
preds_T <- preds %>% filter(CT == 1)
preds_C <- preds %>% filter(CT == 0)

N.out_T <- as.matrix(preds_T[, c(8:(13+for_per))])
N.out_C <- as.matrix(preds_C[, c(8:(13+for_per))])

Y_T = as.matrix(dat_T[, c(8:13)])
Y_C = as.matrix(dat_C[, c(8:13)])

#Summary stats of estimations population volumes
N.sum <- ssm2$BUGSoutput$summary

#plot for examination purposes
```

```
N1.sum <- N.sum[seq(1,196, by = 12),]
N1.sum <- N1.sum[1:(6+for_per),]

plot(N.out[1,], type = 'l', ylim = c(0, max(N1.sum[,7])),
        ylab = "Volume", xlab = "Time Step" ,
        main = "Estimated and \n Observed Population at \n Plot 1 Control")
polygon(c(seq(1:6),rev(seq(1:6))),
        c(N1.sum[,3],rev(N1.sum[,7])),
        col = "grey80", border = FALSE)
lines(N.out[1,], type = 'l', col = 'blue')
lines(Y[1,], type ='l', col = 'red')

#Summary stats of estimations population volumes
period <- (6+for_per)
nBeta <- 4
#Number of plots there were recordings in
nPlots <-12
N.sum <- ssm2$BUGSoutput$summary
# mu.lam + lam + N + deviance
No_entries = (2*12*(period-1)) + 12*period +1 + nBeta
deviance.sum <- N.sum[((12*period)+2),]
N.sum<- rbind(N.sum[1:((12*period+2)),], N.sum[((12*period)+4):No_entries,])
No_entries = (2*12*(period-1)) + 12*period  + nBeta
#Summary Statistics for Confidence intervals By Plot Number
N_sum <- vector("list")
for(i in 1:12)
{

  Ni.sum <-N.sum[seq(i,No_entries, by = 12),]
  N_sum[[i]] <- Ni.sum[1:period,]
}

Add_legend <- function()
{
  par(fig = c(0, 1, 0, 1),
  oma = c(0, 0, 0, 0),
  mar = c(0, 0, 0, 0), new = TRUE)
  plot(0, 0, type = 'l', bty = 'n', xaxt = 'n', yaxt = 'n')
  legend('bottom',
  legend = c("Estimated", "Observed"),
```

```
  col = c("blue", "red"), lwd = 5, xpd = TRUE,
  horiz = TRUE, cex = 1.8, seg.len=1.4, bty = 'n')
}

#Graphs for Renosterveld Treatment Plots
par(oma = c(4,1,1,1), mfrow = c(2, 3), mar = c(2, 2, 1, 1))
for(i in 1:6)
{
  plotNo <- as.numeric(dat_T[i,14])

  title= paste( "Plot", toString(as.numeric(dat_T[i,1])) )

  plot(N.out_T[i,], type = 'l', col = 'blue',
    ylim = c(0, max(c(N_sum[[plotNo]][1:6,7],Y_T[i,])) ) ,
    ylab = "Volume", xlab = "Time Step",
    main = title, cex.main = 1.3)

  polygon(c(seq(1:period),
    rev(seq(1:period))),c(N_sum[[plotNo]][,3],
    rev(N_sum[[plotNo]][,7])),
    col = "grey80", border = FALSE)
  lines(N.out_T[i,], type = 'l', col = 'blue', lwd = 2)
  lines(Y_T[i,], type ='l', col = 'red', lwd = 2)
}
Add_legend()


#Graphs for Renosterveld Control Plots
par(oma = c(4,1,1,1), mfrow = c(2, 3), mar = c(2, 2, 1, 1))
for(i in 1:6)
{
  plotNo <- as.numeric(dat_C[i,14])

  title= paste( "Plot", toString(as.numeric(dat_C[i,1])) )

  plot(N.out_C[i,], type = 'l', col = 'blue',
    ylim = c(0, max(c(N_sum[[plotNo]][1:6,7],Y_C[i,])) ) ,
    ylab = "Volume", xlab = "Time Step",
    main = title, cex.main = 1.3)
```

```
  polygon(c(seq(1:period),rev(seq(1:period))),
    c(N_sum[[plotNo]][,3],
    rev(N_sum[[plotNo]][,7])),
    col = "grey80", border = FALSE)
  lines(N.out_C[i,], type = 'l', col = 'blue', lwd = 2)
  lines(Y_C[i,], type ='l', col = 'red', lwd = 2)
}
Add_legend()

################################################
#--------------Get Stats--------------------#

#Put summary into list
Nplots <- nrow(dat)
nBeta <- 4
#Summary stats of estimations population volumes
period <- (6+for_per)
N.sum <- ssm2$BUGSoutput$summary
No_entries = (2*Nplots*(period-1)) + Nplots*period +1
deviance.sum <- N.sum[((Nplots*period)+1+nBeta),]
beta.out <- N.sum[((Nplots*period)+1):((Nplots*period)+nBeta),]
N.sum<- rbind(N.sum[1:((Nplots*period)),],
    N.sum[((Nplots*period)+nBeta+2):No_entries,])
No_entries = (2*Nplots*(period-1)) + Nplots*period - nBeta
#Summary Statistics for Confidence intervals By Plot Number
N_sum <- vector("list")
for(i in 1:Nplots)
{

  Ni.sum <-N.sum[seq(i,No_entries, by = Nplots),]
  N_sum[[i]] <- Ni.sum
}


#Lambdas
lams <- ssm2$BUGSoutput$mean$lam

lams_mat <- cbind(dat[,7], dat[,1], as.matrix(lams))

lams_T <- lams_mat %>% filter(CT ==1)
```

```
lams_T <- lams_T[,-1]

lams_C <- lams_mat %>% filter(CT ==0)
lams_C <- lams_C[,-1]

#mu_lamdas
mu.lams <- ssm2$BUGSoutput$mean$mu.lam

mu.lams_mat <- cbind(dat[,7], dat[,1], as.matrix(mu.lams))


mu.lams_T <- mu.lams_mat %>% filter(CT ==1)
mu.lams_T <- mu.lams_T[,-1]

mu.lams_C <- mu.lams_mat %>% filter(CT ==0)
mu.lams_C <- mu.lams_C[,-1]

#Betas
beta_tab <- beta.out[,c(1,2,3,7)]
```

7.8 JAGS Model for MARSS model

```
sink("MV_Microdon.jag")
cat("
    model {
    # Priors

    for(i in 1:x) #Loop trough each plot
    {

    for(j in 1:4)#for each data matrix
     {
      N[i,1,j] ~ dunif(0, 40000)
     }#end j
    }#end i


    for(j in  1:4)
    {
```

```
  for(k in 1:4)
  {
    Q[j,k] ~ dunif(0,5000)
    R[j,k] ~ dunif(0,5000)
  }#end k
 }#endj


 for(i in 1:4)
 {
  u[i] ~ dunif(0,10)
  a[i] ~ dunif(0,10)
 }


for(i in 1:4)
 {
 for(j in 1:4)
 {
   beta[i,j] ~ dnorm(0, 0.01)
 }#end j

 }#end i


 mu = c(0,0,0,0)

 # Likelihood
 for(i in 1:(x)){

 #State Process

 w[1:4,i,1] ~ dmnorm.vcov(mu[1:4], Q[1:4,1:4])
 for(t in 1:(T-1)) #For each time step after the first modeling each plot seperat
 {

 N[i,(t+1),1:4] = beta %*%  N[i,(t),1:4] + u + w[1:4,i,t]
 w[1:4,i,(t+1)] ~ dmnorm.vcov(mu[1:4], Q[1:4,1:4])

 }#end t
```

```
    #Observation Process
    for(t in 1:(T))
    {
    y[i,t,1:4] ~ dmnorm.vcov(N[i,(t),1:4], R[1:4,1:4])

    }#end t

    }#end i



    }#end model


    ",fill = TRUE)#end cat
sink()
```